CAPITAL STRUCTURE MODELS

UNDERSTANDING THE CAPITAL STRUCTURE OF A FIRM THROUGH MARKET PRICES

By

ZHUOWEI ZHOU, M.SC.

A Thesis

Submitted to the School of Graduate Studies

in Partial Fulfilment of the Requirements

for the Degree

Doctor of Philosophy

McMaster University

DOCTOR OF PHILOSOPHY (2011)   McMaster University

(Financial Mathematics)   Hamilton, Ontario

TITLE: UNDERSTANDING THE CAPITAL STRUCTURE OF A FIRM THROUGH MARKET PRICES

AUTHOR: Zhuowei Zhou,M.SC.(McMaster University)

SUPERVISOR: Dr. Thomas Hurd

NUMBER OF PAGES: xvi, 128

Abstract

The central theme of this thesis is to develop methods of financial mathematics to understand the dynamics of a firm's capital structure through observations of market prices of liquid securities written on the firm. Just as stock prices are a direct measure of a firm's equity, other liquidly traded products such as options and credit default swaps (CDS) should also be indicators of aspects of a firm's capital structure. We interpret the prices of these securities as the market's revelation of a firm's financial status. In order not to enter into the complexity of balance sheet anatomy, we postulate a balance sheet as simple as $Asset = Equity + Debt$. Using mathematical models based on the principles of arbitrage pricing theory, we demonstrate that this reduced picture is rich enough to reproduce CDS term structures and implied volatility surfaces that are consistent with market observations. Therefore, reverse engineering applied to market observations provides concise and crucial information of the capital structure.

Our investigations into capital structure modeling gives rise to an innovative pricing formula for spread options. Existing methods of pricing spread options are not entirely satisfactory beyond the log-normal model and we introduce a new formula for general spread option pricing based on Fourier analysis of the payoff function. Our development, including a flexible and general error analysis, proves the effectiveness of a fast Fourier transform implementation of the formula for the computation of spread option prices and Greeks. It is found to be easy to implement, stable, and applicable in a wide variety of asset pricing models.

Acknowledgements

Needless to say, the list of people in this section is far from being complete.

I would like to thank my thesis advisor Professor Tom Hurd for being a great mentor and friend. Tom has not only indoctrinated me with financial mathematics knowledge, but also has taught me to think about problems with passion. His insight and dedication in this area have been influential to me. Moreover, I really appreciate the delicious meals amidst our research discussion at his home.

I am also very grateful to Professor Peter Miu and Professor Shui Feng, the members of my PHD committee, who have made an enormous commitment to giving me research suggestions, as well as carefully reading and commenting on my thesis draft. Their expertise in their own areas has provided me with important supplementary knowledge. I also would like thank my external examiner Professor Adam Metzler for carefully reading my thesis and making valuable suggestions.

Many thanks to Professor Matheus Grasselli, Professor David Lozinski, Professor Roman Viveros-Aguilera and Professor Lonnie Magee for stimulating discussions on financial mathematics, statistics and econometrics.

I would like to thank participants in the Thematic Program on Quantitative Finance at Fields Institute in 2010. Communications with them have broadened my scope in financial mathematics at large and their comments on my presentation in the 6th World Congress of the Bachelier Finance Society have enlightened my subsequent exploration of the contents in chapter 3 of this thesis in particular.

I also would like to thank the SIAM Journal on Financial Mathematics for issuing permission license for reprinting my published journal article in chapter 4 of this thesis. I also appreciate two anonymous referees from the journal, whose valuable suggestions have led to significant improvements of the article before it was accepted.

Last but not the least, I am indebted to my parents Angen and Yixiang, my wife Youhai and my new born daughter Mia. Their love and support are my fortune.

Contents

List of Tables

List of Figures

List of Acronyms

APT   Arbitrage Pricing Theory

BC   Black-Cox

BDLP   Background Driving Lévy Processes

BIS   Bank for International Settlements

BK   Black-Karasinski

BMO   Bank of Montreal

CDF   Cumulative Density Function

CDO   Collateralized Debt Obligation

CDS   Credit Default Swap

CLO   Collateralized Loan Obligation

CMS   Constant Maturity Swap

CVA   Credit Valuation Adjustment

DtD   Distance-to-Default

EAD   Exposure at Default

EC   Economic Capital

EMM   Equivalent Martingale Measure

EXP   Exponential

FP   First Passage

FFT   Fast Fourier Transform

FX   Foreign Exchange

GBM   Geometric Brownian Motion

GCorr   Global Correlation

IID   Independent Identical Distribution

ITM   In-the-Money

IV   Implied Volatility

KF   Kalman Filter

LGD   Loss Given Default

LOC   Line of Credit

LSBM   Lévy Subordinated Brownian Motion

MBS   Mortgage-Backed Security

MKMV   Moody's KMV

MLE   Maximum Likelihood Estimation

MtM   Mark-to-Market

NYSE   New York Stock Exchange

OTC   Over-the-Counter

OTM   Out-of-the-Money

PD   Default Probability

PDE   Partial Differential Equation

PDF   Probability Density Function

PIDE   Partial Integro-Differential Equation

RBC   Royal Bank of Canada

RMSE   Root Mean Squared Error

RV   Realized Variance

SEA   Self-Exciting Affine

SD   Structural Default

S & P   Standard & Poor's

SV   Stochastic Volatility

TCBM   Time-Changed Brownian Motion

TTM   Time to Maturity

UAW   United Auto Workers

VG   Variance Gamma

Declaration of Academic Achievement

My "sandwich thesis" includes three self-contained and related financial mathematics papers completed during my PhD study from 2007 to 2011.

The first paper "Statistical Inference for Time-changed Brownian Motion Credit Risk Models" in chapter 2 has been submitted for peer review [60] in early 2011. This paper demonstrates how common statistical inference, in particular maximum likelihood estimation (MLE) and Kalman filter (KF) can be efficiently implemented for a new class of credit risk models introduced by Hurd [57]. For this class of models, traditional estimation methods face challenges such as computational cost due to a non-explicit probability density function (PDF). My coauthor Professor Hurd and I have made significant improvement on resolving these issues and a study on Ford Motor Co. historical data shows our new method is fast and reliable. Professor Hurd and I are both equal contributors in the writing of this paper. More specifically I have made the following contributions: 1. Numerous studies leading to the statistical solution as the core of the paper including alternative approaches; 2. Most of the technical aspects of this paper, including mathematical derivations, data collection, computer programming and numerical analysis; 3. An equal share of drafting and finalizing of the paper.

The second paper "Two-Factor Capital Structure Models for Equity and Credit" in chapter 3 is ready to be submitted for peer review [61]. This paper extends the classical Black-Cox (BC) model in credit risk to a model of the capital structure of a firm that incorporates both credit risk and equity risk. In contrast to other extensions to the BC model that are restricted by a one-factor and/or diffusive nature, our model contains a two-factor characterization of firm asset and debt, and allows their dynamics to diffuse and jump. With much greater flexibility, our model retains satisfactory tractability and important financial derivatives can be priced by numerical integrations. We demonstrate the strength of the model by showing its improved fit

to market data. My coauthor Professor Hurd and I are both equal contributors in the writing of this paper. More specifically I have made the following contributions: 1. An equal share of the original idea of this paper that evolved from our discussions; 2. Most of the technical aspects of this paper, including mathematical derivations, data collection, computer programming and numerical analysis; 3. An equal share of drafting and finalizing of the paper.

The third paper "A Fourier Transform Method for Spread Option Pricing" in chapter 4 has been published in the *SIAM Journal of Financial Mathematics* [59][1]. This paper introduces a new formula for general spread option pricing based on Fourier analysis of the payoff function. This method is found to be easy to implement, stable, efficient and applicable in a wide variety of asset pricing models. On the other hand, most existing tractable methods are not entirely satisfactory beyond the log-normal model. Few exceptions are either computationally costly or subject to unsatisfactory numerical errors. My coauthor Professor Hurd and I are both equal contributors in the writing of this paper. More specifically I have made the following contributions: 1. Setting up the theoretical framework; 2. Most of the technical aspects of this paper, including mathematical derivations, computer programming and numerical analysis; 3. An equal share of drafting and finalizing of the paper.

Chapter 1

Background and Motivation

In the private sector, a firm finances its assets through a combination of equity, debt, or hybrid securities, leaving itself liable to various financial stakeholders. The composition or "structure" of these liabilities makes up its capital structure. A detailed capital structure tells rich information about a firm, such as its creditworthiness, its access to financing options, and even regulatory restrictions on the firm.

The management of a firm knows its capital structure well enough to make strategies that help the firm grow. Outsiders, such as rating agencies and stakeholders, need to know capital structure better to make forecasts of the firm. Balance sheets unveiled in quarterly financial statements provide a good snapshot of the capital structure to the public. However, balance sheets are inconvenient for real-time analysis as they are not available between reporting dates. Their relevance can also be obscured by accounting specifics and time delay. In addition, investors usually gather information from a firm's issued securities. For example, equity dilution can lead to the stock price dropping, while debt restructuring can lead to a slashing of bond prices. However, such analyses are ad hoc and intuitive, and they are difficult to extend to more quantitative problems.

We believe financial mathematics is a more sophisticated tool that can reveal non-intuitive and in-depth connections between market prices and a firm's capital structure. Its advantages are mainly two fold. First of all, by replacing a real world problem by a mathematical model one focuses critical attention on the underlying

idealizing assumptions. Once the assumptions have been accepted the rules of mathematics lead to clear results that can improve intuition. Also, mathematical modeling can simplify each problem by retaining only key factors and omitting others. For example, in our models we postulate a balance sheet as simple as $Asset = Debt + Equity$, which we write as

$$V_t = D_t + E_t \tag{1.1}$$

for each time t. Second of all, it is flexible and can take as inputs a broad spectrum of market prices. In addition to the "baseline" cases of stocks and bonds, one can include liquidly traded financial derivatives such as options, credit default swaps (CDS), which should also be indicators of aspects of a firm's capital structure. The values of capital structure can be learnt by comparing or calibrating model prices to these market prices.
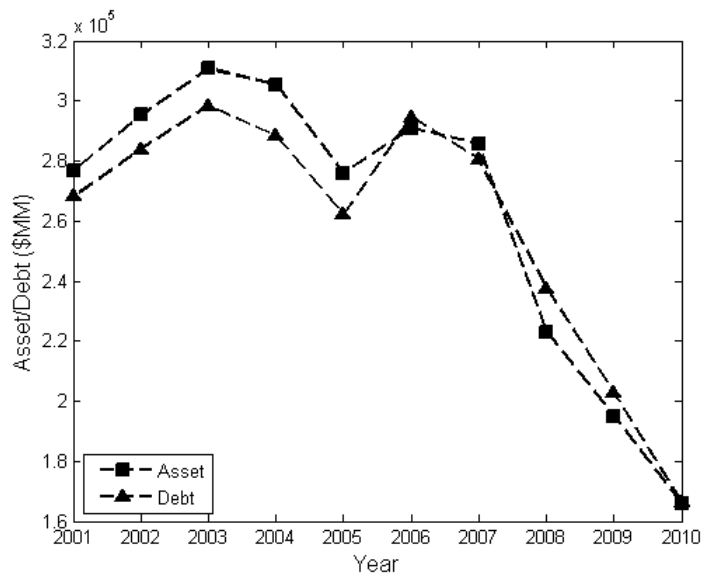
Figure 1.1: Ford's total asset and debt according to annual financial statements from 2001 to 2010.

While financial mathematics provides alternatives to understand a firm's capital structure, a caveat needs to be mentioned. The model implied capital structure represents market values of asset, debt *etc.* in a "mark-to-market" (MtM) sense,

as are the traded instruments used for calibration. However, the capital structure in a balance sheet represents accounting values that are calculated and interpreted differently [105]. So it is not important for us to reproduce the accounting balance sheet or even to obtain a capital structure similar to it. Instead, our aim is to provide an independent measure of the capital structure implied from market prices. To illustrate this point, we see from figure 1.1 that Ford's accounting $V - D$ became negative for several years which is impossible in our MtM calibration.

The value of any model can only be fully realized in real life applications. Admittedly, there are numerous firms worthy of detailed case study and in this thesis we chose one firm that is of particular interest. Ford Motor Company (NYSE: F) is the second largest automaker in the US and was the fifth largest in the world based on annual vehicle sales in 2010. It is the eighth-ranked overall American-based company in the 2010 Fortune 500 list, based on global revenues in 2009 of \$118.3 billion. However, this giant name in the global auto industry really stumbled in the last decade. As a result of declining market share, corporate bond rating agencies had downgraded the bonds of Ford to junk status by 2005. In 2006 in the wake of a labor agreement with the United Auto Workers (UAW), the automaker reported the largest annual loss in company history of \$12.7 billion. At the peak of the financial crisis, Ford announced a \$14.6 billion annual loss, making 2008 its worst year in history.

We note that Ford Motor Company experienced a large number of credit rating changes during this period. The history of Standard & Poor's (S & P) ratings is as follows: A to BBB+ on October 15, 2001; BBB+ to BBB on October 25, 2002; BBB to BBB- on November 12, 2003; BBB- to BB+ on May 5, 2005; BB+ to BB- on January 5, 2006; BB- to B+ on June 28, 2006; B+ to B on September 19, 2006; B to B- on July 31, 2008; B- to CCC+ on November 20, 2008. The downgrades continued into 2009, with a move from CCC+ to CC on March 4, 2009 and to SD ("structural default") on April 6, 2009. The latest news was improving: on April 13, 2009, S & P raised Ford's rating back to CCC, on November 3, 2009 to B-, and on August 2, 2010 to B+, the highest since the onset of the credit crisis. On February 2, 2011, it rose to BB-.

In hindsight we see that Ford never actually defaulted during this period, although
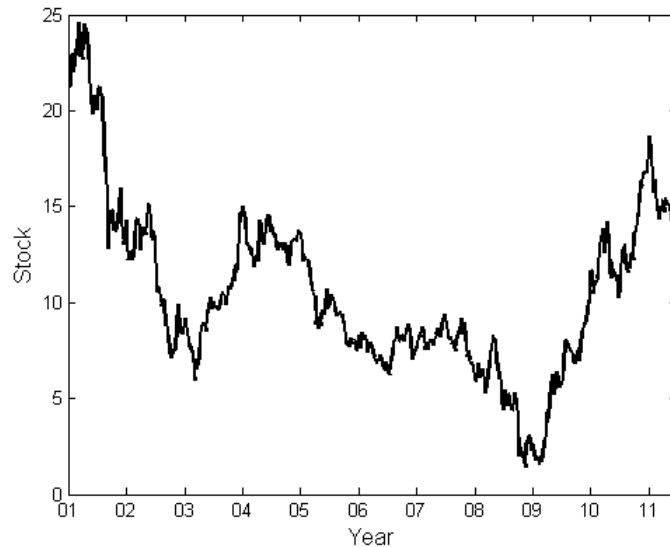
Figure 1.2: Ford stock prices after adjustments for dividends and splits from 2001 to 2011.

it came close. It implies that this company stays solvent in the MtM sense as its asset has a narrow margin over debt. From market prices, we not only see that its stock volatility and CDS have been priced high, but also that they evolved quite dynamically. It is therefore of particular interest to use Ford as a case study in this thesis to understand how much market prices tell about its capital structure.

1.1 How Good is Mathematical Modeling for Financial Derivatives?

In financial markets, a derivative is a security whose value depends on other, more basic, underlying variables [53]. The global financial derivative markets have seen staggering growth during the last two decades. According to the Bank for International Settlements (BIS) in March 2011 [9] the notional outstanding amounts of Over-the-Counter (OTC) derivatives reached \$583 trillion with gross market values of \$25 trillion in June 2010. The notional outstanding amounts of exchange traded

derivatives reached \$78 trillion in December 2010.

Paralleling the burgeoning in market size has been financial innovation. Market makers who provide financial market liquidity have tailored existing derivatives or invented entirely new ones to meet customers' financial needs. For example, variance swaps [21] provide investors with opportunities to hedge and speculate on market volatilities. Credit Default Swap (CDS) contracts provide investors with default protection on sovereign, municipal and corporate bonds. The highest profile innovation of Wall Street is probably securitization, among the associated securities are so-called structured instruments such as Mortgage-Backed Securities (MBS), Collateralized Loan Obligations (CLO) and Collateralized Debt Obligations (CDO). These instruments attract capital from international investors to provide less costly funding in otherwise illiquid housing markets, loan markets and speculative bond markets. For example, the CDO issuance grew from an estimated \$20 billion in Q1 2004 to its peak of over \$180 billion by Q1 2007 [101], while the numbers for MBS are even greater [88].

Even if intended as a way to off-load or manage risk, such complex derivatives may also harm holders with unexpected risks. Warren Buffett famously called derivatives "financial weapons of mass destruction", which illuminates the risky side of derivatives. Narrowly speaking, because of leverage, a trader could lose everything in option trading with only a modest movement of the underlying stock. From a global perspective, the 2007-2010 financial crisis (for a description of the crisis see [51] and its references therein) would have been contained within the housing market where it originated if complex derivatives such as MBS, MBS CDO had not become so widespread (See [51][52]). The subprime mortgage market only amounted to a small part of the US economy or even of the prime mortgage market. However, its impact swiftly propagated into US capital markets and eventually eroded the global economy. Among many other causes of the crisis is OTC derivatives' role in transferring risks, that can lead to systemic risks (See [28] for a good illustration of so-called contagion and systemic risks). A panacea might be to go back to the old, simple days when there was no room for complex, toxic securities. However, this view misses the fact that complex derivatives serve the same primary purpose as stocks and bonds,

in a more sophisticated way, to direct limited resources (funding) to promote social development. The technology of risk pooling and risk transfer has been an essential component of capital markets for centuries, with innovations that have arisen in response to legitimate needs of individuals and corporations. Their real benefits are the basis for people's good faith on them.

Until recently, market participants have been content to use the modern mathematical finance theory, pioneered by Black, Scholes and Merton in the 1970s [11][85][106], to hedge and price derivatives. Experienced traders make estimates of their bid/ask prices starting from the bare-bones model prices. They also quantify their risk exposures in terms of model dependent risk metrics such as Greeks. During the financial crisis people have seen the predictions of financial models diverge dramatically from empirical observations, and consequently much criticism has been cast on quantitative modeling in general, and sometimes even a particular formula [94][102]. The basis of this negative voice is that quantitative analysts ("quants") failed to build "right" models to capture dangerous risks that ultimately pushed the financial system to the brink. To provide an opposite view, several renowned researchers wrote on this subject in their columns or papers [36][77][100][107]. These authors contrasted financial models with physics models and illustrated why financial models have yet to achieve the level of accomplishment of physics models. In Lo and Mueller's Taxonomy [77], physics has been very successful in modeling a world with "complete certainty" and "risk without uncertainty". This physics world involves deterministic motions such as planetary orbits and harmonic oscillation and controlled lab experiments such as atomic collisions and crystal growth. In contrast, financial models must cope with the mental world of monetary value. They aim at reducing humans' irreversible and unrepeatable behavior to a simplified mechanism. Modeling this realm of "partially reducible uncertainty" is a much more ambitious undertaking than physics. There is no "right" model because the world changes in response to the models we use [1]. On the other hand, there is the "right" use of models. In the course of modern mathematical finance theory, models are developed that work for different markets

---

[1]Take arbitrage trading for example. Arbitrage trading always annihilates existing arbitrage opportunities. So the same trading algorithms would fail after short-term usage.

under different scenarios, to maximize their utility and accuracy. There are some best available models for specific finance or economics problems. The right use of models also requires users' good judgment. As Steve Shreve put it [100], *. . . a good quant also needs good judgment. A wise quant takes to heart Albert Einstein's words, "As far as the laws of mathematics refer to reality, they are not certain; and as far as they are certain, they do not refer to reality. . . "*. The right use of models involves much more than finding a generic model that works for all.

This thesis presents mathematical models of capital structure that are more robust and have weaker assumptions than some existing ones. Our aim will be to show that these models work reasonably well in the markets we investigated. We also provide mathematical techniques that make these models tractable and therefore be applied to real industry problems. We hope that these works will complement and extend the current financial literature and provide new tools to improve risk management of the financial markets.

1.2   A Filtered Probability Space

In modern mathematical finance theory, underlying dynamic market variables are modeled as stochastic processes. The probabilistic specifications of these selected stochastic processes must reflect empirical market observations to diminish the so-called "model risk". On top of these processes, there is a filtered probability space $(\Omega, \mathcal{F}, \mathcal{F}_t, \mathbb{Q})$ that formalizes their evolution with respect to time. Here Ω is a non-empty set that includes all possible "outcomes" or realizations of the underlying stochastic processes and $\mathcal{F}$ is a $\sigma-$algebra of subsets of Ω. With the calendar time starting from 0 and denoted by t, the filtration $(\mathcal{F}_t, t \geq 0)$ is a family of sub $\sigma-$algebras of $\mathcal{F}$ such that $\mathcal{F}_s \subseteq \mathcal{F}_q$ whenever $s \leq q$. Each subset A in $\mathcal{F}$ is called an event, and its probability of occurrence is given by the probability measure $\mathbb{Q}(A)$. It is naturally required that $\mathbb{Q}(A) \geq 0$ and $\mathbb{Q}(\Omega) = 1$.

It is standard in probability theory to require some further conditions on a filtration, and the following pair of conditions are referred as the *usual hypotheses*:

- (completeness) $\mathcal{F}_0$ contains all sets of $\mathbb{Q}-$measure zero;

- (right continuity) $\mathcal{F}_t = \mathcal{F}_{t+}$ where $\mathcal{F}_{t+} = \cap_{\epsilon>0} \mathcal{F}_{t+\epsilon}$.

Let the underlying stochastic process $X = (X(t), t \geq 0)$ be a mapping from $\mathbb{R}^+$ to $\mathbb{R}^d$. We say that it is adapted to the filtration (or $\mathcal{F}_t-$adapted) if $X(t)$ is $\mathcal{F}_t-$measurable for each $t \geq 0$. Any process X is adapted to its own filtration $\mathcal{F}_t^X = \sigma\{X(s); 0 \leq s \leq t\}$ and this is usually called the *natural filtration*.

In mathematical finance modeling, the filtration is intimately connected to the information revealed by the market at a time on-going basis. The most accessible information is given by the "market filtration" $\mathcal{G}_t \subset \mathcal{F}_t$ defined by the market observables. Hidden variables such as the short rate and stochastic volatilities are adapted to hidden filtrations that may or may not be "backed out" from observables such as traded options. When some investors gain access to a larger filtration, either from superior information channels or better modeling, they may be able to create a so-called *dynamic arbitrage* [19] to risklessly cash-out at the expense of others. In this thesis, we work with probability space. Our market observables include stock prices, implied volatility (IV) surfaces and CDS term structures that are made available to the public. In addition, our models have a small dimensional family of hidden Markov variables, or latent variables that includes firm asset, debt and leverage ratio. Inference of these hidden values is made from traded securities on the firm, and possibly its balance sheets as well.

For formal descriptions of probability theory and stochastic processes, one can refer to standard probability textbooks such as [3] and [65]. [99] also provides mathematical finance interpretations of probability theory.

1.3 Literature Review

1.3.1 Understanding a Firm's Capital Structure

Balance Sheet Analysis

The straightforward way to understand a firm's capital structure is to read off its balance sheet from published quarterly financial statements. In a simplified and stylized balance sheet, a firm's capital structure consists of assets and an equal ("balanced") amount of liabilities that consist of shareholders' equity and debt holders' debt [2]. Table 1.1 illustrates a simplified balance sheet. In this case, a financial firm is funded by \$10 billion from equity holders and \$90 billion from debt holders, the total of which is invested in assets which are mostly securities. If we define the leverage ratio as the ratio of asset over debt [3], the firm's leverage ratio is $\frac{10}{9}$. Typically, a standard balance sheet in financial accounting further breaks down assets into current assets and non-current assets, debt into short term current debt and long term non-current debt, equity into paid-in capital and retained earnings *etc.* [105]. A detailed balance sheet is very useful for static performance analysis of a firm. Altman [1] used seven quantities in a balance sheet to calculate the famous Z-score to determine firms' survivability. Rating agencies rely heavily on balance sheets to estimate the default probability (PD), exposure at default (EAD) and loss given default (LGD) of different bonds issued by a firm.

Assets	Liabilities
Securities, 100	Debt, 90
	Equity, 10

Table 1.1: A simplified and stylized balance sheet for a financial firm (in \$ billion).

---

[2]In many occasions, liabilities are used to represent debt exclusively. Our definition of liabilities stresses that a firm is also liable to equity holders.

[3]In financial accounting, leverage ratio of a firm is usually defined as the ratio of debt over asset or debt over equity. We use this definition to conform to the log leverage ratio $X_t = \log(V_t/D_t)$ in chapter 2.

The Collapse of Enron

The demise of the giant energy corporation Enron was the highest profile bankruptcy reorganization in American history up to that time. Its quick fall a couple of months after its first quarterly loss report in years shocked investors and auditors:

- Enron headed into 2001 with a stock price of about $80. On June 19, Jeffrey Skilling, the incumbent chief executive officer, reiterated "strong confidence" in Enron's earning guidance to investors. On the same day, Enron's daily realized variance (RV) jumped dramatically from 66 percent to 158 percent.

- On August 14, Skilling resigned unexpectedly, triggering Wall Street's concern about Enron's real financial status. The equity price fell from $42.93 to $36.85 in two days. Daily RV increased from 29 percent on August 13 to 84 percent and 131 percent on August 14 and 15 respectively.

- On October 16, Enron's first quarterly loss in more than four years was made public through its financial statement, accompanied by a $1.2 billion charge against shareholders' equity. Its equity price dropped from $33.84 to $20.65 in the next four days. Daily RV moved up into the range of 85-210 percent.

- On November 8, Enron announced that it would restate its earnings from 1997 through 2001, which further brought down its equity to $8.63 during that week. Daily RV reached 262 percent.

- On November 28, credit-rating agencies downgraded Enron's bonds to junk status, and Enron temporarily suspended all payments before filing for Chapter 11 bankruptcy protection on December 2. The daily RV experienced its highest spike of 1027 percent.

From the Enron case, we can see that infrequently published balance sheet information does not fit well with a dynamic analysis of capital structure, especially for short term, since apart from the share value, balance sheet entries are only available quarterly and with time delay. The main theme of this thesis is to explore an alternative, namely
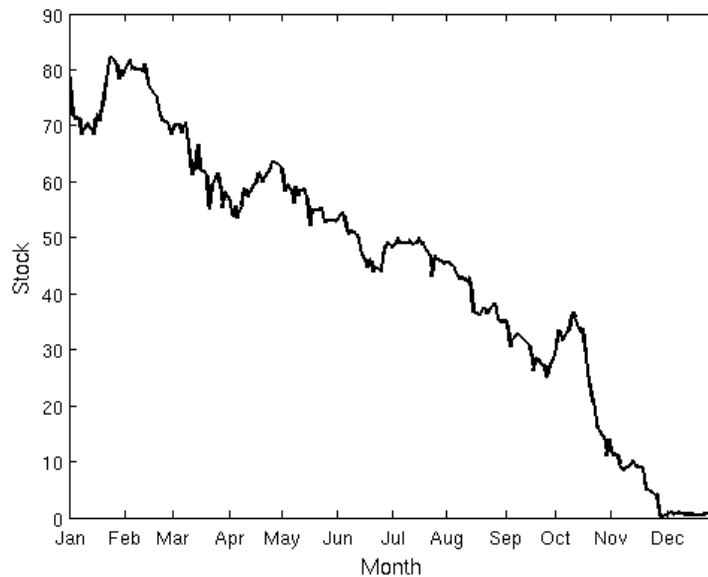
Figure 1.3: Enron historical stock prices in 2001.

to deduce a simplified capital structure from prices of market observables which are more abundant and reliable, using tractable mathematical finance models.

Structural Approach in Credit Modeling

The structural approach to credit risk models balance sheet parameters of a firm such as asset, debt or leverage as underlying processes, and treats securities issued by the firm such as bonds and stock as contingent claims on the firm's assets. This stream of modeling begins with the seminal works of Merton [86] and Black and Cox [10], in which they assumed a geometric Brownian motion (GBM) for the firm asset process and modeled the firm default as the time the asset value hits a continuous or discrete barrier equal to the debt value. While Merton assumed default can only happen at a bond maturity, Black and Cox made default a first passage (FP) event that can happen any time within the maturity horizon. Because its first passage concept in credit modeling is used throughout this thesis, we now outline the Black-Cox framework. We work in a filtered probability space $(\Omega, \mathcal{F}, \mathcal{F}_t, \mathbb{Q})$, where $\mathcal{F}_t$ is the natural filtration of a Brownian motion W_t and $\mathbb{Q}$ is the risk-neutral measure.

In such a probability space, the total value V_t of a firm's assets follow a geometric Brownian motion

$$\frac{dV_t}{V_t} = (\mu - \delta)dt + \sigma dW_t \tag{1.2}$$

where μ is the mean rate of return on the asset, δ is a proportional cash pay-out rate and σ is the volatility. The firm's capital structure includes a single outstanding debt with a deterministic value D_t, which has a maturity T and face value $D_T = D$. Black and Cox postulated that default occurs at the first time that the firm's asset value drops below the debt value. That is, the default time is given by

$$\tau = \inf\{t > 0 : V_t < D_t\} \tag{1.3}$$

This is a simplification of the notion of a safety covenant in corporate finance which gives debt holders legal rights to force liquidation of the asset of a firm if it fails to service any coupon or par obligations. Consistent with the limited liability for equity holders, the pay-off for equity holders at maturity is

$$(V_T - D_T)^+ \mathbf{1}_{\{\tau > T\}} \tag{1.4}$$

A natural choice of the debt value process assumes a constant growth rate $k \geq 0$ so $D_t = De^{-k(T-t)}$ which leads to an explicit formula for the density function of τ as well as a formula for the value of equity.

Beyond the Merton and Black-Cox Models

Along the lines of Merton and Black-Cox, there have been various extended versions in credit risk modeling. Hull and White [55] revised the Black-Cox model by using piecewise constant default barriers and were able to fit perfectly a given term structure of default rates derived from market CDS rates. Nielsen *et.al.* [91], Briys *et.al.* [15], and Schobel [96] modeled stochastic interest rates that brought randomness to the default boundary. Leland [72], Leland and Toft [73], and Mella-Barral and Perraudin [83] considered strategic default which is exercised by a firm's management (*i.e.* the equity holders) to maximize its equity value. Vendor's software, such as Moody's KMV (MKMV) [30], stemmed from the Merton model. Rather than

looking at asset and debt individually, Moody's KMV models its proprietary accounting ratio called distance-to-default (DtD) that serves as a normalized measure of the margin between the asset and debt. Other authors have incorporated more financial intuition into the definition of default. Cetin *et.al.* [27] defined default as the time when a firm's cash balance hits a secondary barrier after staying below the primary barrier of zero (financial stress) for an extended period of time. Yildirim [108] defined default as the first time the firm value stays under a barrier for an extended period measured by the integral of the firm value with respect to time. The financial implication is that when a firm becomes financially stressed, it still has some chance of revival by accessing liquidity or bank lines of credit (LOC) before default is triggered. The performance of several structural models has been tested by Eom *et.al.*[42].

While the Merton and Black-Cox models have been widely accepted due to their consistency with financial intuition and tractability in mathematical treatment, their shortcomings are also well known. They predict that term structures of credit spreads must have a zero short spread and a particular hump shape that is unrealistic. At least for investment grade credits there is evidence against humps and for increasing credit spreads [76][95][50]. Moreover, the Merton model has a time inconsistency problem when it comes to derive the PD term structure. For more detailed discussion of these models, one can refer to standard credit risk books for example [39][69][97].

Within the structural approach the majority of works that succeed in producing flexible term structures start from one of two fundamental ideas:

1. Introduce jumps into the firm asset, debt or leverage ratio processes so that the creditworthiness of a firm can have a good opportunity for a substantial move in a short period of time, making default an "unpredictable" event. Various numerical methods have been developed to improve tractability. Zhou [111] is the first to use Monte Carlo simulation in this kind of structural models to make the connection between jumps and non-zero short spread. Kou and Wang [68] used Kou's earlier asset price model and took advantage of the "memoriless" feature of the exponential jumps to derive an explicit Laplace transform of the first passage time, leading to the formulas for the first passage time density and

credit spreads involving Laplace inversion [8]. More generally, the Wiener-Hopf factorization gives the Laplace transform of the joint characteristic function of a Lévy process and its running maximum, and has been used to price barrier options under Lévy processes [29]. Similarly, it can be used to calculate the first passage time density in the structural approach. Moreover, a first passage time of the second kind invented by Hurd [57] has a semi-closed form density function in terms of a spectral expansion for a broad class of time changed Brownian motions (TCBM), so that credit spreads can be efficiently calculated by one dimensional numerical integrations.

2. Introduce uncertainties into the current observation of a firm's asset or debt so that the firm's default event becomes unpredictable. Duffie and Lando [38] assumed that a firm's asset is observed with accounting noises, only at certain points in time. Giesecke [46] assumed that a firm's default threshold has some prior distribution known to investors, and which can be updated with new information from bond markets. In the vendor software CreditGrades [45], the default threshold is a log-normally distributed random variable drawn at time zero.

There are several notable merits of the structural approach. First of all, it has a clear economic interpretation. The framework links balance sheet parameters of asset and debt to the market tradable stocks and bonds, and is consistent with arbitrage pricing theory (APT). People have been able to implement reverse engineering of structural models using readily available equity and bond data to estimate unobserved asset and debt values of a firm. In Bensoussan *et.al* [7], the asset volatility of a firm is analytically derived from the equity volatility. The interpretation of the leverage effect in equity markets is also addressed. Duan [37] and Ericsson and Reneby [43] used maximum-likelihood estimation (MLE) to obtain a firm's asset value from equity data. The best-known vendor software of this kind Moody's KMV uses a proprietary structural approach [4] to estimate time series of asset values for a vast

---

[4]Moody's KMV is (understandably) reluctant to release all details of the model as they are trying to sell the model.

pool of public firms in its database. Its "GCorr" (Global Correlation) model provides asset correlation matrices calculated from these time series. Very recently, Eberlein and Madan [41] went further to use both traded equity options and balance sheet statements to evaluate a firm's impact on the economy. They argued that limited liability applies to all of a firm's stakeholders not just the shareholders, and claimed the shortfall amounted to a "taxpayer put" option written by the economy at large. They model both a firm's risky assets and debts as exponential Lévy processes. After calibration to balance sheet statements and equity options for six US banks, their model is able to put a value on these taxpayer put options and an acceptable level of capital reserves.

Second of all, the structural approach is naturally suited to analyze one type of relative value strategy commonly used in hedge funds and investment banks, namely capital structure arbitrage[109]. Capital structural arbitrage relies on model dependent links between seemingly unrelated securities of the same firm and explains security prices inconsistent relative to others as mispricing by the market. The statistical arbitrage profits by investing in expectation that this mispricing eventually vanishes, forced by the fundamental value of the firm. Built on a structural model, CreditGrades is an industry benchmark model for evaluating CDS prices from a firm's current share price, historical equity volatility, debt per share, historical recovery rate and model assumptions. Yu [110] used CreditGrades to study possible arbitrage opportunities achievable by trading on the relative values of equity and CDS.

Third of all, the structural approach allows for flexible asset and default correlation. For pure diffusive processes, correlation of names can be parameterized in a correlation matrix and for a large portfolio one can introduce factor models in which correlations are parameterized by a reduced number of factor loadings. The popularity of the structural approach has reached various multi-name problems, such as economic capital (EC)[30][47], credit valuation adjustment (CVA)[55][14][12][75], CDO pricing [56][54]. Due to the fact that a broad class of Lévy processes is subordinated Brownian motion [57][29], some far-reaching research has studied correlation for this class of Lévy processes.

In spite of the success of the structural approach, one should always recall a

line of caveat in its usage. No direct correspondence of the market value of asset, debt or leverage to a firm's balance sheet parameters is necessary for the validity of this approach: all that matters is that there are such processes (observable or unobservable), and that they indicate the creditworthiness of the firm.

1.3.2 Spread Options are Akin to Capital Structure

The stylized balance sheet (1.1) can be written $E_t = V_t - D_t$. This implies that an equity option is akin to a spread option, and it suggests that one can model capital structure by modeling the two underlying factors V_t, D_t.

Spread options are a fundamental class of derivative contracts written on multiple assets that are widely traded in a range of financial markets, such as equity, fixed-income, foreign exchange (FX), commodity and energy markets. The majority of the academic literature focuses on basic European spread options with two underlying assets. If we denote by $S_{jt}, j = 1, 2, t \geq 0$ the two asset price processes and $K \geq 0$ the strike of the contract, the spread option pays $(S_{1T} - S_{2T} - K)^+$ at maturity T. When we take $S_{1t} = V_t$ and $S_{2t} = D_t$ this becomes our equity option payoff function $(V_T - D_T - K)^+$. So the understanding of spread options pricing may be quite helpful for cracking capital structure problems. In general, we can identify two main streams of modeling approaches to spread options.

Modeling the Asset Spread

The first stream reduces the dimension of the problem by directly modeling the spread of the two assets or the combination of one asset and the strike. The motivation for this stems from avoiding modeling individual assets and correlations which can be volatile in some markets. In the Bachelier appoximation [104][98][92], the spread of the two assets follows an arithmetic Brownian motion, leading to an analytic Bachelier formula for pricing spread options similar to pricing plain-vanilla options. Ultimately, this becomes a moment matching technique, and is commonly used for pricing more general basket options. Brigo *et.al.* [13] has tested the accuracy of such distributional approximations using notions of distance on the space of probability densities. Others

[79] have been able to obtain higher accuracy for the spread distribution by using a Gram-Charlier density function as pioneered in finance by Jarrow and Rudd [63]. The Gram-Charlier density function approximates the terminal spread distribution in terms of a series expansion related to its higher order moments. This higher order expansion is able to capture more features of the true distribution, especially in its tails. With a different treatment but a similar idea, Kirk [66] combined the second asset with the fixed strike and assumed a log normal distribution for the sum of the two. He then used the Margrabe formula to price spread options. In [35] [5], it was pointed out that the Kirk method is equivalent to a linearization of the nonlinear exercise boundary and they implemented a second-order boundary approximation and demonstrated an improved accuracy. In a parallel paper, Deng *et. al.* [34] extended the two-asset setting to multi-asset setting. This was achieved by approximating the arithmetic average of asset prices by the corresponding geometric average, and again the moment matching technique commonly used in pricing basket options. Dempster, Medova and Tang [33] used more sophisticated one factor and two-factor Ornstein-Uhlenbeck (OU) processes to model the spread, which again have normal terminal distributions.

Having closed-form solutions similar to Black-Scholes formula is the greatest advantage of this stream of modeling framework. Not only is the pricing very fast and reliable, but also hedging comes easily with convenient calculation of the Greeks. The downside of this stream of model framework is also obvious: it is doubtful that the spread empirically follows a normal or log-normal distribution. If not, the model misspecification may lead to unacceptable pricing and hedging errors. The calibration also faces challenges. It is hard to draw forward looking information of the spread dynamics from the typically illiquid multi-name derivative market. Sometimes, the spread model parameters can only be regressed from historical time series, a less than satisfactory way since historical data tells little about today's pricing.

---

[5]Strictly speaking, their work belongs to the second stream. We introduce it in the first stream to recognize it as an extension of the Kirk method.

Modeling Assets

The second stream of modeling framework more naturally models each asset individually, and recognizes their explicit correlation structure. In the common case of geometric Brownian motions, the unconditional spread option price is written as a one dimensional integral of conditional Black-Scholes call option prices with respect to a Gaussian Kernel, and can be accurately computed using numerical recipes such as quadrature rules. As discussed in [17], numerical algorithms have weaknesses compared to analytical algorithms. Notably, the former does not evaluate prices and the Greeks as rapidly as the latter, making it less favored in trades that require fast pricing and hedging. It also makes static comparative analysis difficult. Carmona and Durrleman [18] designed an approximate analytical formula for spread option pricing and Greeks. Their pricing formula needs no numerical integration, but uses parameters as solutions to nonlinear systems of equations which require numerical recipes and can be computationally costly. More recently, Deng *et. al.* [35] derived their approximate analytical formula for spread option pricing and Greeks by approximating the option exercise boundary to quadratic order in a Taylor series expansion.

The above analytical algorithms usually do not fit easily with more general asset models outside the Gaussian world. Such models require slow algorithms such as Monte Carlo simulation, numerical integration, PDE/PIDE or Fourier transforms. In line with Carr and Madan [23], Dempster and Hong [32] derived spread option prices as Fourier transform in the log strike variable. In particular, they derived tight lower and upper bounds for spread option prices and found the lower bounds to be more accurate than their Monte Carlo benchmark. In the line of Lewis [74], Leentvaar and Oosterlee [71] derived general basket option prices as Fourier transforms in the log asset variables. A general framework using Lewis type Fourier transforms in log asset variables is presented in [62], which they demonstrated in the pricing of different financial derivatives. The Fourier transform method is well suited for a wide range of asset models, as long as the characteristic functions of the log asset processes are calculable.

1.4 What Can Be Learnt From This Thesis

The central theme of this thesis is to understand a firm's capital structure through its traded underlying and derivatives. Just as stock prices are a direct measure of a firm's equity, other liquidly traded products such as options, credit default swap (CDS) should also be indicators of aspects of a firm's capital structure. Via mathematical modeling we interpret the values of these products as market's revelation of a firm's financial status. In order not to enter into the complexity of balance sheet anatomy, we postulate a balance sheet as simple as $Asset = Equity + Debt$. We demonstrate that this reduced dimension is rich enough to reproduce CDS term structure, implied volatility surface that are consistent with market observations. Therefore, reverse engineering fed with market observation provides concise and crucial information of the capital structure.

We demonstrate these ideas by building mathematical models of capital structure based on the foundations laid down in the modern martingale approach to arbitrage pricing theory as developed by Harrison and Kreps [48], Harrison and Pliska [49], and Delbaen and Schachermeyer [31]. Thus we propose to model the dynamics of the balance sheet parameters as stochastic processes within the filtered probability space $(\Omega, \mathcal{F}, \mathcal{F}_t, \mathbb{Q})$, where $\mathbb{Q}$ is an equivalent martingale measure (EMM). From this will follow the pricing formulas of stocks, bonds, options and CDS.

The main body of this thesis consists of chapters 2, 3 and 4, each of which is a self-contained and structurally independent paper that addresses certain aspects of our central theme.

Chapter 2 uses an extended Black-Cox model to study arguably the single most important financial parameter in a firm's capital structure, namely its leverage ratio defined as the ratio of asset to debt. We assume that a firm's log-leverage ratio X_t evolves as a time changed Brownian motion (TCBM), a regular Brownian motion running with an independent stochastic business clock. For this rich class of processes, we construct the default of a firm as a first passage problem of the TCBM, with an explicit first passage density function in special cases. In particular, we explore the variance gamma (VG) model and the exponential (EXP) jump model. Given a time

series of historical CDS term structures for Ford Motor Co. over more than a four-year horizon, we develop an inference scheme to estimate the model parameters and log-leverage ratio time series. A performance analysis of the resulting fit reveals that the TCBM models outperform the Black-Cox model. Based on this, we find that the implied time series of the log leverage ratio X_t is quite dynamic and strongly correlated with stock prices. Our estimation problem is more challenging than [37] and [43] as we need to deal with the contribution of measurement error in the likelihood function. We also distinguish our model estimation with the so-called "daily calibrations" often used in finance as we only allow the natural state variables, not the model parameters, to be time varying. Beyond the log-leverage models proposed, the main mathematical or statistical contribution made in this chapter is called the "linearized measurement scheme". This amounts to making a specific nonlinear transformation of the market data before formulating the partial likelihood function and leads to a more efficient statistical inference.

Chapter 3 is partly motivated by the results in chapter 2 that show a strong but imperfect correlation between log-leverage ratios and stock prices. To capture these two factors, we model a firm's asset V_t and debt D_t by correlated exponential TCBM. From these, we define the stock price and log-leverage as

$$S_t = E_t = V_t - D_t, \quad X_t = \log(V_t/D_t).$$

Thus this model adds in the extra flavor of debt dynamics, an aspect usually overlooked by existing models. The default problem depends on solving first passage for the log-leverage ratio and is identical to chapter 2, and the new work here is to price an equity call option as a down-and-out spread option. We find that the pricing formulas for bonds, CDS and implied volatility are not only very tractable for most common TCBMs, but also fit well to market observations such as volatility skew and CDS term structure. Based on our familiar VG model and EXP model, we make daily co-calibrations of the implied volatility surface and CDS term structure. The implied asset and debt values are comparable to the balance sheet parameters observed in quarterly financial reports. Moreover, the price fitting of the calibration indicates that the model simultaneously captures the risks from both equity and credit markets

reasonably well. As a generic structural model, this model has a natural potential for constructing relative value strategies, equity and credit cross-hedging *etc.* One important mathematical contribution we have made in this chapter is the result that a down-and-out spread option is equivalent to the difference of two vanilla spread options in our TCBM models.

Chapter 4 explores the pricing of spread options, a common product in almost every type of financial market. This chapter develops a flexible numerical method based on the Fourier transform that applies to price spread options on multiple underlying assets with specified joint characteristic functions. Compared with other existing methods for spread options, our method achieves higher accuracy with a very competitive computational cost, and thus this result has interest far beyond our applications to capital structure models.

To price financial derivatives, there is an inevitable trade-off between modeling sophistication and mathematical tractability. In all three subjects of this thesis, we try to optimize this trade-off by using robust models with little compromise to empirical observations and semi-closed form pricing formulas that lead to efficient computation by the fast Fourier transform (FFT). This effort is also convenient for hedging and model calibration, which usually are more important than direct pricing in practical uses of a model.

In chapter 5, we conclude with a summary that envisions what can be extended from results developed in this thesis.

Chapter 2

Statistical Inference for Time-changed Brownian Motion Credit Risk Models

This chapter is originated from a paper coauthored with Professor Hurd and submitted to *SIAM Journal of Financial Mathematics*[60] in early 2011, to which the author of the thesis is an equal contributor. It should be noted that the references of the chapter are indexed to adapt to the thesis, therefore differ from the submitted paper. Another difference is the section *Additional Material* in the end of this chapter which is not included in the submitted paper.

2.1   Abstract

We consider structural credit modeling in the important special case where the log-leverage ratio of the firm is a time-changed Brownian motion (TCBM) with the time-change taken to be an independent increasing process. Following the approach of Black and Cox, one defines the time of default to be the first passage time for the log-leverage ratio to cross the level zero. Rather than adopting the classical notion of first passage, with its associated numerical challenges, we accept an alternative notion applicable for TCBMs called "first passage of the second kind". We demonstrate how

statistical inference can be efficiently implemented in this new class of models. This allows us to compare the performance of two versions of TCBMs, the variance gamma (VG) model and the exponential jump model (EXP), to the Black-Cox model. When applied to a 4.5 year long data set of weekly credit default swap (CDS) quotes for Ford Motor Co, the conclusion is that the two TCBM models, with essentially one extra parameter, can significantly outperform the classic Black-Cox model.

2.2   Introduction

Next to the Merton credit model of 1974 [86], the Black-Cox (BC) model [10] is perhaps the best known structural credit model. It models the time of a firm's default as the first passage time for the firm's log-leverage process, treated as an arithmetic Brownian motion, to cross zero. The BC model is conceptually appealing, but its shortcomings, such as the rigidity of the resulting credit spread curves, the counterfactual behaviour of the short end of the credit spread curve and the difficulty of computing correlated multifirm defaults, have been amply discussed elsewhere, see e.g. [69]. Indeed remediation of these different flaws has been the impetus for many of the subsequent developments in credit risk.

One core mathematical difficulty that has hampered widespread implementation of Black-Cox style first passage models has been the computation of first passage distributions for a richer class of processes one might want to use in modeling the log-leverage process. This difficulty was circumvented in [57], enabling us to explore the consequences of using processes that lead to a variety of desirable features: more realistic credit spreads, the possibility of strong contagion effects, and "volatility clustering" effects. [57] proposed a structural credit modeling framework where the log-leverage ratio $X_t := \log(V_t/K(t))$, where V_t denotes the firm asset value process and $K(t)$ is a deterministic default threshold, is a time-changed Brownian motion (TCBM). The time of default is the first passage time of the log-leverage ratio across zero. In that paper, the time change was quite general: our goal in the present paper is to make a thorough investigation of two simple specifications in which the time change is of Lévy type that lead to models that incorporate specific desirable

characteristics. For illustrative purpose, we focus here on a single company, Ford Motor Co., and show that with careful parameter estimation, TCBM models can do a very good job of explaining the observed dynamics of credit spreads. TCBMs have been used in other credit risk models, for example [87], [44], [5] and [84].

One model we study is an adaptation of the variance gamma (VG) model introduced by [81] in the study of equity derivatives, and remaining very popular since then. We will see that this infinite activity pure jump exponential Lévy model adapts easily to the structural credit context, and that the extra degrees of freedom it allows over and above the rigid structure of geometric Brownian motion correspond to desirable features of observed credit spread curves. The other model, the exponential (EXP) model, is a variation of the Kou-Wang double exponential jump model [68]. Like the VG model it is an exponential Lévy model, but now with a finite activity exponential jump distribution. We find that the EXP model performs remarkably similarly to the VG model when fit to our dataset.

We apply these two prototypical structural credit models to a dataset, divided into 3 successive 18 month periods, that consists of weekly quotes of credit default swap spreads (CDS) on Ford Motor Company. On each date, seven maturities are quoted: 1, 2, 3, 4, 5, 7, and 10 years. The main advantages of CDS data over more traditional debt instruments such as coupon bonds are their greater price transparency, greater liquidity, their standardized structure, and the fact that they are usually quoted for more maturities.

Our paper presents a complete and consistent statistical inference methodology applied to this time series of credit data, one that takes full advantage of the fast Fourier transform to speed up the large number of pricing formula evaluations. In our method, the model parameters are taken as constants to be estimated for each 18 month time period: in contrast to "daily calibration" methods, only the natural dynamical variables, not the parameters, are allowed to be time varying.

Section 2 of this paper summarizes the financial case history of Ford Motor Co. over the global credit crisis period. Section 3 reviews the TCBM credit modeling framework introduced in [57]. There we include the main formulas for default probability distributions, defaultable bond prices and CDS spreads. Each such formula

is an explicit Fourier transform representation that will be important for achieving a fast algorithm. Section 4 gives the detailed specification of the two TCBM models under study. Section 5 outlines how numerical integration of the default probability formula can be cast in terms of the fast Fourier transform. The main theoretical innovation of the paper is the statistical inference method unveiled in section 6. In this section, we argue that the naive measurement equation is problematic due to nonlinearities in the pricing formula, and that an alternative measurement equation is more appropriate. We claim that the resultant inference scheme exhibits more stable and faster performance than the naive method. In Section 7, we outline an approximate numerical scheme that implements the ideal filter of Section 6. The detailed results of the estimation to the Ford dataset are summarized in Section 8.

2.3 Ford: The Test Dataset

We chose to study the credit history of Ford Motor Co. over the 4.5 year period from January 2006 to June 2010. The case history of Ford over this period spanning the global credit crisis represents the story of a major firm and its near default, and is thus full of financial interest. We have also studied the credit data for a variety of other types of firm over this period, and achieved quite similar parameter estimation results. Thus our study of Ford truly exemplifies the capabilities of our modeling and estimation framework.

We divided the period of interest into three nonoverlapping successive 78 week intervals, one immediately prior to the 2007-2008 credit crisis, another starting at the outset of the crisis, the third connecting the crisis and its early recovery. We used Ford CDS and US Treasury yield data, taking only Wednesday quotes in order to remove weekday effects.

1. Dataset 1 consisted of Wednesday midquote CDS swap spreads $\widehat{\text{CDS}}_{m,T}$ and their bid-ask spreads $w_{m,T}$ on dates $t_m = m/52, m = 1, \ldots, M$ for maturities $T \in \mathcal{T} := \{1, 2, 3, 4, 5, 7, 10\}$ years for Ford Motor Co., for the $M = 78$ consecutive Wednesdays from January 4th, 2006 to June 27, 2007, made available from

Bloomberg.

2. Dataset 2 consisted of Wednesday midquote CDS swap spreads $\widehat{\text{CDS}}_{m,T}$ and their bid-ask spreads $w_{m,T}$ on dates $t_m = m/52, m = M + 1, \ldots, 2M$ for maturities $T \in \mathcal{T} := \{1, 2, 3, 4, 5, 7, 10\}$ years for Ford Motor Co., for the $M = 78$ consecutive Wednesdays from July 11, 2007 to December 31, 2008, made available from Bloomberg.

3. Dataset 3 consisted of Wednesday midquote CDS swap spreads $\widehat{\text{CDS}}_{m,T}$ and their bid-ask spreads $w_{m,T}$ on dates $t_m = m/52, m = 2M + 1, \ldots, 3M$ for maturities $T \in \mathcal{T} := \{1, 2, 3, 4, 5, 7, 10\}$ years for Ford Motor Co., for the $M = 78$ consecutive Wednesdays from January 7th, 2009 to June 30, 2010, made available from Bloomberg.

4. The US treasury dataset[1] consisted of Wednesday yield curves (the "zero curve") on dates $t_m = m/52, m = 1, \ldots, 3M$, for maturities

$$T \in \tilde{\mathcal{T}} := \{1m, 3m, 6m, 1y, 2y, 3y, 5y, 7y, 10y, 20y, 30y\}$$

for the period January 4th, 2006 to June 30, 2010.

We note that Ford Motor Company experienced a large number of credit rating changes during this four-and-a-half year period. The history of Standard & Poors (S & P) ratings is as follows: BB+ to BB- on January 5, 2006; BB- to B+ on June 28, 2006; B+ to B on September 19, 2006; B to B- on July 31, 2008; B- to CCC+ on November 20, 2008. The downgrades continued into 2009, with a move from CCC+ to CC on March 4, 2009 and to SD ("structural default") on April 6, 2009. The latest news was good: on April 13, 2009, S & P raised Ford's rating back to CCC, on November 3, 2009 to B-, and on August 2, 2010 to B+, the highest since the onset of the credit crisis.

In hindsight we see that Ford never actually defaulted, although it came close. In the following estimation methodology, we consider the non-observation of default as an additional piece of information about the firm.

---

[1]Obtained from US Federal Reserve Bank, www.federalreserve.gov/datadownload

2.4 The TCBM Credit Setup

The time-changed Brownian motion credit framework of [57] starts with a filtered probability space $(\Omega, \mathcal{F}, \mathcal{F}_t, \mathbb{P})$, which is assumed to support a Brownian motion W and an independent increasing process G where the natural filtration $\mathcal{F}_t$ contains $\sigma\{G_u, W_v : u \leq t, v \leq G_t\}$ and satisfies the "usual conditions". $\mathbb{P}$ is taken to be the physical probability measure.

Assumptions 1.   *1. The log-leverage ratio of the firm, $X_t := log(V_t/K(t)) := x + \sigma W_{G_t} + \beta\sigma^2 G_t$ is a TCBM with parameters $x > 0, \sigma > 0$ and β. The time change G_t is characterized by its Laplace exponent $\psi(u, t) := -log\mathbb{E}[e^{-uG_t}]$ which is assumed to be known explicitly and has average speed normalized to 1 by the condition*

$$\lim_{t \to \infty} t^{-1}\partial\psi(0, t)/\partial u = 1.$$

2. The time of default of the firm is the first passage time of the second kind for the log-leverage ratio to hit zero (see the definition that follows). The recovery at default is modelled by the "recovery of treasury" mechanism[2] with constant recovery fraction $R \in [0, 1)$.

3. The family of default-free zero-coupon bond price processes $\{B_t(T), 0 \leq t \leq T < \infty\}$ is free of arbitrage and independent of the processes W and G.

4. There is a probability measure $\mathbb{Q}$, equivalent to $\mathbb{P}$ and called the risk-neutral measure, under which all discounted asset price processes are assumed to be martingales. Under $\mathbb{Q}$, the distribution of the time change G is unchanged while the Brownian motion W has constant drift.[3] We may write $X_t = x + \sigma W^Q_{G_t} + \beta_Q\sigma^2 G_t$ for some constant β_Q where $W^Q_u = W_u + \sigma(\beta - \beta_Q)u$ is driftless Brownian motion under $\mathbb{Q}$.

---

[2]See [69].

[3]This assumption can be justified by a particular version of the Girsanov theorem. It would be natural to allow the distribution of G to be different under $\mathbb{Q}$, but for simplicity we do not consider this possibility further here.

We recall the definitions from [57] of first passage times for a TCBM X_t starting at a point $X_0 = x \geq 0$ to hit zero.

Definition 1.   • *The standard definition of first passage time is the $\mathcal{F}$ stopping time*

$$t^{(1)} = \inf\{t | X_t \leq 0\} . \tag{2.1}$$

The corresponding stopped TCBM is $X_t^{(1)} = X_{t \wedge t^{(1)}}$. Note that in general $X_{t^{(1)}}^{(1)} \leq 0$.

• *The first passage time of the second kind is the $\mathcal{F}$ stopping time*

$$t^{(2)} = \inf\{t | G_t \geq t^*\} \tag{2.2}$$

where $t^* = \inf\{t | x + \sigma W_t + \beta \sigma^2 t \leq 0\}$. The corresponding stopped TCBM is

$$X_t^{(2)} = x + \sigma W_{G_t \wedge t^*} + \beta \sigma^2 (G_t \wedge t^*) \tag{2.3}$$

and we note that $X_{t^{(2)}}^{(2)} = 0$.

The general relation between $t^{(1)}$ and $t^{(2)}$ is studied in detail in [58] where it is shown how the probability distribution of $t^{(2)}$ can approximate that of $t^{(1)}$. For the remainder of this paper, however, we consider $t^{(2)}$ to be the definition of the time of default.

The following proposition[4], proved in [57], is the basis for computing credit derivatives in the TCBM modeling framework.

Proposition 1. *Suppose the firm's log-leverage ratio X_t is a TCBM with $\sigma > 0$ and that Assumptions 1 hold.*

1. *For any $t > 0, x \geq 0$ the risk-neutral survival probability $P^{(2)}(t, x) := \mathbb{E}_x[\mathbf{1}_{\{t^{(2)} > t\}}]$ is given by*

$$\frac{e^{-\beta x}}{\pi} \int_{-\infty}^{\infty} \frac{u \sin(ux)}{u^2 + \beta^2} e^{-\psi(\sigma^2(u^2 + \beta^2)/2, t)} du + (1 - e^{-2\beta x}) \mathbf{1}_{\{\beta > 0\}}, \tag{2.4}$$

---

[4]Equation (2.6) given in [57] only deals with the case $\beta < 0$. The proof of the extension for all β is available by contacting the authors.

The density for X_t conditioned on no default is

$$\rho(y; t, x) := \frac{d}{dy} \mathbb{E}_x[\mathbf{1}_{\{X_t \leq y\}} | t^{(2)} > t] \tag{2.5}$$

$$= P^{(2)}(t, x)^{-1} \mathbf{1}_{\{y>0\}} \frac{e^{\beta(y-x)}}{2\pi} \int_{\mathbb{R}} \left[e^{iu(y-x)} - e^{-iu(y+x)} \right] e^{-\psi(\sigma^2(u^2+\beta^2)/2, t)} du$$

The characteristic function for X_t conditioned on no default is

$$\mathbb{E}_x[e^{ikX_t} | t^{(2)} > t] = P^{(2)}(t, x)^{-1} \mathbb{E}_x[e^{ikX_t} \cdot \mathbf{1}_{\{t^{(2)}>t\}}] \tag{2.6}$$

$$= P^{(2)}(t, x)^{-1} \frac{e^{-\beta x}}{\pi} \int_{\mathbb{R}} \frac{u \sin(ux)}{(\beta + ik)^2 + u^2} e^{-\psi(\sigma^2(u^2+\beta^2)/2, t)} du$$

$$+ \left(e^{ikx} - e^{-ikx-2\beta x} \right) e^{-\psi(\sigma^2(k^2-2i\beta k)/2, t)} \left(\frac{1}{2} \mathbf{1}_{\{\beta=0\}} + \mathbf{1}_{\{\beta>0\}} \right)$$

2. *The time 0 price $\bar{B}^{RT}(T)$ of a defaultable zero coupon bond with maturity T and recovery of treasury with a fixed fraction R is*

$$\bar{B}^{RT}(T) = B(T)[P^{(2)}(T, x)) + R(1 - P^{(2)}(T, x))] \tag{2.7}$$

3. *The fair swap rate for a CDS contract with maturity $T = N\Delta t$, with premiums paid in arrears on dates $t_k = k\Delta t, k = 1, \ldots, N$, and the default payment of $(1 - R)$ paid at the end of the period when default occurs, is given by*

$$CDS(x, T) = \frac{(1 - R) \left[\sum_{k=1}^{N-1} [1 - P^{(2)}(t_k, x)][B(t_k) - B(t_{k+1})] + B(T)[1 - P^{(2)}(T, x)] \right]}{\Delta t \sum_{k=1}^{N} P^{(2)}(t_k, x) B(t_k)} \tag{2.8}$$

Remarks 2. • *We shall be using the above formulas in both measures $\mathbb{P}$ and $\mathbb{Q}$, as appropriate.*

• *We observe in (2.4) that the survival and default probabilities are invariant under the following joint rescaling of parameters*

$$(x, \sigma, \beta) \rightarrow (\lambda x, \lambda \sigma, \lambda^{-1} \beta), \text{ for any } \lambda > 0. \tag{2.9}$$

It follows that all pure credit derivative prices are invariant under this rescaling.

2.5   Two TCBM Credit Models

The two credit models we introduce here generalize the standard Black-Cox model that takes $X_t = x + \sigma W_t + \beta \sigma^2 t$. They are chosen to illustrate the flexibility inherent in our modeling approach. Many other specifications of the time change are certainly possible and remain to be studied in more detail. The following models are specified under the measure $\mathbb{P}$: by Assumption 1 they have the same form under the risk-neutral measure $\mathbb{Q}$, but with β replaced by β_Q.

2.5.1   The Variance Gamma Model

The VG credit model with its parameters $\theta = (\sigma, \beta, b, c, R)$ arises by taking G to be a gamma process with drift defined by the characteristic triple $(b, 0, \nu)_0$ with $b \in (0, 1)$ and jump measure $\nu(z) = ce^{-z/a}/z, a > 0$ on $(0, \infty)$. The Laplace exponent of G_t is

$$\psi^{VG}(u, t) := -\log E[e^{-uG_t}] = t[bu + c\log(1 + au)]. \tag{2.10}$$

and by choosing $a = \frac{1-b}{c}$ the average speed of the time change is $t^{-1}\partial \psi^{VG}(0, t)/\partial u = 1$. This model and the next both lead to a log-leverage process of Lévy type, that is, a process with identical independent increments that are infinitely divisible.

2.5.2   The Exponential Model

The EXP credit model with its parameters $\theta = (\sigma, \beta, b, c, R)$ arises taking by G to be a Lévy process with a characteristic triple $(b, 0, \nu)_0$ with $b \in (0, 1)$ and jump measure $\nu(z) = ce^{-z/a}/a, a > 0$ on $(0, \infty)$. The Laplace exponent of G_t is

$$\psi^{Exp}(u, t) := -\log E[e^{-uG_t}] = t\left[bu + \frac{acu}{1 + au}\right].$$

and by choosing $a = \frac{1-b}{c}$ the average speed of the time change is $t^{-1}\partial \psi^{VG}(0, t)/\partial u = 1$.

2.6 Numerical Integration

Statistical inference in these models requires a large number of evaluations of the integral formula (2.4) that must be done carefully to avoid dangerous errors and excessive computational costs. To this end, we approximate the integral by a discrete Fourier transform over the lattice

$$\Gamma = \{u(k) = -\bar{u} + k\eta | k = 0, 1, \ldots, N-1\}$$

for appropriate choices of $N, \eta, \bar{u} := N\eta/2$. It is convenient to take N to be a power of 2 and lattice spacing η such that truncation of the u-integrals to $[-\bar{u}, \bar{u}]$ and discretization leads to an acceptable error. If we choose initial values x_0 to lie on the reciprocal lattice with spacing $\eta^* = 2\pi/N\eta = \pi/\bar{u}$

$$\Gamma^* = \{x(\ell) = \ell\eta^* | \ell = 0, 1, \ldots, N-1\}$$

then the approximation is implementable as a fast Fourier transform (FFT):

$$
\begin{aligned}
P^{(2)}(t, x(\ell)) &\sim \frac{-i\eta e^{-\beta x(\ell)}}{\pi} \sum_{k=0}^{N-1} \frac{u(k)e^{iu(k)x(\ell)}}{u(k)^2 + \beta^2} \exp[-\psi(\sigma^2(u(k)^2 + \beta^2)/2, t)] \quad (2.11)\\
&= -i(-1)^n \eta e^{-\beta x(\ell)} \sum_{k=0}^{N-1} \frac{u(k)e^{2\pi i k\ell/N}}{u(k)^2 + \beta^2} \exp[-\psi(\sigma^2(u(k)^2 + \beta^2)/2, t)] \quad (2.12)
\end{aligned}
$$

Note that we have used the fact that $e^{-iN\eta x(\ell)/2} = (-1)^n$ for all $\ell \in \mathbb{Z}$.

The selection of suitable values for N and η in the above FFT approximation of (2.8) is determined via general error bounds proved in [70]. In rough terms, the pure truncation error, defined by taking $\eta \to 0, N \to \infty$ keeping $\bar{u} = N\eta/2$ fixed, can be made small if the integrand of (2.4) is small and decaying outside the square $[-\bar{u}, \bar{u}]$. Similarly, the pure discretization error, defined by taking $\bar{u} \to \infty, N \to \infty$ while keeping η fixed, can be made small if $e^{-|\beta|\bar{x}}P^{(2)}(\bar{x}, t)$, or more simply $e^{-|\beta|\bar{x}}$, is small, where $\bar{x} := \pi/\eta$. One expects that the combined truncation and discretization error will be small if $\bar{u}$ and $\eta = \pi/\bar{x}$ are each chosen as above. These error bounds for the FFT are more powerful than bounds one finds for generic integration by the trapezoid rule, and constitute one big advantage of the FFT. A second important

advantage of the FFT is its $O(N\log N)$ computational efficiency that yields $P^{(2)}$ on a lattice of x values with spacing $\eta^* = 2\pi/N\eta = \pi/\bar{u}$: this aspect will be very useful in estimation. These two advantages are offset by the problem that the FFT computes values for x only on a grid.

We now discuss choices for N and η in our two TCBM models. For $\beta < 0$, the survival function of the VG model is

$$P^{(2)}(0,t,x,\beta) = \frac{e^{-\beta x}}{\pi} \int_{-\infty}^{\infty} \exp[-tb\sigma^2(u^2+\beta^2)/2] \left(1 + \frac{a\sigma^2(u^2+\beta^2)}{2}\right)^{-ct} \frac{u\sin ux}{u^2+\beta^2} du$$

while for the EXP model

$$P^{(2)}(0,t,x,\beta) = \frac{e^{-\beta x}}{\pi} \int_{-\infty}^{\infty} \exp\left[-t\left(b\sigma^2(u^2+\beta^2)/2 + \frac{ac\sigma^2(u^2+\beta^2)}{2+a\sigma^2(u^2+\beta^2)}\right)\right] \frac{u\sin ux}{u^2+\beta^2} du$$

In both models, the truncation error has an upper bound ϵ when $\bar{u} > C|\Phi^{-1}(\epsilon C')|$, where Φ^{-1} is the inverse normal CDF and C, C' are constants depending on t. On the other hand, provided $\beta < 0$, the discretization error will be small (of order ϵ or smaller) if $N > \frac{\bar{u}}{2\pi|\beta|}\log\left(\epsilon^{-1}(1+\exp(-2\beta x))\right)$. Errors for (2.6) can be controlled similarly.

C (depending on t) and a normal CDF related to $\bar{u}$. The truncation error has an upper bound ϵ when $\bar{u} > \frac{-1}{\sqrt{A}}\Phi^{-1}(\frac{\epsilon\sqrt{A}}{2C\sqrt{2\pi}})$, where Φ^{-1} is the inverse normal CDF and A is another constant related to t. On the other hand, provided $\beta < 0$, the discretization error will be small (of order ϵ or smaller) if the number of discretization $N > \frac{\bar{u}}{2\pi|\beta|}\log(\frac{\epsilon}{1+exp(-2\beta x)})$. Similar error control can be conducted for (2.6).

2.7 The Statistical Method

The primary aim of this exercise is to demonstrate that our two TCBM credit models can be successfully and efficiently implemented to fit market CDS data on a single firm, in this case Ford Motor Company, and to compare these models' performance to the original Black-Cox structural model.

We were able to reduce the complexity of our models with negligible loss in accuracy by removing what appear to be two "nuisance parameters". First, we expect, and

it was observed, that parameter estimations were not very sensitive to β near $\beta = 0$, so we arbitrarily set $\beta = -0.5$. Secondly, we observed insensitivity to the parameter b and a tendency for it to drift slowly to zero under maximum likelihood iteration: since $b = 0$ is a singular limit, we set $b = 0.2$. Finally, in view of the rescaling invariance (2.9), and the interpretation of σ as the volatility of X, without loss of generality we set $\sigma = 0.3$ in all models. So specified, the two TCBM models have three free parameters $\Theta = (c, \beta_Q, R)$ as well as three frozen parameters $\sigma = 0.3, \beta = -0.5, b = 0.2$. The Black-Cox model with its free parameters $\Theta = (\beta_Q, R)$ and frozen parameters $\sigma = 0.3, \beta = -0.5$ then nests as the $c = 0$ limit inside both the VG and EXP models.

We summarize the modeling ingredients:

- an unobserved Markov process $X_t \in \mathbb{R}^d$;

- model parameters $\Theta \in D \subset \mathbb{R}^n$. We augment the vector $\Theta \to (\Theta, \eta)$ to include an additional measurement error parameter η;

- model formulas $F^k(X, \Theta)$ for $k = 1, \dots, K$, which in our case are theoretical CDS spreads given by (2.8) for $K = 7$ different tenors;

- a dataset consisting of spreads $Y := \{Y_t\}$ observed at times $t = 1, \dots, M$ where $Y_t = \{Y_t^k\}$ for a term structure of $k = 1, \dots, K$, plus their associated quoted bid/ask spreads w_t^k. We use notation $Y_{\leq t} := \{Y_1, \dots, Y_t\}$ and $Y_{<t} := \{Y_1, \dots, Y_{t-1}\}$ etc.

Since we do not attempt to estimate an underlying interest rate model, we treat the US Treasury dataset as giving us exact information about the term structure of interest rates, and hence the discount factors entering into (2.8). We treat the quoted bid/ask spreads w_t^k as a proxy for measurement error: these will simplify our treatment of the measurement equation. We also treat the non-default status of Ford on each date as an additional observation.

To complete the framework, an arbitrary Bayesian prior density of Θ is taken

$$\rho_0(\Theta) := e^{\mathcal{L}_0(\Theta)}.$$

with support on $D \subset \mathbb{R}^{n+1}$. The statistical method appropriate to a problem like this is thus some variant of a nonlinear Kalman filter, combined with maximum likelihood parameter estimation.

Based on these assumptions, it is rather natural to assume that observed credit spreads provide measurements of the hidden state vector X with independent gaussian errors. Moreover the measurement errors may be taken proportional to the observed bid/ask spread. Thus a natural measurement equation is

$$Y_t^k = F^k(X_t, \Theta) + \eta w_t^k \zeta_t^k \tag{2.13}$$

where ζ_t^k are independent standard gaussian random variables and η is a constant. In this case the full measurement density of Y would be

$$\mathcal{F}(Y|X,\Theta) = \prod_{t=1,\ldots,M} \prod_{k=1,\ldots,K} \left[\frac{1}{\sqrt{2\pi}\eta w_t^k} \exp\left(-\frac{(Y_t^k - F^k(X_t,\Theta))^2}{2\eta^2 (w_t^k)^2} \right) \right] \tag{2.14}$$

However, we observed an important deficiency that seems to arise in any scheme like this where the measurement equation involves a nonlinear function of an unobserved process X. This nonlinearity leads to nonconvexity in the log-likelihood function for X, which in turn can destabilize the parameter estimation procedure. For such reasons, we instead follow an alternative scheme that in our problem, and perhaps many others of this type, gives a great improvement in estimation efficiency. It works in our case because the model formula (2.8) for $F^k(x, \Theta)$, although nonlinear in x, is monotonic and approximately linear in x. We will call our scheme the "linearized measurement" scheme and it is justified as follows.

We define $G^k(Y, \Theta)$ to be the solution x of $Y = F^k(x, \Theta)$, and note that $f^k := \partial_x F^k > 0$. Then, provided ηw^k are small enough, we may linearize the x dependence of the measurement equation using the Taylor expansion

$$\begin{aligned} Y^k - F^k(x) &= Y^k - F^k(G^k(Y^k) + x - G^k(Y^k)) \\ &\approx Y^k - F^k(G^k(Y^k)) + f^k(G^k(Y^k))(G^k(Y^k) - x) \\ &= f^k(G^k(Y^k))(G^k(Y^k) - x) \end{aligned}$$

This equation above justifies the following alternative to the measurement equation

(2.13):

$$\tilde{X}_t^k = X_t + \eta \tilde{w}_t^k \xi_t^k \tag{2.15}$$

Now $\xi_t^k, k = 1, 2, \ldots, K, t = 1, 2, \ldots, M$ are iid $N(0,1)$ random variables and the transformed measurements are

$$\tilde{X}_t^k = \tilde{X}^k(Y_t^k, \Theta) := G^k(Y_t^k, \Theta).$$

Furthermore,

$$\tilde{w}_t^k = \tilde{w}_t^k(\tilde{X}_t^k, \Theta) = f^k(\tilde{X}_t^k, \Theta)^{-1} w_t^k.$$

Note that $\tilde{X}_t^k, k = 1, \ldots, K$ have the interpretation as independent direct measurements of the unobserved state value X_t.

The full measurement density of Y in our linearized measurement scheme is thus:

$$\mathcal{F}(Y|X, \Theta) := \prod_{t=1,\ldots,M} f(Y_t|X_t, \Theta) \tag{2.16}$$

$$f(Y_t|X_t, \Theta) := \prod_{k=1,\ldots,K} \left[\frac{1}{\sqrt{2\pi}\eta w_t^k} \exp\left(-\frac{(\tilde{X}_t^k(Y_t^k, \Theta) - X_t)^2}{2\eta^2 \tilde{w}_t^k(\Theta)^2} \right) \right] \tag{2.17}$$

where we have recombined denominator factors of $\tilde{w}^k$ with Jacobian factors $(f^k)^{-1}$. The multiperiod transition density conditioned on nondefault is

$$\mathcal{P}(X|\Theta, \text{no default}) = \prod_{t=2,\ldots,M} p(X_t|X_{t-1}, \Theta) \tag{2.18}$$

where $p(y|x, \Theta)$ is the one period conditional transition density given by (2.5) with $t = \Delta t$. Finally the full joint density for (X, Y, Θ) is

$$\rho(X, Y, \Theta) := \mathcal{F}(Y|X, \Theta)\mathcal{P}(X|\Theta)\rho_0(\Theta) \tag{2.19}$$

Integration over the hidden state variables X leads to the partial likelihood function, which can be defined through an iteration scheme:

$$\rho(Y, \Theta) = \int f(Y_M|X_M, \Theta)\rho(X_M, Y_{<M}, \Theta)dX_M \tag{2.20}$$

where for $t < M$

$$\rho(X_{t+1}, Y_{\leq t}, \Theta) = \begin{cases} \int p(X_{t+1}|X_t, \Theta) f(Y_t|X_t, \Theta)\rho(X_t, Y_{<t}, \Theta)dX_t, & t > 0 \\ \\ \rho_0(\Theta) & t = 0 \end{cases} \tag{2.21}$$

The following summarizes statistical inference within the linearized measurement scheme.

Statistical Inference using the Linearized Measurement Scheme: Let $(\hat{Y}, w) := \{\hat{Y}_t^k, w_t^k\}$ be the time series of CDS observations.

1. Maximum Likelihood Inference: The maximum likelihood parameter estimates $\widehat{\Theta}$ are the solutions of

$$\widehat{\Theta} = \text{argmax}_{\Theta \in D} \log\left(\rho(\hat{Y}, \Theta)/\rho_0(\Theta)\right) \tag{2.22}$$

where $\rho(\hat{Y}, \Theta)$ is given by (2.20). The log-likelihood achieved by this solution is

$$\widehat{\mathcal{L}} := \log\left(\rho(\hat{Y}, \widehat{\Theta})/\rho_0(\widehat{\Theta})\right),$$

and the Fisher information matrix is

$$\widehat{\mathcal{I}} := -\left[\partial_\Theta^2 \log\left(\rho(\hat{Y}, \widehat{\Theta})/\rho_0(\widehat{\Theta})\right)\right];$$

2. Filtered State Inference: The time series of filtered estimates of the state variables $X_1, \ldots, X_M$ are the solutions $\hat{X}_1, \ldots, \hat{X}_M$ of

$$\hat{X}_t = \text{argmax}_{x \in \mathbb{R}_+} \log\left(f(\hat{Y}_t|x, \widehat{\Theta})\rho(x, \hat{Y}_{\leq t-1}, \widehat{\Theta})\right) \tag{2.23}$$

2.8 Approximate Inference

The previous discussion on inference was exact, but computationally infeasible. Our aim now is to give a natural and simple approximation scheme that will be effective for the problem at hand. Our scheme is to inductively approximate the likelihood function $\rho(X_{t+1}, Y_{\leq t}, \Theta)$ defined by (2.21) by a truncated normal distribution through

matching of the first two moments. The truncation point of 0 is determined by the no default condition. The rationale is that the non-gaussian nature of the transition density p will have only a small effect when combined with the gaussian measurement density f. We expect our approximation to be appropriate for a firm like Ford that spent a substantial period near default. As we discuss at the end of this section, a simpler approximation is available that is applicable to a firm of high credit quality. The more complicated method we now describe is intended to be more robust when applied to firms of a range of credit qualities.

We describe a single step of the inductive computation of ρ given by (2.21). We fix t, denote the time t state variable as x and the time $t+1$ state variable as capital X. The length between t and $t+1$ is denoted as Δt. We also suppress $Y_{\leq t}$ and Θ. In this context, we are looking for $\bar{\mu}$ and $\bar{\sigma}$ that satisfy

$$\rho(X) \approx \frac{m_0 \phi\left(\frac{X-\bar{\mu}}{\bar{\sigma}}\right)}{\Phi\left(\frac{\bar{\mu}}{\bar{\sigma}}\right)}, X > 0 \tag{2.24}$$

where

$$m_0 = \int_0^\infty f(x)\tilde{\rho}(x)dx. \tag{2.25}$$

Here ϕ and Φ are probability density and cumulative distribution functions of the standard normal distribution and $\tilde{\rho}$ is carried over from the previous time step. The first two moments of the truncated normal distribution are straightforward to derive and are given here for completeness:

$$\begin{aligned} m_1^{trunc} &= \bar{\mu} + \bar{\sigma}\lambda(\alpha) \\ m_2^{trunc} &= \bar{\sigma}^2[1 - \delta(\alpha)] + (m_1^{trunc})^2 \end{aligned}$$

where $\alpha = -\frac{\bar{\mu}}{\bar{\sigma}}, \lambda(\alpha) = \frac{\phi(\alpha)}{1-\Phi(\alpha)}, \delta(\alpha) = \lambda(\alpha)[\lambda(\alpha) - \alpha]$. Note that the truncated normal distribution has a larger mean and smaller variance than the original normal distribution.

Using the Fubini theorem, the first two moments of the distribution $\rho(X)$ are:

$$\begin{aligned} m_1 &= m_0^{-1} \int_0^\infty g_1(x)f(x)\tilde{\rho}(x)dx \tag{2.26} \\ m_2 &= m_0^{-1} \int_0^\infty g_2(x)f(x)\tilde{\rho}(x)dx \end{aligned}$$

Here $g_1(x)$ and $g_2(x)$ are the first and second moments of X with respect to the transition density $p(X|x)$ and are given using (2.6) by

$$g_1(x) = \frac{1}{i}\partial_k|_{k=0}\mathbb{E}_x^P[e^{ikX}|t^{(2)} > \Delta t] \qquad (2.27)$$
$$g_2(x) = -\partial_k^2|_{k=0}\mathbb{E}_x^P[e^{ikX}|t^{(2)} > \Delta t]$$

Note that $\tilde{\rho}(x)$ has a gaussian kernel approximation by induction and the measurement density $f(x)$ is also gaussian. Their product gaussian kernel is then simply a scaled normal probability density function:

$$f(x)\tilde{\rho}(x) = \frac{m_0}{\sqrt{\bar{v}}\Phi(\bar{m}/\sqrt{\bar{v}})}\phi\left(\frac{x - \bar{m}}{\sqrt{\bar{v}}}\right) \qquad (2.28)$$

We also notice that the transition density $p(X|x)$ with a short period Δt resembles a Dirac δ function of X and fitting it to a polynomial would require very high order to guarantee accuracy in a local domain. In our method, by contrast, the moment functions $g_1(x)$ and $g_2(x)$ that appear in the integrals in (2.26) are much smoother functions of x and usually low order polynomials can approximate them quite accurately in a local domain. Take a normal transition density for example: $g_1(x)$ is linear in x and $g_2(x)$ is quadratic in x. Their counterparts for time changed Brownian motion conditional on no default can also be well approximated by low order polynomials in a local domain. We stress the word "local" because the product gaussian kernel $f\rho$ typically has a moderate variance $\bar{v}$ and relatively large mean $\bar{m}$: therefore the integrals in Equation (2.26) are dominated by a local domain $[\bar{m} - a\sqrt{\bar{v}}, \bar{m} + a\sqrt{\bar{v}}]$ with a safely taken to be 4. Thus we need to fit $g_1(x)$ and $g_2(x)$ over the interval $[\bar{m} - a\sqrt{\bar{v}}, \bar{m} + a\sqrt{\bar{v}}]$ which can be done quite accurately with quartic polynomials:

$$
\begin{aligned}
g_1(x) &= \Sigma_{k=0}^4 c_{1k}(x - \bar{m})^k \\
g_2(x) &= \Sigma_{k=0}^4 c_{2k}(x - \bar{m})^k.
\end{aligned}
\qquad (2.29)
$$

Equation (2.26) is now approximated by

$$
\begin{aligned}
m_1 &= \frac{1}{m_0\sqrt{\bar{v}}\Phi(\bar{m}/\sqrt{\bar{v}})}\int_0^\infty \Sigma_{k=0}^4 c_{1k}(x - \bar{m})^k \phi\left(\frac{x - \bar{m}}{\sqrt{\bar{v}}}\right)dx \\
m_2 &= \frac{1}{m_0\sqrt{\bar{v}}\Phi(\bar{m}/\sqrt{\bar{v}})}\int_0^\infty \Sigma_{k=0}^4 c_{2k}(x - \bar{m})^k \phi\left(\frac{x - \bar{m}}{\sqrt{\bar{v}}}\right)dx
\end{aligned}
$$

which can be evaluated analytically in terms of the error function. Matching m_1 and m_2 with m_1^{trunc} and m_2^{trunc} determines $\bar{\mu}$ and $\bar{\sigma}$ and completes the iteration scheme for (2.20).

Remarks 3.

- *In our numerical examples, we enlarge the integral domain in Equation (2.30) from $\mathbb{R}^+$ to $\mathbb{R}$ if $\bar{m} > 4\sqrt{\bar{v}}$, which leads to a simpler implementation. It turns out in our study that this condition is satisfied for all sampling periods.*

- *An alternative moment matching approximation is possible which approximates $\rho(X)$ by a regular normal distribution, rather than a truncated normal. Then the truncated density in Equation (2.24) should be replaced by the regular density $\phi\left(\frac{X-\bar{\mu}}{\bar{\sigma}}\right), X \in \mathbb{R}$. Although this approximation conflicts with the default barrier, for a firm that is far from default this does not introduce a serious numerical error. Moreover, this approximation leads to linear gaussian transition density and is thus a Kalman filter.*

Here we summarize the computation of $\rho(Y_{\leq M}, \Theta)$ for a fixed value of Θ:

1. Set $\rho_1 = \rho_0(\Theta)$;

2. Compute the measurement density $f(Y_1|X_1)$ (i.e. compute its mean and variance: this step requires efficient use of the FFT to invert the CDS spread formula);

3. For $t = 1 : M - 1$

    (a) Approximate $\rho(X_{t+1}, Y_{\leq t}, \Theta)$ given by (2.21) by a truncated normal density with mean and variance computed by matching moments. For this one uses the exact formula for the first two moments of the conditional transition density (2.5), and the assumed normal form of $f(Y_t|X_t)$ and $\rho(X_t, Y_{<t}, \Theta)$;

    (b) Compute the measurement density $f(Y_{t+1}|X_{t+1})$ (ie. compute its mean and variance, again with efficient use of FFT);

(c) End loop;

4. Finally compute $\rho(Y_{\leq M}, \Theta)$ by integrating X_M as in (2.20).

2.9 Numerical Implementation

From the considerations described in section 2.7 we fix $\beta = -0.5, \sigma = 0.3, b = 0.2$. We choose $\bar{u} = 300$ which controls the truncation error within 10^{-10}. Depending on Θ, we allowed the size of the FFT lattice, N, to vary from 2^8 to 2^{10}, keeping the discretization error within 10^{-10}. We use the Matlab function *fmincon* to implement the quasi-Newton method to maximize the likelihood function. Since *fmincon* also calculates the gradient and Hessian of the objective function, we also obtain standard errors of the parameter estimates.

Table 2.1 summarizes the estimation results for each of the three models, for the three datasets in 2006-2010, using our time series approximate inference. Estimated parameter values are given with standard errors, as well as summary statistics for the resulting filtered time series of X_t. We also present the root mean square error (RMSE) defined as the average error of the CDS spreads quoted in units of the bid/ask spread.

$$\text{RMSE} = \sqrt{\frac{1}{M \cdot K} \sum_{t=1}^{M} \sum_{k=1}^{K} \frac{\left(F^k(X_t, \Theta) - Y_t^k\right)^2}{(w_t^k)^2}}$$

Overall, the finite activity EXP model shares quite a few similarities with the infinite activity VG model, both in behavior and performance. For these two TCBM models, their model parameters are quite similar between dataset 1 and dataset 3 respectively. It is consistent with Ford's history of credit ratings that dataset 3 has lower, more volatile log-leverage ratios and lower recovery rate than dataset 1. We can also see that during the peak of the credit crisis in dataset 2, the estimated parameters show noticeable signs of stress. The mean time change jump size is up by approximately 50%, driven mainly by the increased short term default probability. The recovery rate is significantly lower. In the very stressed financial environment at that time, a firm's value would be greatly discounted and its capacity to liquidate

		Dataset 1	Dataset 2	Dataset 3
	number of weeks	78	78	78
	$\hat{\sigma}$	0.3	0.3	0.3
	$\hat{b}$	0.2	0.2	0.2
	$\hat{c}$	1.039(0.060)	0.451(0.034)	1.08(0.11)
	$\hat{\beta}_Q$	-1.50(0.12)	-0.879(0.061)	-1.368(0.066)
VG Model	$\hat{R}$	0.626(0.026)	0.450(0.029)	0.611(0.018)
	$\hat{\eta}$	1.53	0.897	1.797
	$\hat{x}_{av}$	0.693	0.457	0.480
	$\hat{x}_{std}$	0.200	0.239	0.267
	RMSE	1.43	0.837	1.792
	$\hat{\sigma}$	0.3	0.3	0.3
	$\hat{b}$	0.2	0.2	0.2
	$\hat{c}$	2.23(0.12)	1.17(0.07)	2.33(0.20)
	$\hat{\beta}_Q$	-1.44(0.12)	-0.780(0.060)	-1.286(0.067)
Exponential Model	$\hat{R}$	0.609(0.028)	0.395(0.033)	0.588(0.022)
	$\hat{\eta}$	1.503	0.882	1.775
	$\hat{x}_{av}$	0.702	0.479	0.486
	$\hat{x}_{std}$	0.199	0.242	0.266
	RMSE	1.41	0.821	1.763
	$\hat{\sigma}$	0.3	0.3	0.3
	$\hat{\beta}_Q$	-2.02(0.10)	-1.793(0.067)	-1.78(0.12)
	$\hat{R}$	0.773(0.011)	0.757(0.009)	0.760(0.013)
Black-Cox Model	$\hat{\eta}$	2.38	1.29	2.18
	$\hat{x}_{av}$	0.624	0.406	0.422
	$\hat{x}_{std}$	0.187	0.214	0.237
	RMSE	2.19	1.19	2.14

Table 2.1: Parameter estimation results and related statistics for the VG, EXP and Black-Cox models. $\hat{X}_t$ derived from (2.23) provide the estimate of the hidden state variables. The numbers in the brackets are standard errors. The estimation uses weekly (Wednesday) CDS data from January 4th 2006 to June 30 2010. $\hat{x}_{std}$ is the square root of the annualized quadratic variation of $\hat{X}_t$.

	VG	EXP	B-C
VG	0	-2.21/-1.41/-2.33	5.42/5.10/2.03
EXP	2.21/1.41/2.33	0	5.46/5.22/2.19
B-C	-5.42/-5.10/-2.03	-5.46/-5.22/-2.19	0

Table 2.2: Results of the Vuong test for the three models, for dataset 1, dataset 2 and dataset 3. A positive value larger than 1.65 indicates that the row model is more accurate than the column model with 95% confidence level.

assets would be limited. On the other hand the risk neutral drift β_Q is significantly higher, reflecting a certain positive expectation on the firm. At the peak of the credit crisis, Ford's annualized credit spreads exceeded 100%. The log-leverage ratios are much suppressed to a level of about 65% of that of dataset 1.

By definition, RMSE measures the deviation of the observed CDS spreads from the model CDS spreads while η measures the deviation of the "observed" log-leverage ratios $\tilde{X}_t$ from the "true" log-leverage ratios X_t. We can see that RMSE and η are very close in all cases, which implies that the objective functions based on the naive CDS measurement density (2.14) and the linearized measurement density (2.16) are fundamentally very similar.

In terms of RMSE and η, both TCBM models performed much better than the Black-Cox model. The TCBM fitting is typically within two times the bid/ask spread across 3 datasets, while the errors of the Black-Cox model are about 30% higher on average. Figure 2.1 shows that on three typical days, the TCBM models can fit the market CDS term structure curves reasonably well while the Black-Cox model, with its restrictive hump-shaped term structures, has difficulties for some tenors. To fit high short spreads, the log-leverage ratio is forced to unreasonably low levels. The TCBM models, with only one extra parameter than the Black-Cox model, generate more flexible shapes, and do a better job of fitting the data.

Figure 2.2 displays histograms of the signed relative error $(w_t^k)^{-1}\big(F^k(X_t, \Theta) - Y_t^k\big)$ for the three models, for the short and long end of the term structure. For both TCBM models we can see that most errors are bounded by ± 2 and are without obvious bias. By comparison, the errors of the Black-Cox model are highly biased downward in the

both the short and long terms. For 1-year spreads the majority of errors stay near -2 and for 10-year spreads there is a concentration of errors near -4. Surprisingly, all the three models perform better and more closely to one another during the crisis period of dataset 2. For the TCBM models, the great majority of errors are near 0 and without obvious bias. The Black-Cox model does not have obvious bias either, but there are more errors beyond the ± 2 range. The performance of all three models is better for intermediate tenors between 1 and 10 years, with the mid-range 5-year and 7-year tenors having the best fit. The histograms for these tenors (not shown) do still indicate that the TCBM models perform better than the Black-Cox model, in regard to both bias and absolute error.

The estimation results (not shown here) using the Kalman filter method described in Remarks 3 are very close to the results shown in Table 2.1, indicating that the transition density can be safely approximated by a gaussian density. The Kalman filter is convenient for calculating the weekly likelihood function, which is needed in the Vuong test [103], a test to compare the relative performance of nested models. If $\bar{X}_t$ and $\bar{P}_t$ denote the ex-ante forecast and variance of time t values of the measurement series obtained from Kalman filtering, the weekly log-likelihood function can be written as

$$l_t = -\frac{1}{2}\log|\bar{P}_t| - \frac{1}{2}(\tilde{X}_t - \bar{X}_t)^\top (\bar{P}_t)^{-1}(\tilde{X}_t - \bar{X}_t) - \sum_k f^k(\tilde{X}_t^k, \Theta). \qquad (2.30)$$

The log-likelihood ratio between two models i and j is

$$\lambda_{ij} = \sum_{t=1}^M (l_{it} - l_{jt})$$

and the Vuong test statistic is

$$\mathcal{T}_{ij} = \frac{\lambda_{ij}}{\hat{s}_{ij}\sqrt{M}},$$

where $\hat{s}_{ij}^2$ is the variance of $\{l_{it} - l_{jt}\}_{t=1,\dots,M}$. Vuong proved that $\mathcal{T}_{ij}$ is asymptotic to a standard normal under the null hypothesis that models i and j are equivalent in terms of likelihood function. Due to the serial correlation within the log-likelihood functions, Newey and West's estimator [90] is used for $\hat{s}$. The Vuong test results are shown in

Table 2.2 and confirm that the Black-Cox model is consistently outperformed by the two TCBM models. Moreover, by this test, the EXP model shows an appreciable improvement over the VG model that could not be easily observed in the previous comparison.

It is interesting to compare the time series of Ford stock prices to the filtered log-leverage ratios X_t. Fig 2.3 shows there is a strong correlation between these two quantities, indicating that the equity market and credit market are intrinsically connected. The empirical observations supporting this connection and thereafter financial modeling interpreting this connection can be found in [84], [26] and their references.

Finally, we mention that a stable model estimation over a 78 week period typically involved about 120 evaluations of the function $\rho(Y, \Theta)$, and took around one minute on a standard laptop.

2.10 Conclusions

In this paper, we demonstrated that the Black-Cox first passage model can be efficiently extended to a very broad class of firm value processes that includes exponential Lévy processes. We tested the fit of two realizations of Lévy subordinated Brownian motion models to observed CDS spreads for Ford Motor Co., a representative firm with an interesting credit history in recent years. We found that the two Lévy process models can be implemented very easily, and give similarly good performance in spite of the very different characteristics of their jump measures. With one extra parameter, both models outperform the Black-Cox model in fitting the time series of CDS term structures over 1.5 year periods. However, they still have limitations in fitting all tenors of the CDS term structure, suggesting that further study is needed into models with more flexible time changes.

We also proposed a new method for filtered statistical inference, based on what we call the linearized measurement equation. This new method inductively creates "quasi-gaussian" likelihood functions that can be approximated either as truncated gaussians, or as true gaussians in which case we are lead to a Kalman filter. By their
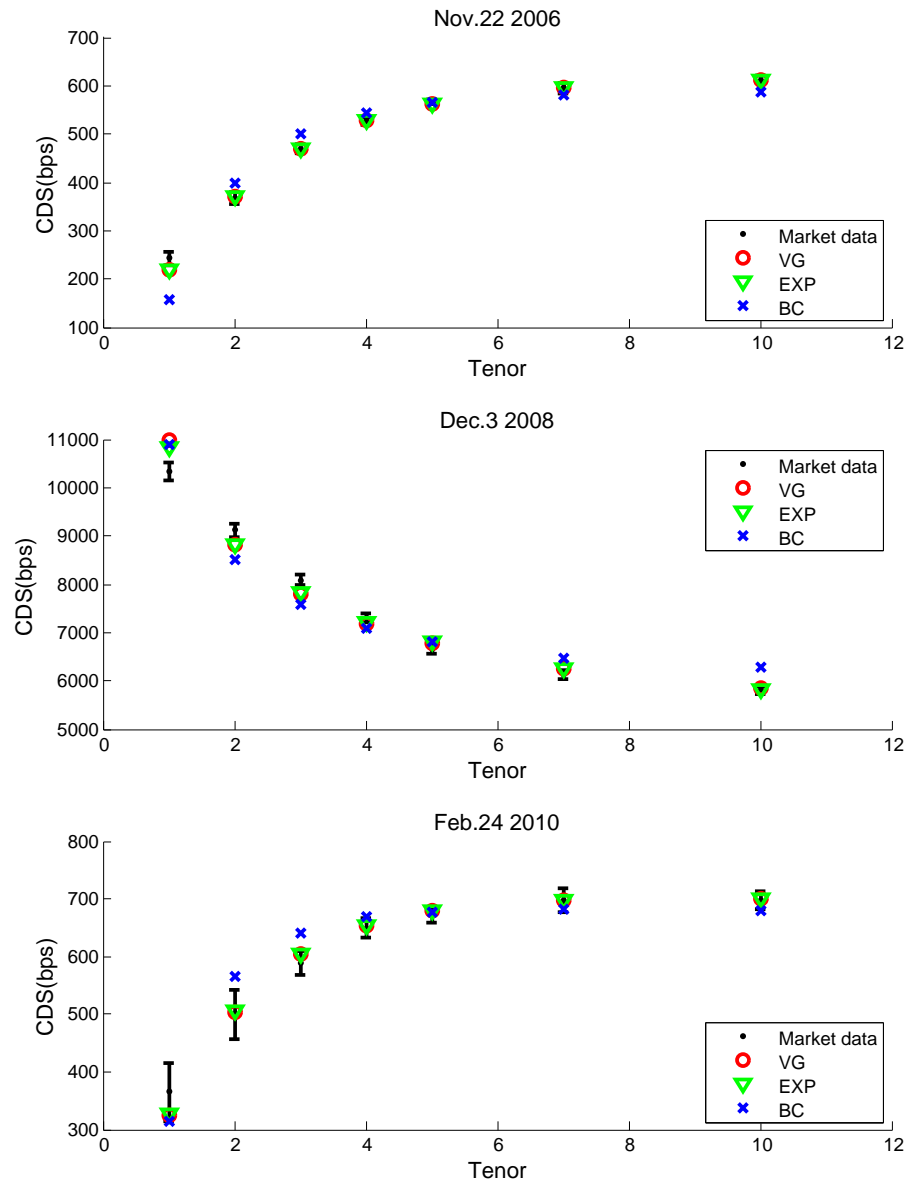
Figure 2.1: The in-sample fit of the two TCBM models and Black-Cox model to the observed Ford CDS term structure for November 22, 2006 (top), December 3, 2008 (middle) and February 24, 2010 (bottom). The error bars are centered at the mid-quote and indicate the size of the bid-ask spread.
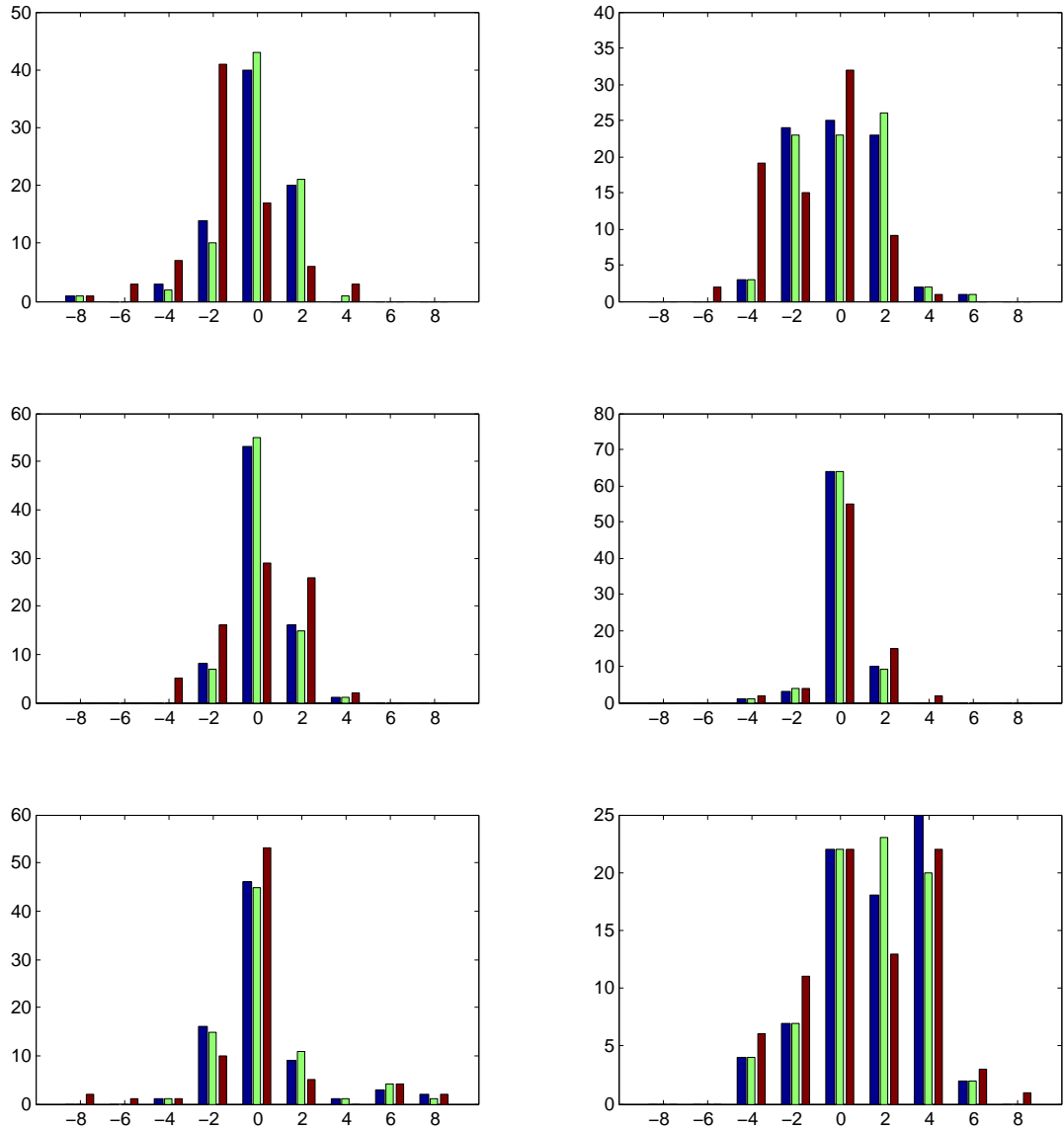
Figure 2.2: Histograms of the relative errors, in units of bid-ask spread, of the in-sample fit for the VG model (blue bars), EXP model (green bars) and Black-Cox model (red bars) for dataset 1 (top), dataset 2 (middle) and dataset 3 (bottom). The tenor on the left is 1-year and on the right, 10-year.
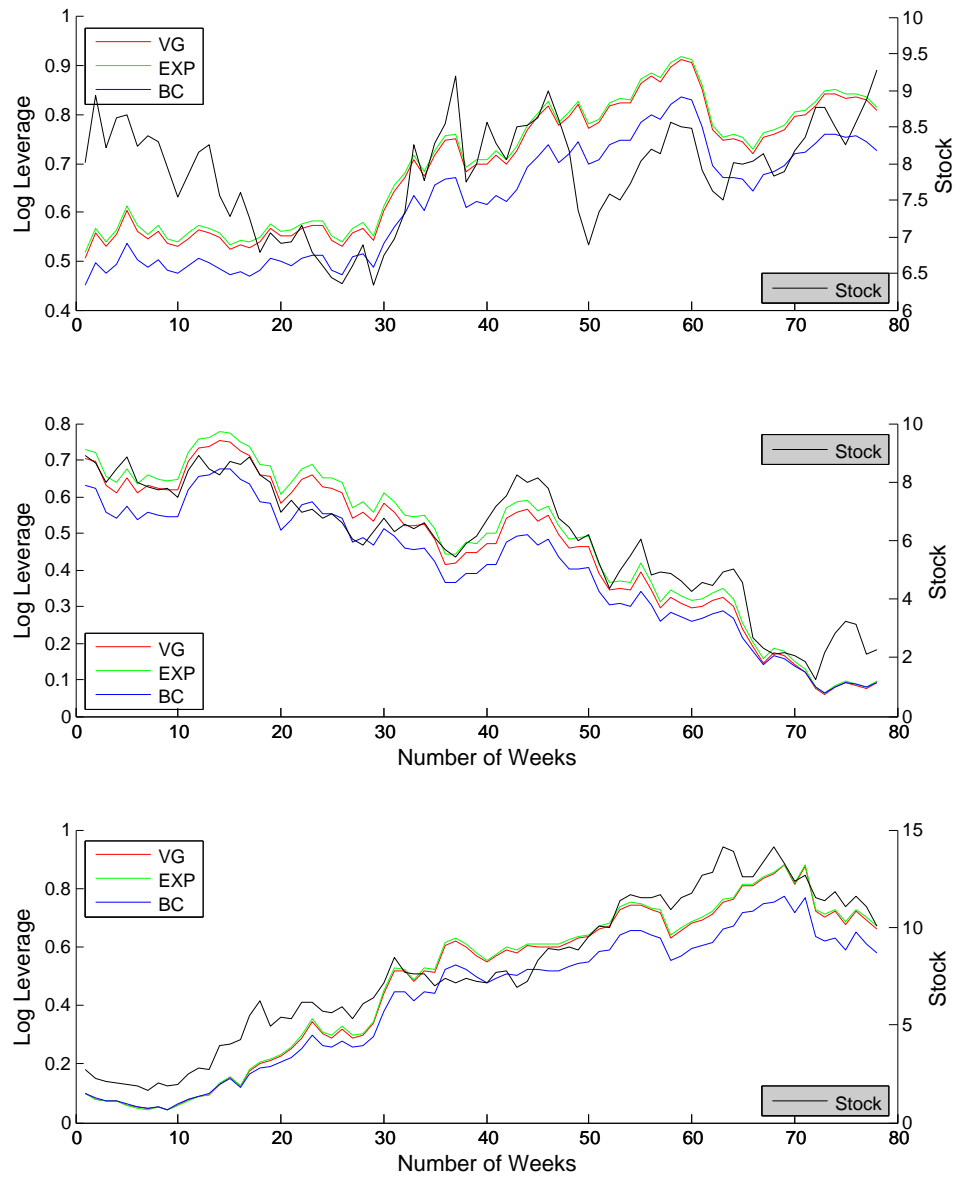
Figure 2.3: Filtered values of the unobserved log-leverage ratios X_t versus stock price for Ford for dataset 1(top), 2 (middle) and 3 (bottom).

strategic use of the fast Fourier transform, both of our two approximation methods turn out to be very efficient: parameter estimation for a time series of term structures for 78 weeks can be computed in about a minute. Finally, we observe a strong correlation between Ford's stock price and the filtered values of its unobserved log-leverage ratios. This final observation provides the motivation for our future research that will extend these TCBM credit models to TCBM models for the joint dynamics of credit and equity.

2.11   Additional Material

This section briefly describes three extensions not discussed in the original paper. The first is called the self-exciting affine (SEA) model and is an example of TCBM credit models with stochastic volatility. The second extension is to include further evidence of the improvement of the VG and EXP models over the BC model. The third extension shows that the transition PDF in these models can be replaced by a Gaussian approximation without significantly degrading the fit and enabling the use of a standard Kalman filter for estimation.

We introduce the self-exciting affine (SEA) model whose time change activity rate follows a mean reverting process with one sided pure Lévy jumps, termed background driving Lévy processes (BDLP) by Barndorff-Nielson and Shephard [4]. Thus we take the time change with an absolutely continuous part and a pure jump part:

$$dG_t = \lambda_t dt + m dJ_t,$$
$$d\lambda_t = -b\lambda_t dt + dJ_t$$

where J is the nondecreasing pure jump Lévy diffusion with an exponential Lévy measure $\nu(dx) = ace^{-ax}dx$ and Laplace exponent

$$\psi^{SEA}(u,t) := -\log(E[e^{-uJ_t}]) = t[\int_{\mathbb{R}^+}[1 - e^{-ux}]ace^{-ax}dx]$$

We impose the condition that the long term average speed of the time change is 1 by taking

$$\frac{c(mb+1)}{ab} = 1.$$

Proposition 2. *The Laplace exponent* $\psi(u;t,\lambda) = -logE_\lambda[e^{-uG_t}]$ *is given by*

$$\psi(u;t,\lambda) = \exp[A(u,t) + B(u,t)\lambda] \tag{2.31}$$

where

$$
\begin{aligned}
A(u,t) &= log\left[\left(1 - \frac{B(u,t)}{a+um}\right)^\alpha \left(1 + \frac{bB(u,t)}{u}\right)^\gamma\right] \\
B(u,t) &= -\frac{u}{b}(1 - e^{-bt}).
\end{aligned}
$$

where

$$\alpha = \frac{ac}{ab + u(mb+1)}, \;\; \gamma = \frac{cu(m+1/b)}{ab + u(mb+1)} \tag{2.32}$$

Thus our version is parsimonious, with 5 parameters $\theta = (\beta, \sigma, b, c, m, R)$. Moreover, the time change has a state variable λ.

The extra power of the SEA model over VG and EXP is mainly three-fold. First of all, VG and EXP have independent and identically distributed (IID) increments, which determines that one log leverage ratio value has an invariant CDS term structure. This characteristic for general Lévy processes also make them inadequate to price options across maturities as well as strikes [67]. The two-factor nature of the SEA model determines that fixing the log leverage ratio alone does not fully capture the CDS term structure, rather, a second source of randomness, the activity rate can still add degree of freedom to it. In [20] some inhomogenous Lévy processes (called Sato process herein) have been shown to successfully calibrate options. So the SEA model is expected to attain even better performance. Second of all, VG and EXP models exhibit constant volatility for the log leverage ratio. SEA model is a stochastic volatility model which captures the volatility clustering effect, an observation frequently seen in equity market and likely seen for log leverage ratios. Third of all, the SEA model also incorporates a simple self-exciting effect ("contagion"). This effect is intended to mimic the observation that when a shock hits the credit market, spreads rise and some clustering of defaults might occur. In SEA model, a shock (*i.e.* a jump) causes both an increase in the volatility (hence a rise in spreads) and an increased likelihood of defaults at that instant.

Beyond SEA model and TCBM one can consider the more sophisticated time changed Lévy processes [25] usually used in option pricing. While these models provide broader generality, their first passage time of second kind may not have explicit density function and their transition density function is also less tractable.

In section 2.9 we mention that the performance of all three models is better for intermediate tenors between 1 and 10 years, with the mid-range 5-year and 7-year tenors having the best fit. Here we supplement the histograms for tenors of 3-year, 4-year, 5-year and 7-year in Figure 2.4 and 2.5. The histograms do still indicate that the TCBM models perform better than the Black-Cox model, in regard to both bias and absolute error. We also mention that the estimation results using the Kalman filter method described in Remarks 3 are very close to the results shown in Table 2.1, indicating that the transition density can be safely approximated by a gaussian density. Here we present the estimation results using the Kalman filter in Table 2.3 to verify our points.
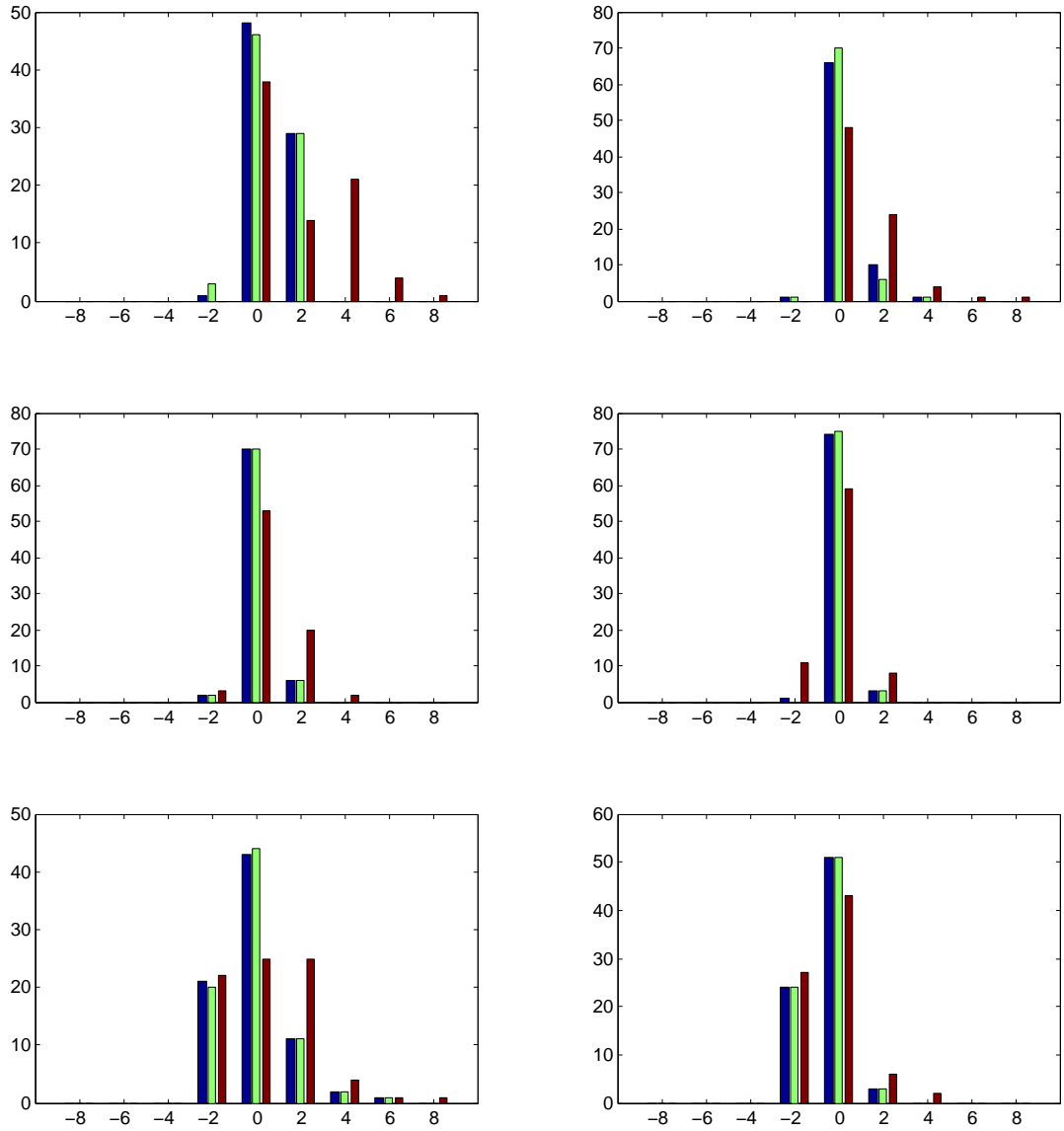
Figure 2.4: Histograms of the relative errors, in units of bid-ask spread, of the in-sample fit for the VG model (blue bars), EXP model (green bars) and Black-Cox model (red bars) for dataset 1 (top), dataset 2 (middle) and dataset 3 (bottom). The tenor on the left is 3-year and on the right, 4-year.
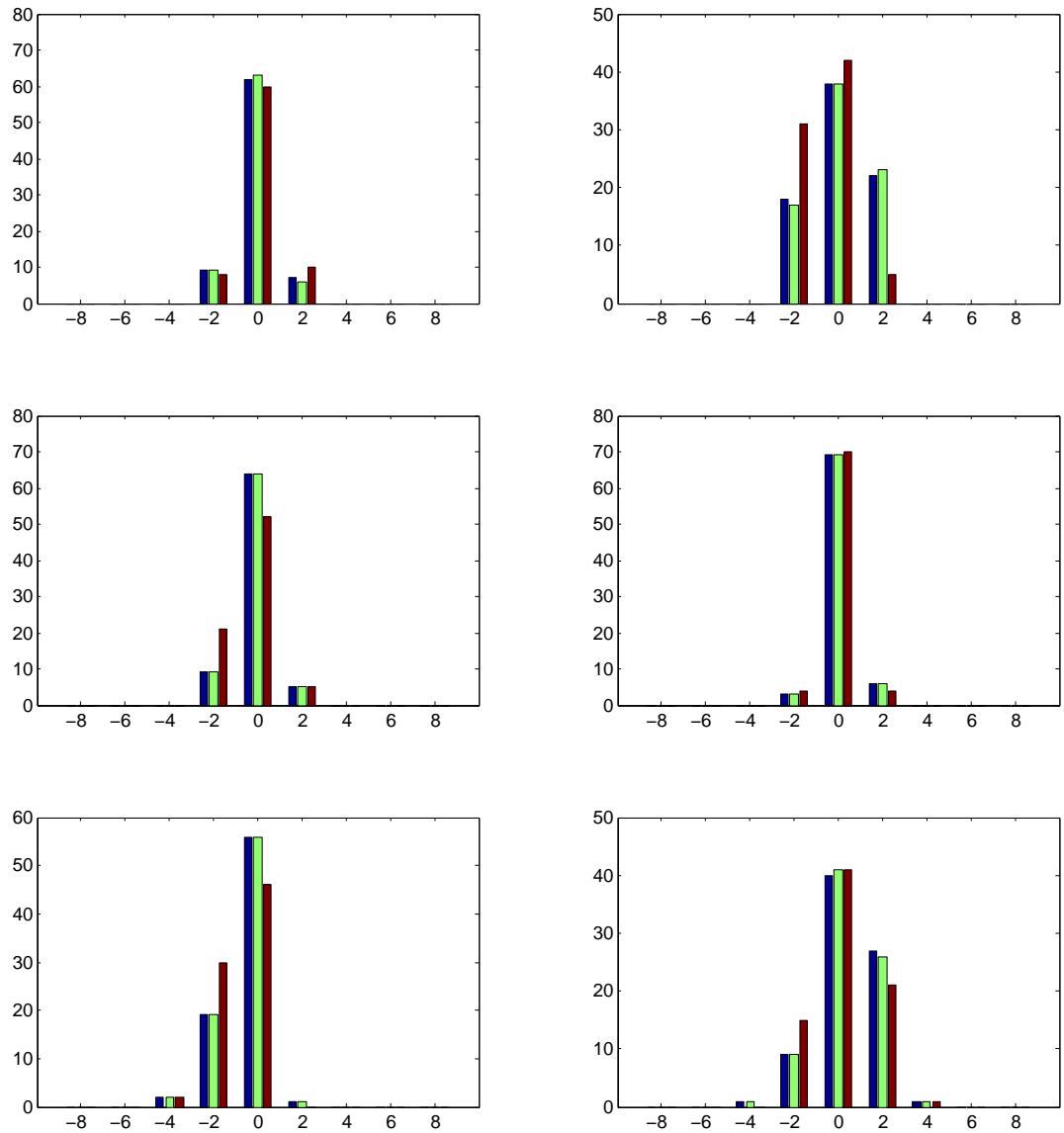
Figure 2.5: Histograms of the relative errors, in units of bid-ask spread, of the in-sample fit for the VG model (blue bars), EXP model (green bars) and Black-Cox model (red bars) for dataset 1 (top), dataset 2 (middle) and dataset 3 (bottom). The tenor on the left is 5-year and on the right, 7-year.

		Dataset 1	Dataset 2	Dataset 3
	number of weeks	78	78	78
	$\hat{\sigma}$	0.3	0.3	0.3
	$\hat{b}$	0.2	0.2	0.2
	$\hat{c}$	1.033(0.056)	0.434(0.033)	1.08(0.11)
	$\hat{\beta}$	-1.49(0.11)	-0.865(0.058)	-1.388(0.071)
VG Model	$\hat{R}$	0.624(0.026)	0.452(0.027)	0.616(0.020)
	$\hat{\eta}$	1.516	0.849	1.806
	$\hat{x}_{av}$	0.695	0.452	0.480
	$\hat{x}_{std}$	0.200	0.237	0.267
	RMSE	1.43	0.844	1.791
	$\hat{\sigma}$	0.3	0.3	0.3
	$\hat{b}$	0.2	0.2	0.2
	$\hat{c}$	2.23(0.11)	1.14(0.06)	2.34(0.19)
	$\hat{\beta}$	-1.43(0.12)	-0.765(0.056)	-1.307(0.068)
Exponential Model	$\hat{R}$	0.606(0.029)	0.397(0.031)	0.594(0.022)
	$\hat{\eta}$	1.492	0.835	1.783
	$\hat{x}_{av}$	0.704	0.474	0.485
	$\hat{x}_{std}$	0.199	0.241	0.266
	RMSE	1.409	0.827	1.762
	$\hat{\sigma}$	0.3	0.3	0.3
	$\hat{\beta}$	-2.02(0.10)	-1.789(0.064)	-1.799(0.082)
	$\hat{R}$	0.773(0.011)	0.759(0.009)	0.762(0.011)
Black-Cox Model	$\hat{\eta}$	2.39	1.24	2.19
	$\hat{x}_{av}$	0.624	0.402	0.422
	$\hat{x}_{std}$	0.187	0.213	0.237
	RMSE	2.19	1.20	2.14

Table 2.3: Parameter estimation results and related statistics for the VG, EXP and Black-Cox models using the likelihood function (2.30) in Kalman filter. The numbers in the brackets are standard errors. The calibration uses weekly (Wednesday) CDS data from January 4th 2006 to June 30 2010. $\hat{x}_{std}$ is the square root of the annualized quadratic variation of $\hat{X}_t$.

Chapter 3

Two-Factor Capital Structure Models for Equity and Credit

This chapter is originated from a paper coauthored with Professor Hurd [61], to which the author of the thesis is an equal contributor. It should be noted that the references of the chapter are indexed to adapt to the thesis, therefore differ from the original paper.

3.1 Abstract

We extend the now classic structural credit modeling approach of Black and Cox to a class of "two-factor" models that unify equity securities (such as options written on the stock price), and credit products like bonds and credit default swaps (CDS). Our "hybrid" models are capable of reproducing the main features of well known equity models such as the variance gamma model, at the same time reproducing the stylized facts about default stemming from structural models of credit risk. Moreover, in contrast to one-factor structural models, they allow for much more flexible dependencies between equity and credit markets. Two main technical obstacles are overcome in our paper. The first obstacle stems from the barrier condition implied by the non-default of the firm, and is overcome by the idea of time-changing Brownian motion in a way that preserves the reflection principle for Brownian motion. The

second obstacle is the difficulty of computing spread options: this was overcome by recent papers that make efficient use of the two dimensional Fast Fourier Transform.

3.2   Introduction

Merton [86], Black and Cox [10], and other pioneering researchers in credit risk well understood that dynamics of a firm's equity and debt should be modeled jointly and that credit derivatives and equity derivatives are linked inextricably. To this day, however, it has proved difficult to capture the dynamical essence of these two aspects of a firm's capitalization. The papers by Leland [72] and Leland and Toft [73] provide a conceptual basis, but they remain strongly attached to the framework of diffusion processes and have a one dimensional source of randomness .

The above structural models can all be classified as one-factor models with the asset process as the only underlying source of randomness. Such models have the severe limitation that the firm's equity and debt are perfectly correlated (*i.e.* they are related by a deterministic function), while it is clear in real life that firms, to a greater or lesser extent, have stochastic liabilities that are not perfectly correlated with assets. As an extreme illustration, hedge funds, with their long/short positions, typically have liabilities as volatile as their assets. Thus the fact is clear that to accurately model capital structure, a stochastic factor process of dimension at least two is necessary. In the context of continuous time finance, the technical and computational challenges implied by this fact have not yet been satisfactorily addressed, and these challenges are the main focus of the present paper. Only a few authors have been able to make substantial headway in modeling actual observed capital structures by two factor models. Benos and Papanastasopouls [6] have extended the Merton model by modeling the asset and default barrier of a firm as independent geometric Brownian motion. They found that their model systematically outperformed the Merton model in both in-sample fitting of credit ratings and out-of-sample predictability of defaults. Eberlein and Madan [41], in a recent working paper, have treated firm asset and liabilities as imperfectly correlated processes. Equity equals the asset/liability spread, and they use this fact to calibrate both the asset and liability values from the

observations of a firm's implied equity volatility surface.

A second deficiency in the standard structural framework is the reliance on diffusion processes, with the consequence that default events are predictable and so instantaneous default is either certain or impossible [97]. Thus in such models the short spreads are either infinity or zero, counter to the fact that short spreads are observed to be positive even for investment grade firms. The natural way to overcome this deficiency is to introduce jumps into the asset process. A number of authors, notably [5],[16], have successfully implemented jump diffusion and pure jump versions of the Merton model. However they share that model's unrealistically simple debt structure. Similar extensions to the Black-Cox first passage framework, however, have had only a limited success, due to the technical difficulty of solving the first passage problem for jump processes. The Kou-Wang model [68] with exponentially distributed jumps was able to work because of the special nature of the underlying process.

This difficulty with predictable defaults was the original motivation for replacing structural models by reduced form models [64] and incomplete information models [38]. Recently, a class of "hybrid" reduced form models that include the stock price and a default hazard process have been developed. These model equity and debt products more realistically by allowing the stock price to jump to zero at the time of default. Carr and Wu [26] take a stochastic volatility model for the stock price and assume that the default arrival rate is driven by the volatility and another independent credit risk factor. In Carr and Linetsky [22], the stock price has a local volatility with constant elasticity of variance, and the default intensity is specified as an affine function of the instantaneous variance of the stock. [84] obtain even more generality while retaining analytic tractability by applying a time change to the hazard rate and stock price processes. All three frameworks are able to capture the so called leverage effect and the co-movement between volatility and default intensity.

Within the structural credit modeling framework, [57] generalizes the Black-Cox model by treating the log-leverage ratio $X_t := \log V_t / K(t)$ as a time-changed Brownian motion (TCBM), where $e^{-rt} V_t := e^{v_t}$ denotes the (per-share) firm asset value process discounted at a constant rate r and $K(t)$ is a deterministic default threshold.

The time of default is the first passage time for the log-leverage ratio to cross zero. Like other structural approaches along these lines, this model cures the inconsistency with observed short spreads and adds the flexibility to include jumps to default and volatility clustering. One contribution of the TCBM approach in [57] lies in an innovative mathematical treatment of the first passage to default that allows the reflection principle and corresponding first passage formulas for Brownian motion to extend to a broader class of processes, leading to analytical tractability in a more general setting.

The object of the present paper is demonstrate how to embed the Black-Cox framework in a simple way into a two-factor framework that allows the firm's equity and debt to be partially correlated while retaining tractability of the underlying default model. We do this by treating the default threshold K as a positive stochastic process $D_t := e^{rt+d_t}$ that we can think of as the market value of the firm's liabilities, per share. Put another way, we treat the firm's debt or liability as a new stochastic process, not fully correlated with the asset process V_t. If we consider as well the stock price S_t (assuming the number of shares is constant and the firm pays no dividends) and the log-leverage X_t, then a minimal set of additional assumptions for combining these processes is:

Assumption 1. *The pre-default dynamics of any two of the four processes V_t, D_t, S_t, X_t is Markovian and time-homogeneous, and determines the dynamics of the remaining two processes by the equations*

$$S_t = V_t - D_t, \quad X_t = log V_t/D_t. \tag{3.1}$$

We assume that the discounted processes $e^{-rt}V_t, e^{-rt}D_t, e^{-rt}S_t$ are martingales under some risk neutral measure $\mathbb{Q}$, and the interest rate r is constant[1]. The time of default is

$$t^* = \inf\{t|X_t \le 0\} = \inf\{t|S_t = 0\}, \tag{3.2}$$

and after default $X_t = S_t = 0$. At the time of default, all securities are assumed to be valued in terms of a "recovery" random variable R.

---

[1]While the arbitrage pricing theory requires only that $e^{-rt}S_t$ be a martingale, we make a stronger assumption to simplify the framework.

In this paper, we will make additional restrictive assumptions on the form of V, D, S, X to obtain a workable tractable framework. Under these restrictions, the pure credit dynamics of two factor models with a constant recovery rate will be consistent with the TCBM credit framework of [57]. In [60] good calibrations of such credit models to a large dataset of CDS spreads for Ford Motor Company were obtained, thus verifying the quality of the framework as a model for credit risk. In addition our two-factor models price equity options as barrier spread options on V, D. Thus option pricing in two factor models faces the type of computational challenges for spread options that have been studied in such papers as [32], [17] and [59]. We are able to use the TCBM structure and properties of Brownian motion to develop an efficient equity option pricing algorithm that uses a two dimensional Fast Fourier Transform (FFT). Such a fast algorithm is needed not just in the forward direction for security pricing, but more importantly to solve the "inverse problem" that arises in calibration to a dataset of observed security prices. In this paper, because we have efficient pricing of the basic securities to be used in the calibration, we are able to demonstrate the feasibility of efficient statistical estimation of two factor models to a dataset of CDS curves and implied equity volatility surfaces.

The above assumptions on the firm's capital structure can only be valid for a period $[0, T]$ over which the firm pays no dividends or debt coupons, and does not issue new shares or debt. A consistent firm model that incorporates such real world features will also be of interest for future research.

This paper will discuss several implementations of the two-factor framework where S, D and V are discounted martingales. In all these implementations, we are able to overcome the two technical obstacles, namely the treatment of the first passage to default and the efficient computation of spread options. In section 2 and section 3 we investigate the case where V_t and D_t are correlated geometric Brownian motions (GBMs). The resultant default model extends the Black-Cox model and shares its known shortcomings, such as zero short spreads. As well it tends to generate rather unrealistic implied volatility surfaces. Therefore in section 4 we allow V_t and D_t to be Lévy subordinated Brownian motions (LSBMs) driven by a single time change, in this case either a gamma process or a process with exponential distributed jumps.

We investigate some of the possible shapes of both the CDS curve and the implied vol surface. In section 5, we investigate how to calibrate such models to market CDS and implied vol data on a single date. We then exhibit the results of a simple calibration of the GBM and LSBM models to data for a typical default risky firm, Ford Motor Company. Finally, section 6 offers a summary and some directions for future exploration.

3.3   Risk-Neutral Security Valuation

As we have explained, the firm's capitalization is modeled by the four processes V_t, D_t, X_t, S_t satisfying Assumption (3.1), and default t^* is the first time $V_t \leq D_t$, or equivalently when $S_t = 0$. We work in a risk-neutral filtered probability space $(\Omega, \mathcal{F}, (\mathcal{F}_t)_{t \geq 0}, \mathbb{Q})$, where V_t, D_t, X_t, S_t are adapted to the filtration $\mathcal{F}_t$ and t^* is an $\mathcal{F}_t$ stopping time. If $\mathcal{G}_t \subset \mathcal{F}_t$ denotes the "market filtration", note that the stock price S_t is $\mathcal{G}_t$ measurable, whereas X, V and D are not. In practice X_t, V_t, D_t must be inferred from the prices of securities trading on the firm, and possibly its quarterly balance sheets.

In this section, we demonstrate that the price of basic credit and equity derivatives can be reduced to computations involving the joint characteristic function of $Y_t := [v_T, d_T]$ conditioned on non-default at time T:

$$\Phi_{ND}(u_1, u_2; T; v_0, d_0) := \mathbb{E}^{\mathbb{Q}}_{v_0, d_0}[e^{i(u_1 v_T + u_2 d_T)} \mathbf{1}_{\{t^* > T\}}] \tag{3.3}$$

As a special case, note that the probability of no default at time T is:

$$P(T; v_0, d_0) = \Phi_{ND}(0, 0; T; v_0, d_0) = \mathbb{E}^{\mathbb{Q}}_{v_0, d_0}[\mathbf{1}_{\{t^* > T\}}] \tag{3.4}$$

The reader can anticipate that in subsequent sections, we will introduce a number of models of dynamics where a generalized reflection principle holds and implies that computations involving Φ_{ND} can be reduced to computations involving the unconstrained characteristic function

$$\Phi(u_1, u_2; T; v_0, d_0) := \mathbb{E}^{\mathbb{Q}}_{v_0, d_0}[e^{i(u_1 v_T + u_2 d_T)}] \tag{3.5}$$

Moreover, our models will have a common property on Y_t:

Assumption 2. *For any $t > 0$, the increment $Y_t - Y_0$ is independent of Y_0.*

This implies that the characteristic function Φ of Y_T factorizes[2]:

$$\mathbb{E}_{T_0}[e^{iuY_T'}] = e^{iuY_0'}\Phi(u;T), \quad \Phi(u;T) := \mathbb{E}_{Y_0}[e^{iu(Y_T - Y_0)'}] . \tag{3.6}$$

where $\Phi(u;T)$ is independent of Y_0. Thus, in the more specialized setting we have in mind, pricing of all important derivatives will be reduced to computation of explicit low dimensional integrals.

3.3.1   Defaultable Bonds and Credit Default Swaps

At any time t prior to default t^*, we consider the value of a zero coupon bond that pays \$1 at maturity T if the firm is solvent. In the event that $t^* < T$, it might be reasonable to suppose that the recovery value of the bond will be dependent on D_{t^*}. However, to avoid a detailed analysis of stochastic recovery modeling, we make a mathematically simple but economically arguable hypothesis:

Assumption 3. *The recovery value of a zero coupon bond with maturity T, at the time of default $t^* < T$ is a constant $R \in [0,1)$.*

This assumption is analogous to the recovery of par mechanism often made in credit risk modeling, and it shares some of its limitations. Then one has the risk-neutral valuation formula for the pre-default price $B_t(T)$ at time t of the maturity T zero coupon bond:

$$B_t(T) = \mathbb{E}^{\mathbb{Q}}_{v_0,d_0}\left[e^{-r(T-t)}\mathbf{1}_{\{t^*>T\}} + R\mathbf{1}_{\{t<t^*\leq T\}}e^{-r(t^*-t)}|\mathcal{F}_t\right] \tag{3.7}$$

which leads to:

Proposition 3.   *1. The pre-default price at time t of a zero coupon bond with maturity T with recovery of par is given by*

$$B_t(T) = e^{-r(T-t)}P(T - t; v_t, d_t) + Re^{-r(T-t)}(1 - P(T - t; v_t, d_t)) \tag{3.8}$$

---

[2]Here and subsequently we adopt matrix notation $u = [u_1, u_2]$, $Y_t = [v_t, d_t]$, and in particular Y' denotes the transpose of Y.

2. *The fair swap rate for a CDS contract with maturity $T = N\Delta t$, with premiums paid in arrears on dates $t_k = k\Delta t, k = 1, \ldots, N$, and the default payment of $(1 - R)$ paid at the end of the period when default occurs, is given by*

$$CDS(T; v_0, d_0) = \frac{(1 - R)\left[\sum_{k=1}^{N-1}[1 - P(t_k; v_0, d_0)][e^{-rt_k} - e^{-rt_{k+1}}] + e^{-rT}[1 - P(T; v_0, d_0)]\right]}{\Delta t \sum_{k=1}^{N} P(t_k; v_0, d_0)e^{-rt_k}}$$

3.3.2 Equity Derivatives

We have assumed that $S_t = 0$ for all $t \geq t^*$. This is a plausible idealization of the observed fact that stocks typically trade near zero for a period after a default plus the fact of limited liability that ensures $S_t \geq 0$. By the martingale assumption it follows that for any $t \leq s$ prior to default

$$S_t = \mathbb{E}^{\mathbb{Q}}[e^{-r(s-t)}(V_s - D_s)\mathbf{1}_{\{t^*>s\}}|\mathcal{F}_t] = (V_t - D_t)\mathbf{1}_{\{t^*>t\}}. \tag{3.9}$$

The second equality comes from Doob's optional stopping theorem [3]. We notice that

$$e^{-rs}(V_s - D_s)\mathbf{1}_{\{t^*>s\}} = e^{-r(s\wedge t^*)}(V_{s\wedge t^*} - D_{s\wedge t^*})$$

is a $\mathbb{Q}$ martingale evaluated at a bounded stopping time $s \wedge t^*$, which is also a $\mathbb{Q}$ martingale. In (3.9), S_t is independent of the debt maturity s. This is different from the standard setup in the Merton model and Black-Cox model, which makes it more parsimonious. Moreover, the time t price of a maturity $T > t$ forward contract with strike K will be $S_t - e^{-r(T-t)}K$. A European call option with (positive) strike K and maturity T has time t pre-default value

$$\text{Call}_t^{KT} = \mathbb{E}^{\mathbb{Q}}[e^{-r(T-t)}(V_T - D_T - K)^+\mathbf{1}_{\{t^*>T\}}|\mathcal{F}_t]. \tag{3.10}$$

Observe that this is equivalent to a down-and-out barrier spread option with a leverage barrier on $X_t = 0$. Put-call parity also holds in such a model, implying that $\text{Call}_t^{KT} - \text{Put}_t^{KT} = S_t - Ke^{-r(T-t)}$.

When a closed or computable form exists for the non-default characteristic function Φ_{ND} the above option pricing formula is amenable to Fourier analysis, following the method developed in [59] for vanilla spread options. There it is proved that the spread option payoff function has an explicit two-dimensional Fourier transform:

Proposition 4. *For any real numbers* $\epsilon = (\epsilon_1, \epsilon_2)$ *with* $\epsilon_2 > 0$ *and* $\epsilon_1 + \epsilon_2 < -1$

$$(e^{x_1} - e^{x_2} - 1)^+ = (2\pi)^{-2} \iint_{\mathbb{R}^2 + i\epsilon} e^{i(u_1 x_1 + u_2 x_2)} \hat{P}(u_1, u_2) d^2 u \qquad (3.11)$$

where $\hat{P}(u_1, u_2) = \frac{\Gamma(i(u_1 + u_2) - 1)\Gamma(-iu_2)}{\Gamma(iu_1 + 1)}$, *where* $\Gamma(z)$ *is the complex gamma function defined for* $\Re z > 0$ *by the integral*

$$\Gamma(z) = \int_0^\infty e^{-t} t^{z-1} dt$$

Combining this formula with the Fubini Theorem leads to the following formula for a call option with strike $K = 1$ and maturity T:

$$\text{Call}^T(v_0, d_0) = \frac{e^{-rT}}{(2\pi)^2} \iint_{\mathbb{R}^2 + i\epsilon} \Phi_{ND}(u_1, u_2; T; v_0, d_0) \hat{P}(u_1, u_2) d^2 u \qquad (3.12)$$

For a general strike $K = e^k$, we use homogeneity to write

$$\text{Call}^{KT}(v_0, d_0) = K \text{Call}^T(v_0 - k, d_0 - k).$$

Such explicit double integrals are sometimes efficiently computable for a full range of v_0, d_0 values using a single two-dimensional Fast Fourier Transform.

3.4   Geometric Brownian Motion Hybrid Model

We now consider the two factor model where $V_t = e^{rt + v_t}$, $D_t = e^{rt + d_t}$ are jointly given by a two-dimensional geometric Brownian motion:

$$\frac{dV_t}{V_t} = r dt + \sigma_v dW_t, \quad \frac{dD_t}{D_t} = r dt + \sigma_d dZ_t; \quad dW_t dZ_t = \rho dt. \qquad (3.13)$$

In this case, the stock price $S_t = V_t - D_t$ and log-leverage ratio $X_t = v_t - d_t$ follow the SDEs

$$\begin{aligned} \frac{dS_t}{S_t} &= \frac{dV_t - dD_t}{V_t - D_t} \\ dX_t &= -\frac{1}{2}(\sigma_v^2 - \sigma_d^2) dt + \sigma_v dW_t - \sigma_d dZ_t \end{aligned} \qquad (3.14)$$

Intuitively one normally expects to find $\sigma_v > \sigma_d \geq 0$, and to have the correlation $\rho \in (-1, 1)$.

3.4.1 Stochastic Volatility Model

Before investigating the form of Φ and hence the pricing formulas, it is worthwhile to note that this two factor model is identical to a specific stochastic volatility equity model, analogous to the Heston model. To see this, first we note that we can write

$$X_t = X_0 + \sigma_X[\alpha t + B_t] \qquad (3.15)$$

Here $\sigma_X^2 = \sigma_v^2 - 2\rho\sigma_v\sigma_d + \sigma_d^2$ and $\alpha = \frac{\sigma_d^2 - \sigma_v^2}{2\sigma_X}$, and the Brownian motion B is correlated to W, Z with

$$
\begin{aligned}
dBdW &= \rho_{vX}dt, \quad \sigma_X\rho_{vX} = \sigma_v - \sigma_d\rho \\
dBdZ &= \rho_{dX}dt, \quad \sigma_X\rho_{dX} = \rho\sigma_v - \sigma_d
\end{aligned}
$$

Next we apply the Itô formula to obtain the SDE for the pre-default stock price

$$
\begin{aligned}
\frac{dS_t}{S_t} &= \frac{r(e^{v_t} - e^{d_t})dt + (\sigma_v e^{v_t}dW_t - \sigma_d e^{d_t}dZ_t)}{e^{v_t} - e^{d_t}} \\
&= rdt + \frac{\sigma_v e^{X_t}dW_t - \sigma_d dZ_t}{e^{X_t} - 1}.
\end{aligned}
$$

The martingale term has stochastic quadratic variation with increment $dS_t^2/S_t^2 = f(X_t)dt$ where

$$f(x) := \frac{(\sigma_v e^x - \sigma_d\rho)^2 + (1 - \rho^2)\sigma_d^2}{(e^x - 1)^2}. \qquad (3.16)$$

Furthermore, the cross variation increment is $dX_t dS_t/S_t = g(X_t)\sigma_X\sqrt{f(X_t)}dt$ where

$$g(x) := \frac{\sigma_v^2 e^x - \rho\sigma_v\sigma_d(e^x + 1) + \sigma_d^2}{\sigma_X\sqrt{(\sigma_v e^x - \sigma_d\rho)^2 + (1 - \rho^2)\sigma_d^2}}. \qquad (3.17)$$

Therefore, using the Lévy theorem to define a new Brownian motion, one can prove

Proposition 5. *In the GBM hybrid model, there are independent Brownian motions $B, B^\perp$ such that the log-leverage process is given by*

$$X_t = X_0 + \sigma_X[\alpha t + B_t]$$

and the stock price follows a stochastic volatility process

$$dS_t/S_t = rdt + \sigma_t[\rho_{SX,t}dB_t + \bar{\rho}_{SX,t}dB_t^\perp] \qquad (3.18)$$

with

$$\sigma_t^2 = f(X_t), \quad \rho_{SX,t} = g(X_t), \quad \bar{\rho}_{SX,t} = \sqrt{1 - g(X_t)^2} \tag{3.19}$$

Moreover, the default time t^* is the first passage time for X_t to cross zero, and is predictable.

Remark 4. *The processes v_t, d_t can be expressed in terms of the independent drifting BMs $B_t + \alpha t$ and $B_t^\perp + \alpha^\perp t$ where $\alpha^\perp = -\frac{\sigma_v}{2\bar{\rho}_{vX}} = -\frac{\sigma_d}{2\bar{\rho}_{dX}}$:*

$$\begin{aligned} v_t &= v_0 + \sigma_v \left[\rho_{vX}(B_t + \alpha t) + \bar{\rho}_{vX}(B_t^\perp + \alpha^\perp t)\right] \\ d_t &= d_0 + \sigma_d \left[\rho_{dX}(B_t + \alpha t) + \bar{\rho}_{dX}(B_t^\perp + \alpha^\perp t)\right] \end{aligned} \tag{3.20}$$

where

$$\bar{\rho}_{vX} = \sqrt{1 - \rho^2}\sigma_d/\sigma_X, \quad \bar{\rho}_{dX} = \sqrt{1 - \rho^2}\sigma_v/\sigma_X$$

Finally, we note that in the GBM hybrid model, the explicit characteristic function is

$$\Phi^{GBM}(u; T, Y_0) = \exp\left[iuY_0 - \frac{T}{2}u\Sigma u' - i\frac{uT}{2}(\sigma_v^2, \sigma_d^2)'\right] \tag{3.21}$$

where $\Sigma = [\sigma_v^2, \rho\sigma_v\sigma_d; \rho\sigma_v\sigma_d, \sigma_d^2]$.

3.4.2 Pricing

Basic securities we need to price, namely, defaultable bonds and equity call options, have payoffs that vanish on the set $\{v_T \leq d_T\}$ and are subject to a "down-and-out" barrier condition. The next proposition shows how the barrier condition can be easily dealt with for such securities. First we note that the linear change of variables $[X_t, X_t^\perp]' = MY_t, Y_t := [v_t, d_t]'$ for the matrix $M = [1, \ -1; 1, \ m]$ with $m = \frac{\rho\sigma_v\sigma_d - \sigma_v^2}{\rho\sigma_v\sigma_d - \sigma_d^2}$ leads to independence of $X_t = v_t - d_t$ and $X_t^\perp$. This fact allows us to state and prove the following important result:

Proposition 6. *Consider an option with maturity T and bounded payoff function $F(v, d)$ that vanishes on the set $\{v < d\}$. Let $f(v_0, d_0; T)$ denote its value at time 0. In the geometric Brownian motion model, the down-and-in barrier option with initial state $v_0 > d_0$ and terminal payoff F is equivalent to a vanilla option with the*

same payoff, but with linearly transformed initial state $[\tilde{v}_0, \tilde{d}_0]$ and an extra factor. Precisely,

$$f_{DI}(v_0, d_0; T) = e^{-2\alpha(v_0 - d_0)/\sigma_X} f(\tilde{v}_0, \tilde{d}_0; T) \tag{3.22}$$

where $[\tilde{v}_t, \tilde{d}_t]' = R[v_t, d_t]', R = M^{-1}[-1, 0; 0, 1]M$.

Proof: Note that the matrix R is a skewed reflection matrix, which hints that this result is essentially a consequence of the reflection principle for Brownian motion. By intermediate conditioning,

$$\mathbb{E}_{v_0, d_0}[F(v_T, d_T)\mathbf{1}_{\{t^* \leq T\}}] = \mathbb{E}_{X_0^\perp}[\mathbb{E}_{X_0}[F(M^{-1}[X_T, X_T^\perp]')\mathbf{1}_{\{X_T > 0\}}\mathbf{1}_{\{t^* \leq T\}}|X^\perp]]$$

For fixed $X^\perp$, the reflection principle governs that the inner expectation can be written as an integral

$$\int_0^\infty G(x, X_T^\perp)\frac{e^{-2\alpha X_0/\sigma_X}}{\sigma_X\sqrt{T}}\phi\left(\frac{-X_0 - x + \alpha\sigma_X T}{\sigma_X\sqrt{T}}\right)$$

where $G(x, y) := F(M^{-1}[x, y]')$. Here we have used a standard result for Brownian motion conditioned on crossing a barrier. The vanilla option with the same payoff can be written

$$f(v_0, d_0) = \mathbb{E}_{v_0, d_0}[F(v_T, d_T)] = \mathbb{E}_{X_0^\perp}[\mathbb{E}_{X_0}[F(M^{-1}[X_T, X_T^\perp]')\mathbf{1}_{\{X_T > 0\}}|X^\perp]]$$

where the inner expectation equals

$$\int_0^\infty G(x, X_T^\perp)\frac{1}{\sigma_X\sqrt{T}}\phi\left(\frac{X_0 - x + \alpha\sigma_X T}{\sigma_X\sqrt{T}}\right)dx$$

The desired result follows by a direct comparison of these two formulas for the inner expectations. $\square$

Corollary 7. *In the geometric Brownian motion hybrid model with initial state $v_0 > d_0$*

1. *The survival probability by time T can be written*

$$P[t^* > T|v_0, d_0] = P[v_T > d_T|v_0, d_0] - e^{-2\alpha X_0/\sigma_X}P[v_T > d_T|\tilde{v}_0, \tilde{d}_0]$$

and the price of a zero-recovery defaultable zero-coupon bond is given by $e^{-rT}P[t^* > T|v_0, d_0]$.

2. *The price of an equity call option can be written*

$$F(v_0, d_0; T) - e^{-2\alpha X_0/\sigma_X} F(\tilde{v}_0, \tilde{d}_0; T)$$

where $F(v_0, d_0; T) = e^{-rT}\mathbb{E}_{v_0,d_0}[(e^{v_T} - e^{d_T} - K)^+ \mathbf{1}_{\{v_T > d_T\}}]$. The vanilla call option price with maturity T and strike $K = 1$ can be computed by the two-dimensional FFT:

$$F(v_0, d_0; T) = \frac{e^{-rT}}{(2\pi)^2} \iint_{\mathbb{R}^2 + i\epsilon} \Phi^{GBM}(u_1, u_2; T; v_0, d_0)\hat{P}(u_1, u_2)d^2u \qquad (3.23)$$

3.5 Lévy Subordinated Brownian Motion Hybrid Models

We have seen that the two-factor GBM model implies that the stock process S is a rather specific stochastic volatility process with continuous paths. Moreover the log-leverage process X is an arithmetic Brownian motion with constant drift, and the resultant Black-Cox credit model is well known to be unable to capture the fine effects in observed credit spreads.

The time-changed Brownian motion (TCBM) credit framework of [57] introduces a non-decreasing "time-change" process G_t independent of B and replaces the Brownian log-leverage process by its time-change $X_t = X_0 + \sigma_X[B_{G_t} + \alpha G_t]$ to create a much richer range of dynamics, allowing for purely discontinuous components as well as "stochastic volatility". The relevant notion of default by first-passage of the log-leverage process to zero has been well understood in this setting. A non-decreasing Lévy process G_t is called a subordinator, and a Lévy subordinated Brownian motion (LSBM) in general includes purely discontinuous components. Any LSBM $W_{G_t} + \alpha G_t$ has the independent increment property and is Markovian and therefore we can say it is a one-factor process. An important consequence of this one-factor property is that it excludes stochastic volatility effects that by definition involve further factors.

The same time-change ideas can be applied to our two-factor GBM hybrid model, and will provide a dramatic increase in flexibility to match effects observed in market data. To retain the simplicity of two-factor models, we focus here on the LSBM case

with a single subordinator G_t and the two uncorrelated drifting Brownian motions $B_{G_t} + \alpha G_t, B_{G_t}^\perp + \alpha^\perp G_t$. We assume the natural filtration $\mathcal{F}_t$ contains $\sigma\{G_u, B_v, B_v^\perp : 0 \leq u \leq t, 0 \leq v \leq G_t\}$.

The assumptions underlying the LSBM two-factor hybrid model are:

Assumption 4. *1. The time-change process G_t is a Lévy subordinator with mean $\mathbb{E}^Q[G_t] = t$.*

2. The log discounted firm value $v_t = -rt + log(V_t)$ and log discounted firm liability $d_t = -rt + log(D_t)$ are both LSBMs, with the same time change G_t, i.e.

$$
\begin{aligned}
v_t &= v_0 + \sigma_v \left[\rho_{vX}(B_{G_t} + \alpha G_t) + \bar{\rho}_{vX}(B_{G_t}^\perp + \alpha^\perp G_t) \right] \\
d_t &= d_0 + \sigma_d \left[\rho_{dX}(B_{G_t} + \alpha G_t) + \bar{\rho}_{dX}(B_{G_t}^\perp + \alpha^\perp G_t) \right]
\end{aligned}
\tag{3.24}
$$

Here, the parameters are chosen as in section 3.

3. The log-leverage ratio $X_t := log(V_t/D_t) = X_0 + \sigma_X[B_{G_t} + \alpha G_t]$ is also a LSBM, and $S_t = V_t - D_t$.

4. The time of default is t^*, the first passage time of the second kind for X to cross zero, defined by

$$
t^* = \inf\{t | G_t \geq \tau\}
\tag{3.25}
$$

where $\tau = \inf\{t | B_t + \alpha t \leq -X_0/\sigma_X\}$. All processes are stopped at t^*.

5. The interest rate r and recovery fraction R are assumed constant.

In the model calibration that follows in Section 3.6 we will consider two specific forms for the subordinator G_t:

1. The first type of time change is an exponential (EXP) jump process with constant drift, that is, G has characteristics $(b, 0, \nu)$ where $b \in (0,1)$ and $\nu(z) = ce^{-z/a}/a, a > 0$ on $(0, \infty)$, the Lévy measure, has support on $\mathbb{R}^+$. The Laplace exponent of G_t is

$$
\psi^{Exp}(u, t) := -\log E[e^{-uG_t}] = t \left[bu + \frac{acu}{1 + au} \right]
\tag{3.26}
$$

and by choosing $a = \frac{1-b}{c}$ the average speed of the time change is normalized to 1;

2. The second type of time change is a variance gamma (VG) process [80], that is, G is a gamma process with drift having characteristics $(b, 0, \nu)$ where $b \in (0, 1)$ and $\nu(z) = ce^{-z/a}/z, a > 0$ on $(0, \infty)$, the Lévy measure, has support on $\mathbb{R}^+$. The Laplace exponent of G_t is

$$\psi^{VG}(u, t) := -\log E[e^{-uG_t}] = t[bu + c\log(1 + au)] \tag{3.27}$$

and by choosing $a = \frac{1-b}{c}$ the average time change speed is normalized to 1;

The practical consequence of the precise way the time-change is introduced, and in particular the associated definition of default t^* as a first passage of the second kind, is that all expectations relevant for the pricing of securities can be done efficiently by iterated expectations. For example, we have a simple formula for the characteristic function of (v_T, d_T):

$$\begin{aligned}
\Phi^{LSBM}(u_1, u_2; T, v_0, d_0) &= \mathbb{E}^{\mathbb{Q}}[\mathbb{E}^{\mathbb{Q}}_{v_0, d_0}[e^{i(u_1 v_T + u_2 d_T)}]|G_T] \\
&= \mathbb{E}^{\mathbb{Q}}[\Phi^{GBM}(u_1, u_2; G_T, v_0, d_0)]
\end{aligned}$$

Since Φ^{GBM} given by (3.21) has the nice feature that the T dependence takes an exponential affine form which implies that the GBM pricing formula easily extends to TCBM with a Lévy subordinator.

Proposition 8. *Consider an option with maturity T and bounded payoff function $F(v, d)$ that pays only if $t^* > T$. Let $f^{GBM}(v_0, d_0; T)$ denote its value at time 0 under the GBM hybrid model, and $f^{LSBM}(v_0, d_0; T)$ its value under the LSBM model. Then*

$$f^{LSBM}(v_0, d_0; T) = \mathbb{E}^{\mathbb{Q}}[f^{GBM}(v_0, d_0; G_T)]$$

Proof: We suppose that $f^{GBM}(v_0, d_0; T) = \mathbb{E}^{\mathbb{Q}}_{v_0, d_0}[F(v_T, d_T)\mathbf{1}_{\{t^* > T\}}]$. Then in the LSBM model,

$$\begin{aligned}
f^{LSBM}(v_0, d_0; T) &= \mathbb{E}^{\mathbb{Q}}_{v_0, d_0}[F(v_T, d_T)\mathbf{1}_{\{t^* > T\}}] \tag{3.28} \\
&= \mathbb{E}^{\mathbb{Q}}[\mathbb{E}^{\mathbb{Q}}_{v_0, d_0}[F(v_T, d_T)\mathbf{1}_{\{\tau > G_T\}}]|G_T] \\
&= \mathbb{E}^{\mathbb{Q}}[f^{GBM}(v_0, d_0; G_T)]
\end{aligned}$$

□

As an important example, we can see that combining the above result with Corollary 7 leads to the following formula for the equity call option with maturity T and strike $K = 1$ in any LSBM model where the time-change G has Laplace exponent ψ:

$$F^{LSBM}(v_0, d_0; T) - e^{-2\alpha(v_0-d_0)/\sigma_X} F^{LSBM}(\tilde{v}_0, \tilde{d}_0; T)$$

where the vanilla spread option price is

$$F^{LSBM}(v_0, d_0; T) = \frac{e^{-rT}}{(2\pi)^2} \iint_{\mathbb{R}^2+i\epsilon} \exp\left[iuY_0 - \psi\left(u\Sigma u'/2 - iu(\sigma_v^2, \sigma_d^2)'/2, T\right)\right] \hat{P}(u_1, u_2)d^2u$$

$$(3.29)$$

3.6   Calibration of LSBM Models

The aim of this calibration exercise is to demonstrate that the simple two-factor LSBM hybrid framework is capable of fitting simultaneous market CDS and implied volatility prices on a firm, in this case Ford Motor Company, at any moment in time. We chose Ford as an example of a large, highly traded, firm, that has been very near to default in recent years. We do not here attempt to conduct a large scale survey of how the model performs for a broad range of firms over different periods of time. However, we will see encouraging results from our small study, that suggest that acquiring and analyzing such a dataset may be worth the considerable expense and effort involved.

3.6.1   Data

We observed equity and credit market data for Ford Motor Co. obtained from Bloomberg at two moments during the post credit-crunch period: once on July 14, 2010 and once on February 16, 2011. On these dates we noted:

1. The stock price was \$11.81 and \$16.05 respectively.

2. Midquote implied volatilities $IV_{D,T}$ for moneyness
   $\mathcal{D} := \{0.4, 0.6, 0.8, 0.9, 0.95, 0.975, 1, 1.025, 1.05, 1.1, 1.2, 1.3, 1.5\}$ and with times

to maturity $\mathcal{T} := \{37, 65, 156, 191, 555\}$ calendar days on July 14, 2010 $\mathcal{T} :=$ $\{30, 58, 93, 121, 212, 338\}$ calendar days on February 16, 2011;

3. Midquote CDS spreads CDS_T for tenors $\tilde{\mathcal{T}} := \{1, 2, 3, 4, 5, 7, 10\}$ years;

4. US treasury yields for maturities
$\bar{\mathcal{T}} := \{1m, 3m, 6m, 1y, 2y, 3y, 5y, 7y, 10y, 20y, 30y\}$.

From 2009 to 2011, Ford Motor Co. steadily recovered from its near default during the 2007/08 credit crunch and expectations from the financial market correspondingly rose. This improvement in the firm's fortunes is manifested in an observed decrease of both its implied volatilities and CDS spreads between the two observation dates.

Remark 5. *We found that deep in-the-money (ITM) options are not very liquid and deep out-of-the-money (OTM) options are difficult to control numerical errors as their prices are very close to nil. For very short time to maturity options, our FFT formulas 3.23 and 3.29 are subject to higher truncation errors as the integrand does not decay fast enough. Therefore in our calibration, we did not use implied volatility data with extreme moneyness $D = 0.4, 1.5$ and with short time to maturity (TTM) $T = 30, 37, 58$ calendar days.*

3.6.2 Daily Calibration Method

To test the GBM, EXP and VG models described above, we performed independent daily calibrations to the data on the above two dates. It is natural to assume that stock prices are perfectly liquid and hence are perfect observations of the process $S_t = e^{v_t} - e^{d_t}$. On the other hand, CDS and equity option markets are much less liquid therefore the $N = 7$ observed CDS spreads and $M \sim 50$ observed implied volatilities are not assumed to match our model prices exactly. Thus at any moment, S_t is exactly observed, while X_t must be filtered from the market data.

On any given date t, under these assumptions, the risk neutral parameters for both LSBM models to be calibrated are $\Theta = (\rho, \sigma_v, \sigma_d, b, c, R, X_t) \in \mathbb{R} \times \mathbb{R}^6$. The GBM hybrid model nests inside both LSBM models as the limit with $c = 0$.

Our method is a least-squares minimization of the relative error between the model and market CDS spreads and implied volatilities observed at a single instant in time. For each $T \in \tilde{\mathcal{T}}$, let $\widehat{CDS}_T$ and $CDS_T(\Theta)$ denote market and model CDS spread with maturity T. Similarly, for each $T \in \mathcal{T}$ and $D \in \mathcal{D}$ let $\widehat{IV}_{D,T}$ and $IV_{D,T}(\Theta)$ denote the observed and model implied volatilities with the given D, T. The objective function to be minimized is a sum of squared relative errors. We introduce a weight factor between the CDS and IV terms to offset a natural overweighting stemming from the large number of equity securities relative to the credit securities. Without this factor, the IV terms would dominate the calibration and wash out the credit effects we aim to capture. Thus we define the objective function to be

$$\mathbb{J}(\Theta) = \sum_{T \in \tilde{\mathcal{T}}} \frac{|\widehat{CDS}_T - CDS_T(\Theta)|^2}{\widehat{CDS}_T^2} + \frac{1}{C^2} \sum_{T \in \mathcal{T}, D \in \mathcal{D}} \frac{|\widehat{IV}_{D,T} - IV_{D,T}(\Theta)|^2}{\widehat{IV}_{D,T}^2}$$

where the subjective value $C^2 = 7$ is roughly the ratio between the number of IV quotes and CDS quotes and proves to provide a nice balance between the credit and equity datasets. The model calibration is required to minimize $\mathbb{J}$ over the domain $\Theta \in \mathbb{R} \times \mathbb{R}^6$:

$$\hat{\Theta} = \operatorname{argmin}_{\Theta} \mathbb{J}(\Theta)$$

Remark 6. *1. The above objective function corresponds to the measurement hypothesis that individual spreads and implied volatilities are observed with independent Gaussian relative errors. Of course, this is likely far from true. In reality, the raw data has been "cleaned up" and transformed by Bloomberg in many different ways, and we would always expect correlations between different measurement errors.*

2. Another important point is that the weights in our objective function were to some extent chosen by us subjectively to give a nice balance between the credit and equity datasets. We have tried other two choices of weight factors: 1. $C^2=1$ gives each quote equal weight which necessarily under-weighs CDS data; 2. A square of bid/ask spread gives each quote a weight proportional to its liquidity which turns out to under-weigh CDS data as well because IV market is much

more liquid. Unbalanced weighting gives rise to good fit to equity while ruining the fit to CDS spreads.

The calibration was implemented on a laptop using standard MATLAB. Minimization of $\mathbb{J}$ was performed using "fmincon": typically around 200 evaluations of $\mathbb{J}$ were needed to find an acceptable minimum. The model CDS and call option prices entering $\mathbb{J}$ are computed by one and two dimensional Fast Fourier Transforms using MATLAB's functions "FFT" and "FFT2". Since each FFT2 is computationally intensive, and calibration involves a great number of evaluations, it was effective to use interpolation from a single grid of FFT-generated prices to compute the range of option prices across moneyness. We used the truncation and discretization error analysis in [59] and [60] to optimize these computations. During the calibration, we found that the down-and-in barrier option terms in (3.28) are always much smaller than the vanilla terms. This can be explained because the credit quality of Ford is reasonably high, and therefore the linear transformation $(\tilde{v}_t, \tilde{d}_t)' = R(v_t, d_t)'$ generates a point $\tilde{v}_t < \tilde{d}_t$ equivalent to a deep out-of-the-money vanilla spread option.

3.6.3 Calibration Results

The calibration results for the three models and two dates are shown in table 3.1. Table 3.2 records the balance sheet entries V, D, S implied by each of these calibrations. For comparison, we also give the summary asset and liability values taken from Ford's quarterly reports on the dates closest to the calibration dates. Clearly there is no obvious correspondence between the market and balance sheet values, so it will be a nontrivial task to identify the extent to which the balance sheet numbers can in principle be predicted by the market implied values.

Many points can be made about our calibration results, and we note those that seem most significant. First, we see that as expected, the GBM hybrid model is able to provide only a qualitative fit to the observed market data. As a stochastic volatility model, and unlike the Black-Scholes model, it does generate an implied volatility smile however, the details of the fitted shapes are not very good. In contrast, with one more parameter than GBM, both the VG and EXP (LSBM) models lead to CDS and IV

curves that capture the correct levels and more of the quantitative features of the market data. The VG and EXP models have similar RMSE lower than the GBM, especially for February 16, 2011.

A second important point is that both LSBM models (but not the GBM model) lead in all cases to implied recovery $R = 0$, at the boundary of the parameter domain. Since reducing R to zero raises the level of CDS curves while leaving IV curves unchanged, this observation suggests a mismatch of risk neutral pricing between equity and credit markets: The CDS spreads are somewhat high relative to the level of the implied volatility surface and the calibration is forced to choose a zero recovery rate in order to narrow the gap as much as possible. In our calibrations it appears that this gap is completely closed with $R = 0$. A similar observation has been made and discussed in Carr and Wu [26] who find essentially a zero recovery rate for 6 out of 8 companies studied, with significant biases remaining between model prices and market quotes.

In the LSBM models, implied volatility always turns out higher than the asset and debt volatility: this is as expected since our model incorporates the well-documented leverage effect described in [69]. The correlations between asset and debt are slightly negative indicating a slight tendency for the asset and debt to move in opposite directions.

The calibrations on the two dates for both LSBM models (but not the GBM model) illuminate distinct financial situations. In the earlier stage of recovery, the July 14 2010 data exhibit higher asset volatility and a higher jump component in the time change, indicating more discontinuity in asset and debt processes as well as higher jump to default probability. The log-leverage ratio is also lower to render higher overall default probability. The second date, February 16, 2011, shows slightly higher debt volatility.

As the VG and EXP (LSBM) models have very similar performance in various measures, an observation already made in credit modeling in chapter 2, we describe their fitting to market data together. As shown in figures 3.1 and 3.4, the LSBM models capture the credit risk quite well. The discrepancies on February 16 2011 are negligible. On July 14 2010, the short term and intermediate term CDS are fit tightly.

However for the longer terms of more than five years, the market CDS spreads seem too wide for our model to fit.

The implied volatility data on July 14 2010 are shown in figures 3.2 and 3.5. The LSBM models fit the market quotes quite well over a broad range of moneyness and time to maturity. However, there are some tensions between them and the market quotes. For shorter time to maturity, they tend to generate volatility smile for market volatility skew. For longer time to maturity, they tend to produce positive biases.

The implied volatility data on February 16 2011 are shown in figures 3.3 and 3.6. The LSBM models fit the market quotes quite well at the near the money range for all time to maturity. However, some tensions between them and the market quotes for deep in the money and deep out of the money range. In particular, the LSBM models overestimate the option prices for those moneyness. For shorter time to maturity, they also tend to generate volatility smile for market volatility skew.

For July 14 2010 calibration of the EXP model, we perturb the log-asset value by its standard deviation and observe the impact on CDS and implied volatilities. The results are shown in figure 3.10 and 3.11. This sensitivity test shows that increasing asset value reduces default probability to lower CDS spread. Implied volatilities also decreases due to the structural connections intrinsically built between equity and credit in our model settings. If the asset value moves to the other direction, both CDS and implied volatility increase for the same reason. Our model is capable of producing the empirically observed correlations between CDS and implied volatilities and interpreting the correlations as interplay between asset and debt processes.

3.7   Conclusions

We have used two-factor LSBM models to characterize a firm's simplified capital structure. Treating the firm asset value and debt value as correlated stochastic processes, we also derive the firm equity value and define the default trigger, therefore achiving hybrid modeling. Similar to the classical Black-Cox model, the equity value comes from an equivalent barrier call option and the default is triggered by a first passage event. However, our models are enriched by the LSBM flexibility to gener-

ate stochastic volatility with jumps for equity dynamics and unpredictable jump to default. In fitting market data, we have found that the VG and EXP models give similarly good performance in spite of the very difference characteristics of their Lévy measures. With one extra parameter, both models outperform the Black-Cox model in capturing key empirical features of credit and equity markets. The CDS term structure can be fit into different shapes and the implied volatility surface exhibits skew and smile. Furthermore, the necessary computations are comparable in difficulty to formulas used routinely in industry, such as the VG model of Madan and Seneta [81]. The default probability and implied volatility are computed by one and two dimensional FFT respectively.

A significant application of the model is to provide a modeling approach to extract a firm's capital structure information from trading securities. We have studied Ford Motor Co. by calibrating its asset and debt values from CDS term structure and implied volatility surface in two days. This approach supplements the dynamic analysis of capital structure for quarterly financial reports. While the latter usually comes infrequently with time-lag our approach takes advantage of readily available, real-time trading assets. Other important parameters, including asset, debt volatilities, correlation and firm recovery rate, inaccessible from financial reports can also be calibrated from the same data.

Interestingly, we find that our LSBM models have recovery rate calibration of zero, even in 2011 after Ford bounced off its worst situation. It implies that the either the market CDS spreads are too wide for our models or the market options prices are too low for our models. We interpret this as pricing inconsistency between the equity and credit markets. Observing this inconsistency and uncovering its evolvement can be of practical significance. If it has a tendency to diminish over time, one can make capital structure arbitrage in single name stocks, options and CDS trading, with long positions in relatively underpriced instruments and short positions in relatively overpriced instruments. Alternatively, we can use asset and debt values of balance sheets as inputs to compute model implied stocks, options and CDS prices. The differences between model prices and market prices also lead to strategies for capital structure arbitrage. For example, Yu [110] studied several strategies for stocks and

CDS trading using CreditGrades [45].

The present paper, indeed, is merely an introduction to what can be done. Our results seem to align with the established knowledge that exponential Lévy models price option well across strikes but have limitations across maturities. The more general inhomogenous Lévy processes, with independent and non-stationary increments, can potentially provide improvement. As demonstrated in [57], it turns out to be quite straightforward technically to move beyond the present TCBM model with Lévy subordinators to the far broader modeling framework of time-changed Brownian motions. However, the huge range of implementation and calibration issues one meets when using general TCBM, notably stochastic volatility and jump effects, makes this a major research and development undertaking, to be carried out in future works.
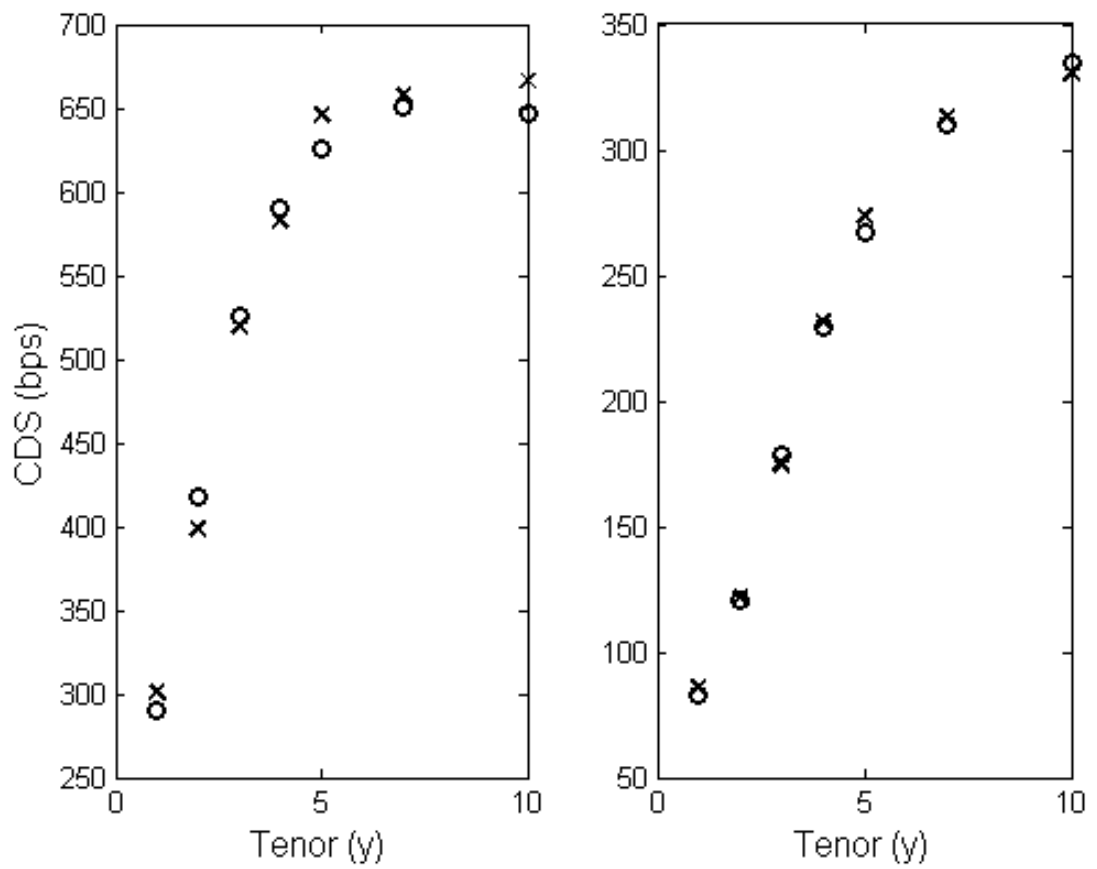
Figure 3.1: CDS market data ("×") versus the VG model data ("∘") on July 14 2010 (left) and February 16 2011(right).

		2010/07/14	2011/02/16
	$\hat{\sigma}_v$	0.2433	0.2005
	$\hat{\sigma}_d$	0.1344	0.1473
	$\hat{\rho}$	-0.0699	-0.0143
	$\hat{b}$	0.4966	0.6948
VG Model	$\hat{c}$	0.0474	0.0240
	$\hat{R}$	0	0
	$\hat{v}$	3.1796	3.3393
	$\hat{d}$	2.5036	2.4973
	RMSE	0.0804	0.0271
	$\hat{\sigma}_v$	0.2502	0.2011
	$\hat{\sigma}_d$	0.1324	0.1553
	$\hat{\rho}$	-0.1687	-0.0383
	$\hat{b}$	0.3700	0.7232
Exponential Model	$\hat{c}$	0.0519	0.0416
	$\hat{R}$	0	0
	$\hat{v}$	3.2786	3.3248
	$\hat{d}$	2.6898	2.4633
	RMSE	0.0801	0.0265
	$\hat{\sigma}_v$	0.0469	0.0612
	$\hat{\sigma}_d$	0.0130	0.0095
	$\hat{\rho}$	-0.8175	-0.9508
Black-Cox Model	$\hat{R}$	0.1900	0.4225
	$\hat{v}$	4.5640	4.4767
	$\hat{d}$	4.4327	4.2752
	RMSE	0.0983	0.1461

Table 3.1: Parameter estimation results and related statistics for the VG, EXP and Black-Cox models.

	Accounting	VG	EXP	GBM
Asset	119.0/109.5	82.9/107.2	91.6/105.6	331.1/334.2
Debt	78.3/77.7	42.2/46.2	50.8/44.6	290.3/273.2

Table 3.2: Ford accounting asset and debt (in $Bn) reported in the nearest quarterly financial statements (June 2010 and March 2011) and estimated from models on July 14 2010 and February 16 2011. The outstanding shares of Ford are approximately 3450 MM shares and 3800 MM shares respectively according to Bloomberg. In the financial statements, we take the total current assets plus half of the total long-term assets as the asset, and the current liabilities as the debt.
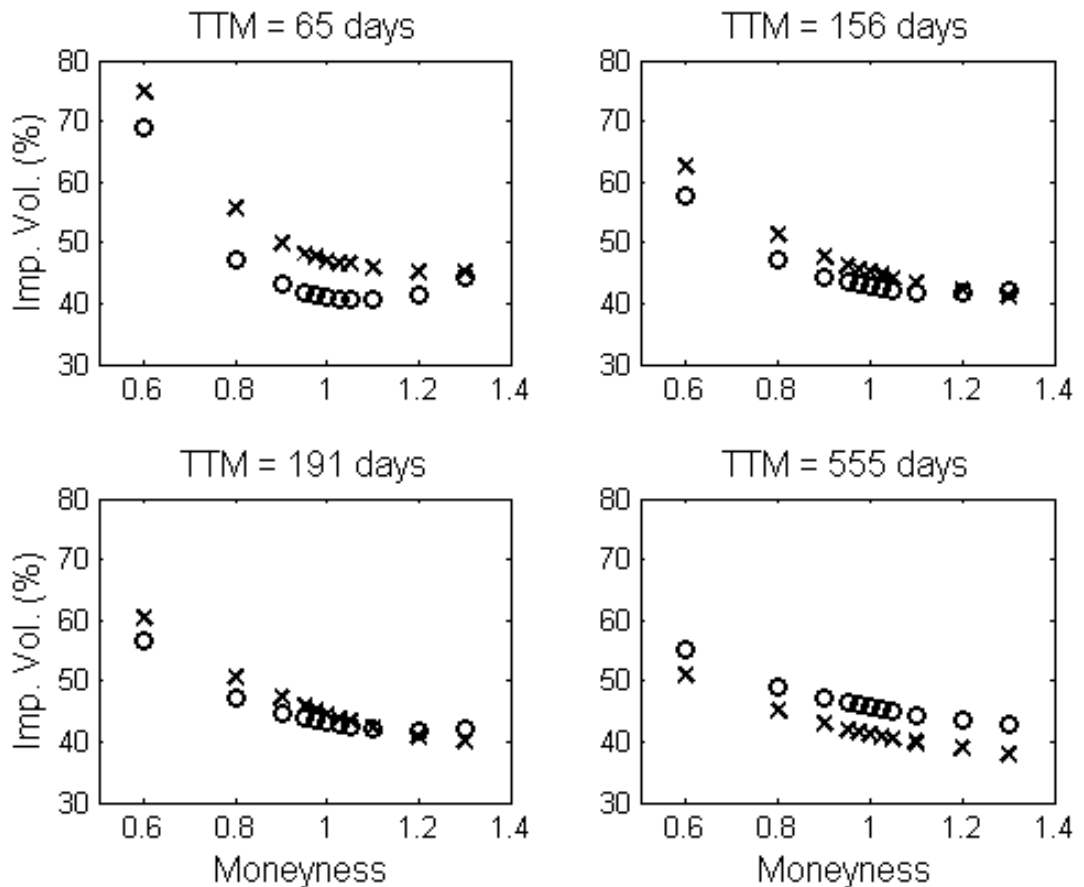
Figure 3.2: Implied volatility market data ("×") versus the VG model data ("○") on July 14 2010.
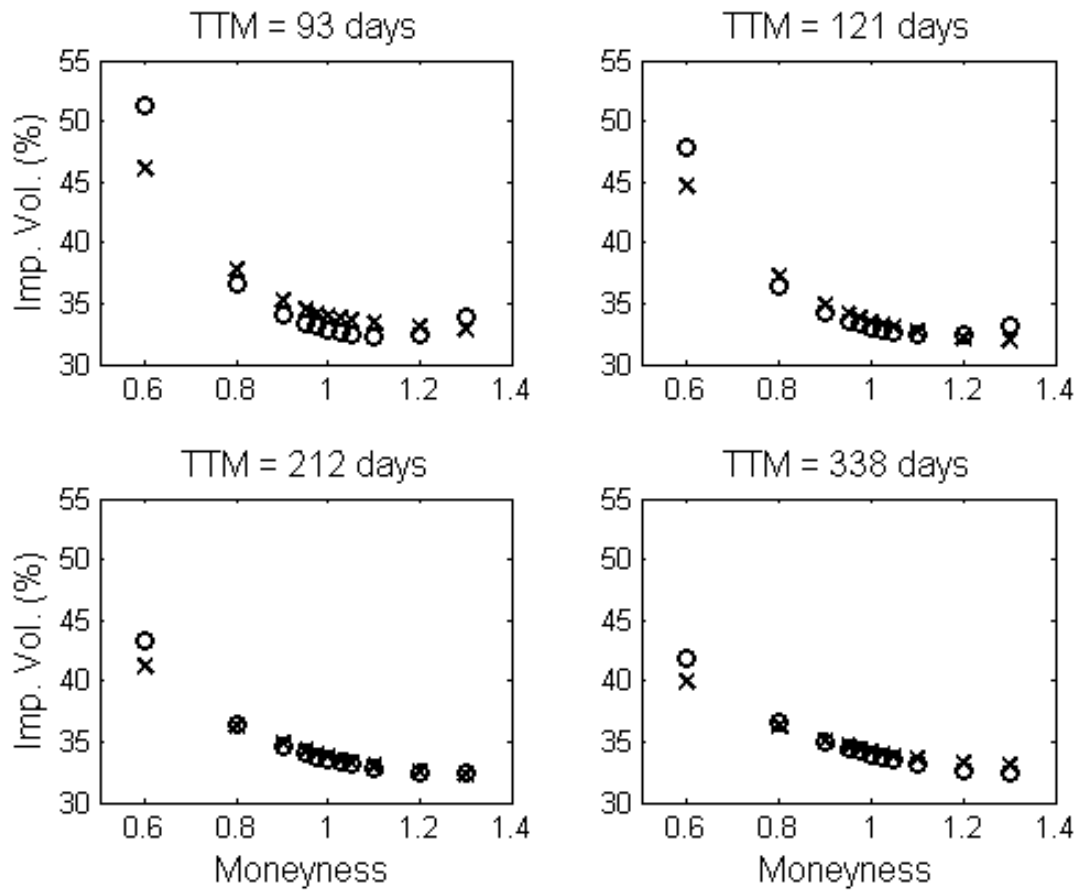
Figure 3.3: Implied volatility market data ("×") versus the VG model data ("○") on February 16 2011.
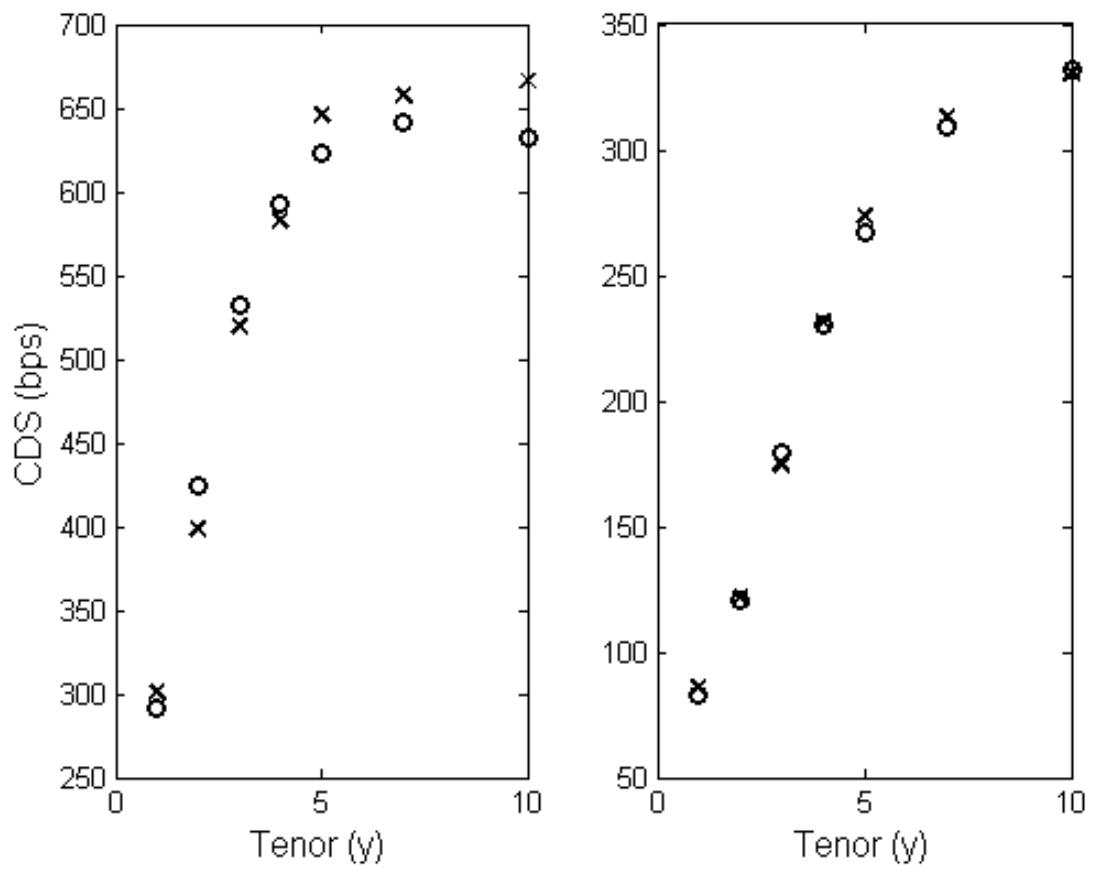
Figure 3.4: CDS market data ("×") versus the EXP model data ("○") on July 14 2010 (left) and February 16 2011(right).
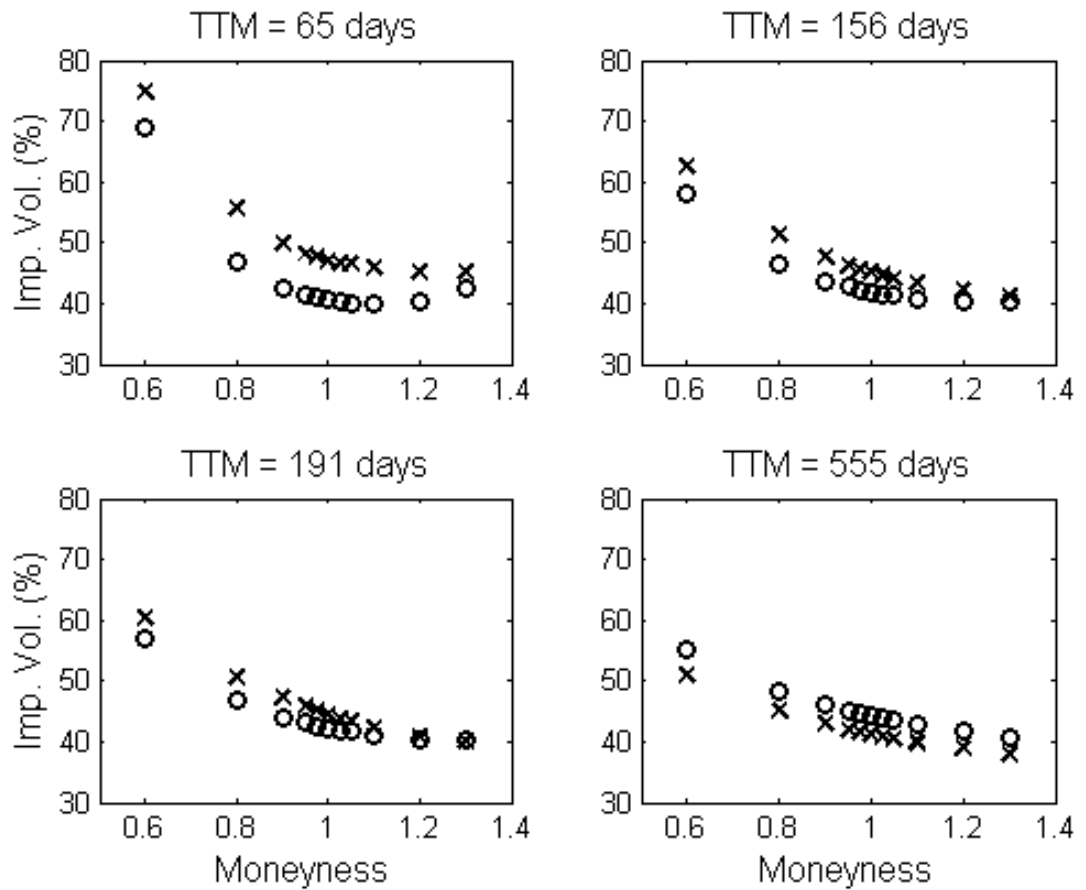
Figure 3.5: Implied volatility market data ("×") versus the EXP model data ("○") on July 14 2010.
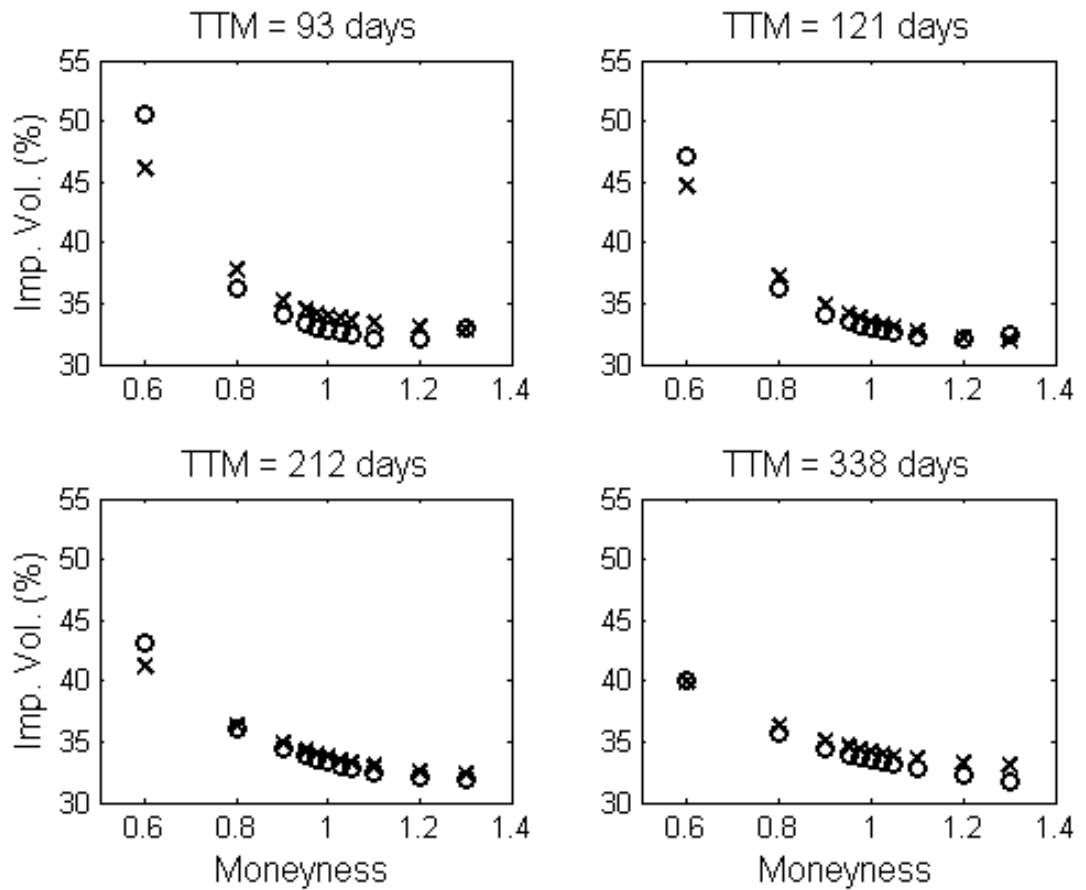
Figure 3.6: Implied volatility market data ("×") versus the EXP model data ("○") on February 16 2011.
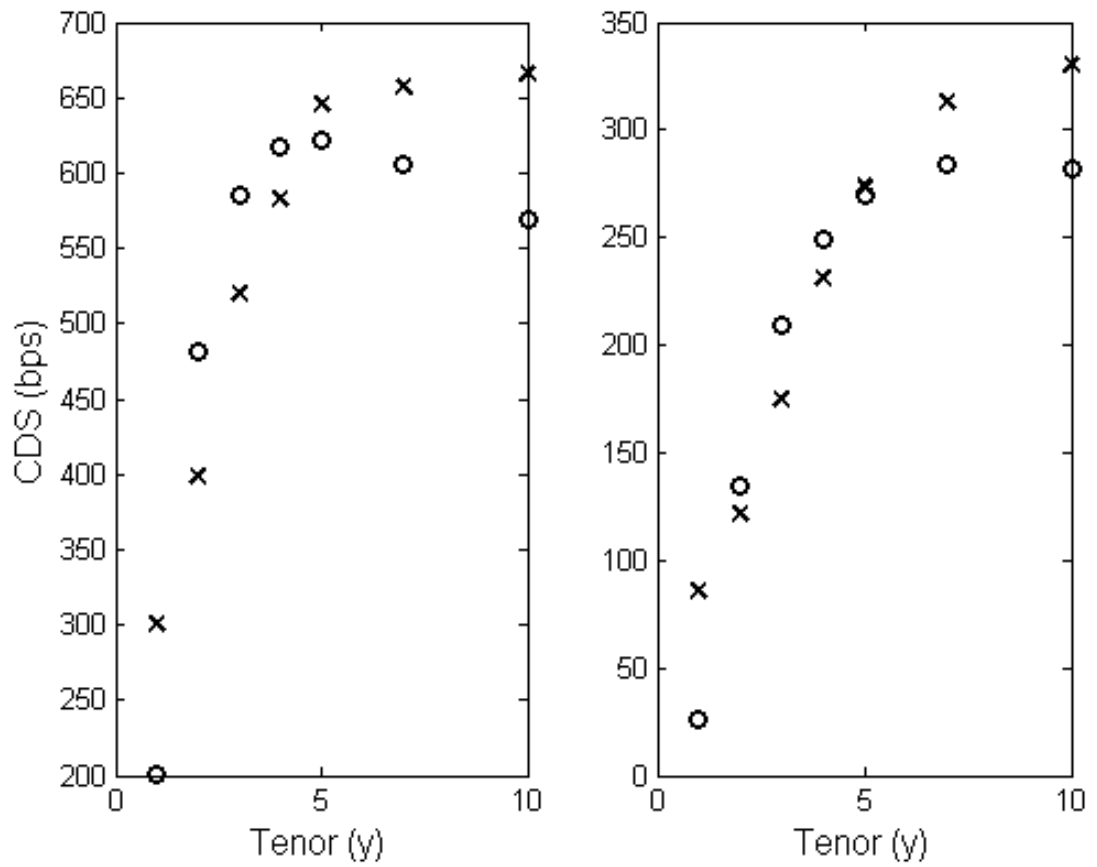
Figure 3.7: CDS market data ("×") versus the GBM model data ("○") on July 14 2010 (left) and February 16 2011(right).
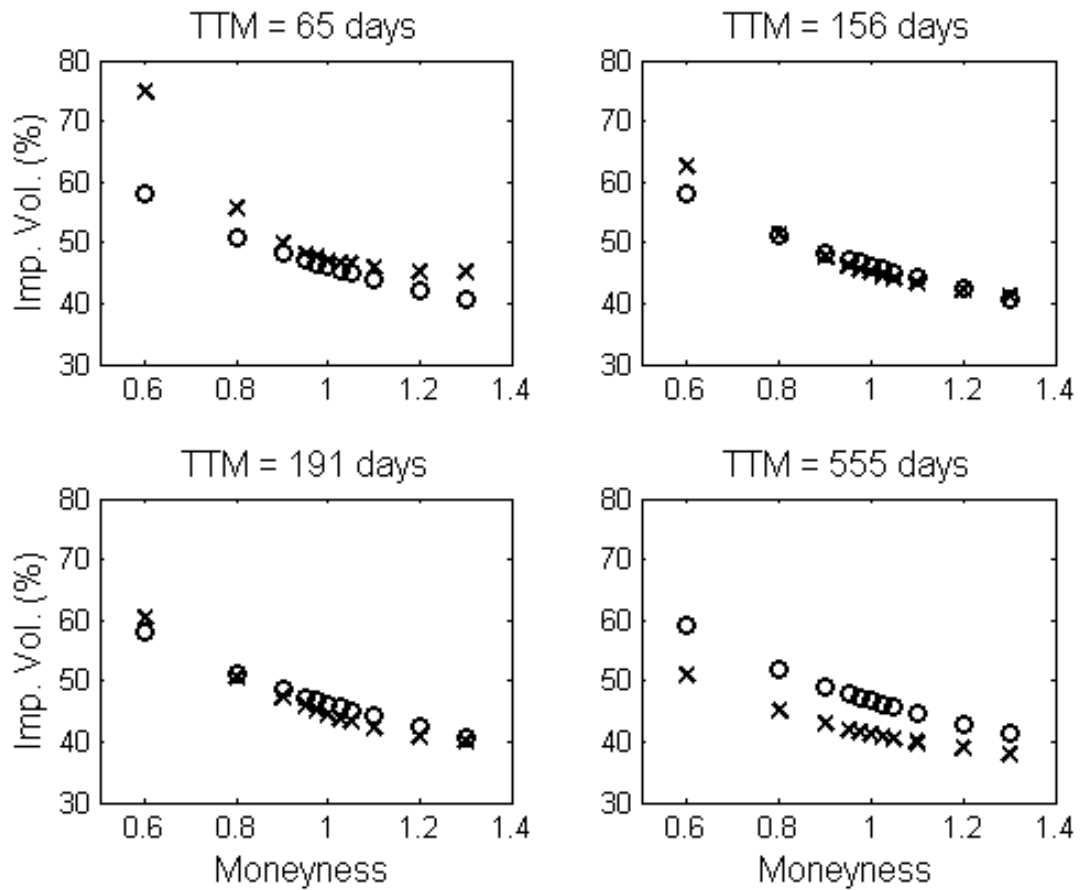
Figure 3.8: Implied volatility market data ("×") versus the GBM model data ("○") on July 14 2010.
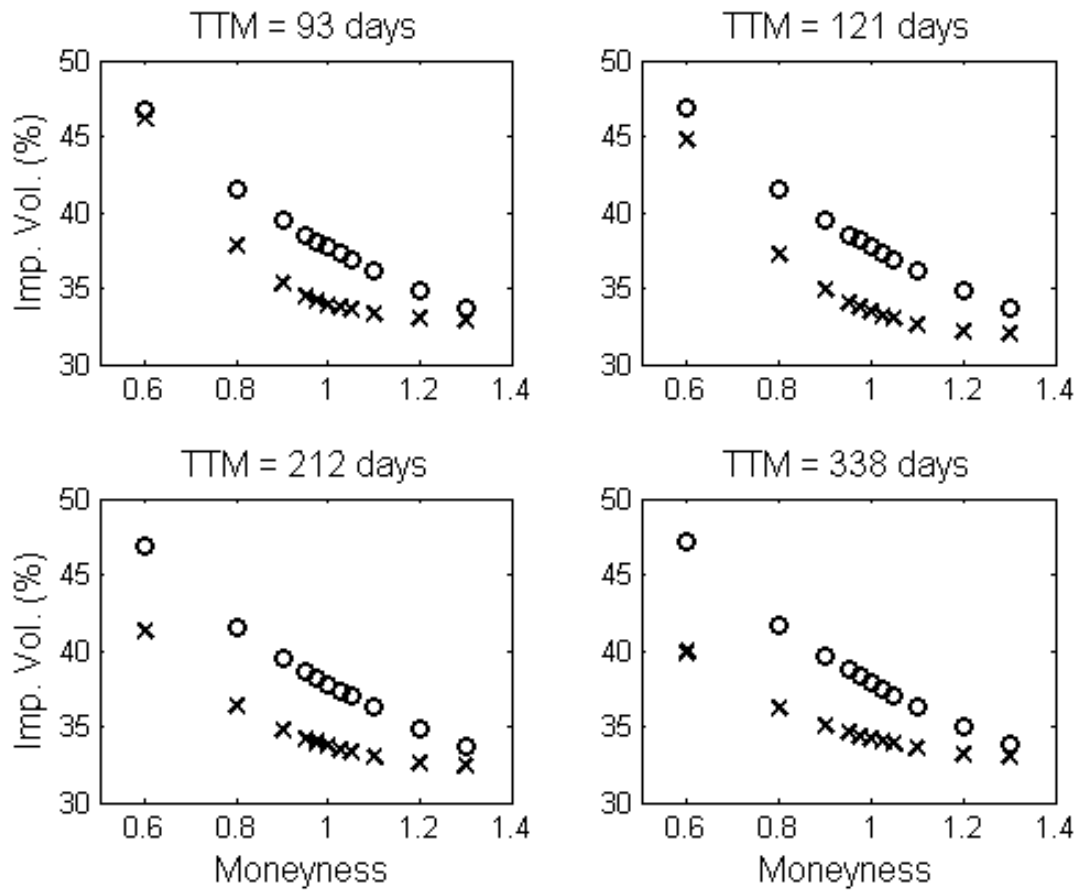
Figure 3.9: Implied volatility market data ("×") versus the GBM model data("○") on February 16 2011.
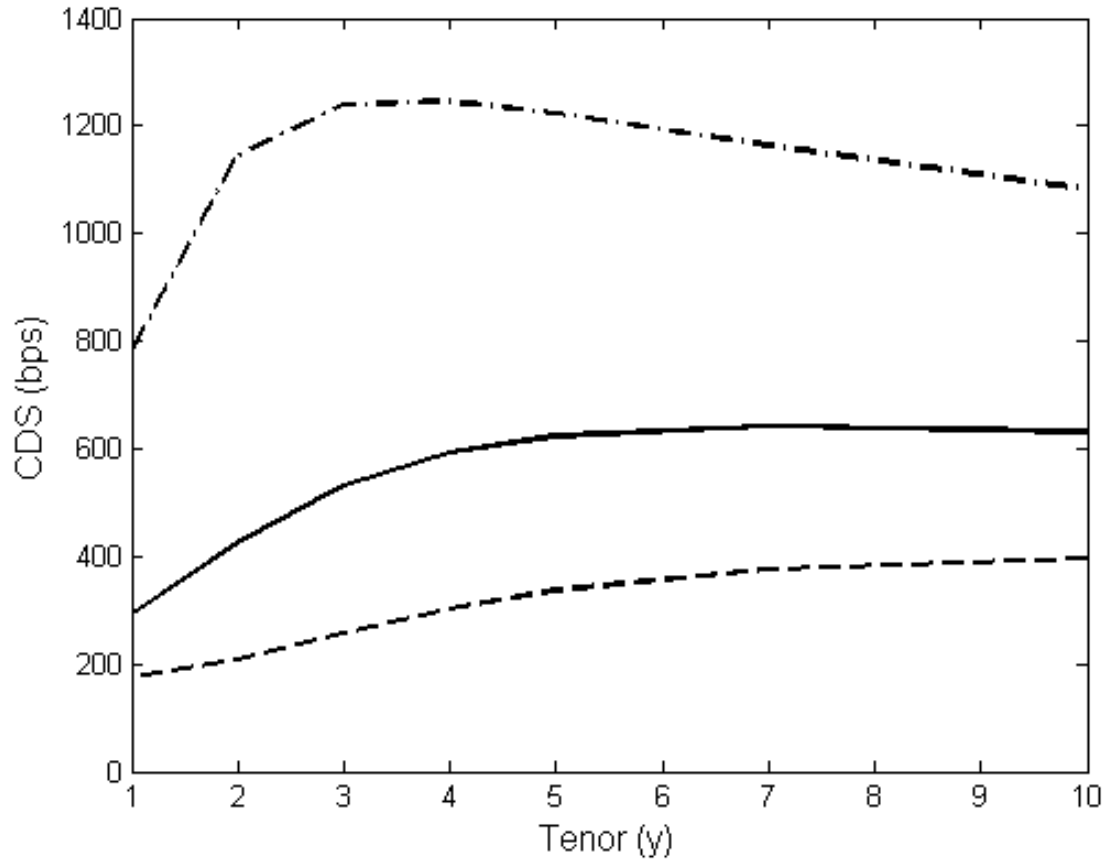
Figure 3.10: CDS spread sensitivities for the EXP model: computed from the 14/07/10 calibrated parameters (solid line), and from setting the log-asset value v_0 one standard deviation (σ_v) up (dashed line) and down (dash-dotted line) from the calibration.
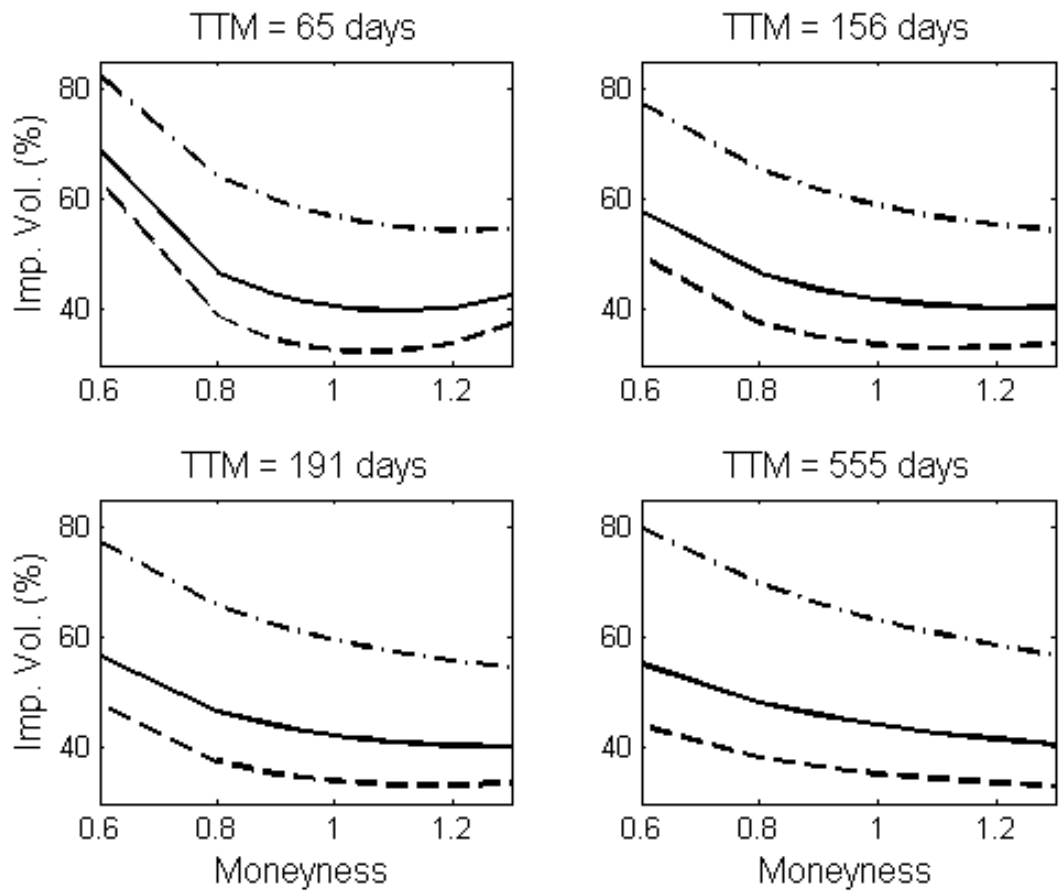
Figure 3.11: Implied volatility sensitivities for the EXP model: computed from the 14/07/10 calibrated parameters (solid line), and from setting the log-asset value v_0 one standard deviation (σ_v) up (dashed line) and down (dash-dotted line) from the calibration.

Chapter 4

A Fourier Transform Method for Spread Option Pricing

This chapter is originated from a published paper coauthored with Professor Hurd [59], to which the author of the thesis is an equal contributor. The full citation of the paper is: T. Hurd and Z. Zhou. A Fourier transform method for spread option pricing. *SIAM J. Financial Math.*, 1:142-157, 2010[1]. It should be noted that the references of the chapter are indexed to adapt to the thesis, therefore differ from the published paper. Another difference is the section *Additional Material* in the end of this chapter which is not included in the published paper.

4.1   Abstract

Spread options are a fundamental class of derivative contract written on multiple assets, and are widely traded in a range of financial markets. There is a long history of approximation methods for computing such products, but as yet there is no preferred approach that is accurate, efficient and flexible enough to apply in general asset models. The present paper introduces a new formula for general spread option pricing based on Fourier analysis of the payoff function. Our detailed investigation, including

a flexible and general error analysis, proves the effectiveness of a fast Fourier transform implementation of this formula for the computation of spread option prices. It is found to be easy to implement, stable, efficient and applicable in a wide variety of asset pricing models.

4.2 Introduction

When $S_{jt}, j = 1, 2, t \geq 0$ are two asset price processes, the basic spread option with maturity T and strike $K \geq 0$ is the contract that pays $(S_{1T} - S_{2T} - K)^+$ at time T. If we assume the existence of a risk-neutral pricing measure, the risk-neutral expectation formula for the time 0 price of this option, assuming a constant interest rate r, is

$$\text{Spr}(S_0; T, K) = e^{-rT}\mathbb{E}_{S_0}[(S_{1T} - S_{2T} - K)^+] . \tag{4.1}$$

The literature on applications of spread options is extensive, and is reviewed by Carmona and Durrleman [17] who explore further applications of spread options beyond the case of equities modelled by geometric Brownian motion, and in particular to energy trading. For example, the difference between the price of crude oil and a refined fuel such as natural gas is called a "crack spread". "Spark spreads" refer to differences between the price of electricity and the price of fuel: options on spark spreads are widely used by power plant operators to optimize their revenue streams. Energy pricing requires models with mean reversion and jumps very different from geometric Brownian motion, and pricing spread options in such situations can be challenging.

Closed formulas for (4.1) are known only for a limited set of asset models. In the Bachelier stock model, $S_t = (S_{1t}, S_{2t})$ is an arithmetic Brownian motion, and in this case (4.1) has a Black-Scholes type formula for any T, K. In the special case $K = 0$ when S_t is geometric Brownian motion, (4.1) is given by the Margrabe formula [82].

In the basic case where S_t is geometric Brownian motion and $K > 0$, no explicit pricing formula is known. Instead there is a long history of approximation methods for this problem. Numerical integration methods, typically Monte Carlo based, are often

employed. When possible, however, the fastest option pricing engines by numerical integration are usually those based on the fast Fourier transform methods introduced by Carr and Madan [23]. Their first interest was in single asset option pricing for geometric Lévy process models like the variance gamma (VG) model, but their basic framework has since been adapted to a variety of option payoffs and a host of asset return models where the characteristic function is known. In this work, when the payoff function is not square integrable, it is important to account for singularities in the Fourier transform variables.

Dempster and Hong [32] introduced a numerical integration method for spread options based on two-dimensional fast Fourier transforms (FFT) that was shown to be efficient when the asset price processes are geometric Brownian motion or to have stochastic volatility. Three more recent papers study the use of multi-dimensional convolution FFT methods to price a wide range of multi-asset options, including basket and spread options. These newer methods also compute by discretized Fourier transforms over truncated domains, but unlike earlier work using FFT, they apparently do not rely on knowing the analytic Fourier transform of the payoff function or integrability of the payoff function. Lord et.al [78] provide error analysis that explains their observation that errors decay as a negative power of the size N of the grid used in computing the FFT, provided the truncation is taken large enough. Oosterlee [71] propose a parallel partitioning approach to tackle the so-called curse of dimensionality when the number of underlying assets becomes large. Jackson et.al [62] proposed a general FFT pricing framework for multi-asset options, including variations with Bermudan early exercise features. These three papers all find that the FFT applied to the payoff function can perform well even if the payoff function is not square integrable and observe that errors can be made to decay as a negative power of N.

As an alternative to numerical integration methods, another stream uses analytical methods applicable to log normal models that involve linear approximations of the nonlinear exercise boundary. Such methods are often very fast, but their accuracy is usually not easy to determine. Kirk [66] presented an analytical approximation that performs well in practice. Carmona and Durrleman [18] and later Deng, Li and Zhou [35] demonstrate a number of lower and upper bounds for the spread option price

that combine to produce accurate analytical approximation formulas in log normal asset models. These results extend to approximate values for the Greeks.

The main purpose of the present paper is to give a numerical integration method for computing spread options in two or higher dimensions using the FFT. Unlike the above multi-asset FFT methods, it is based on square integrable integral formulas for the payoff function, and like those methods is applicable to a variety of spread option payoffs in any model for which the characteristic function of the joint return process is given analytically. Since our method involves only smooth square integrable integrands, the error estimates we present are quite straightforward and standard. In fact, we demonstrate that the asymptotic decay of errors is exponential, rather than polynomial, in the size N of the Fourier grid. For option payoffs that can be made square integrable, our method has the flexibility to handle a wide range of desirable asset return models, all with a very competitive computational expense.

The results we describe stem from the following new formula[2] that gives a square integrable Fourier representation of the basic spread option payoff function $P(x_1, x_2) = (e^{x_1} - e^{x_2} - 1)^+$.

Theorem 9. *For any real numbers $\epsilon = (\epsilon_1, \epsilon_2)$ with $\epsilon_2 > 0$ and $\epsilon_1 + \epsilon_2 < -1$ and $x = (x_1, x_2)$[3],*

$$P(x) = (2\pi)^{-2} \iint_{\mathbb{R}^2 + i\epsilon} e^{iux'} \hat{P}(u) d^2 u, \quad \hat{P}(u) = \frac{\Gamma(i(u_1 + u_2) - 1)\Gamma(-iu_2)}{\Gamma(iu_1 + 1)} . \quad (4.2)$$

Here $\Gamma(z)$ is the complex gamma function defined for $\Re e(z) > 0$ by the integral $\Gamma(z) = \int_0^\infty e^{-t} t^{z-1} dt$.

Using this theorem, whose proof is given in the Appendix, we will find we can follow the logic of Carr and Madan to derive numerical algorithms for efficient computation of a variety of spread options and their Greeks. The basic strategy to compute

---

[2]It came to our attention after the submission of our paper that the result of this Theorem has been simultaneously and independently stated in another working paper by A. Antonov and M. Arneguy [2].

[3]Here and in rest of the paper, some variables such as u, ϵ, x are defined to be row vectors with components $u = (u_1, u_2)$ etc. We use implied matrix multiplication so that $ux' = u_1 x_1 + u_2 x_2$ where x' denotes the (unconjugated) transpose of x.

(4.1) is to combine (4.2) with an explicit formula for the characteristic function of the bivariate random variable $X_t = (\log S_{1t}, \log S_{2t})$. For the remainder of this paper, we make a simplifying assumption.

Assumption 5. *For any $t > 0$, the increment $X_t - X_0$ is independent of X_0.*

This implies that the characteristic function of X_T factorizes:

$$\mathbb{E}_{X_0}[e^{iuX_T'}] = e^{iuX_0'}\Phi(u;T), \quad \Phi(u;T) := \mathbb{E}_{X_0}[e^{iu(X_T-X_0)'}] \ . \tag{4.3}$$

where $\Phi(u;T)$ is independent of X_0. Although the above assumption rules out mean-reverting processes that often arise in energy applications, it holds for typical stock models: moreover, the method we propose can be generalized to a variety of mean-reverting processes. Using Theorem 9 and (4.3), the spread option formula can be written as an explicit two-dimensional Fourier transform in the variable X_0:

$$
\begin{aligned}
\text{Spr}(X_0;T) &= e^{-rT}\mathbb{E}_{X_0}[(e^{X_{1T}} - e^{X_{2T}} - 1)^+] \\
&= e^{-rT}\mathbb{E}_{X_0}\left[(2\pi)^{-2}\iint_{\mathbb{R}^2+i\epsilon}e^{iuX_T'}\hat{P}(u)d^2u\right] \\
&= (2\pi)^{-2}e^{-rT}\iint_{\mathbb{R}^2+i\epsilon}\mathbb{E}_{X_0}[e^{iuX_T'}]\hat{P}(u)d^2u \\
&= (2\pi)^{-2}e^{-rT}\iint_{\mathbb{R}^2+i\epsilon}e^{iuX_0'}\Phi(u;T)\hat{P}(u)d^2u \ . \tag{4.4}
\end{aligned}
$$

The Greeks are handled in exactly the same way. For example, the Delta $\Delta^1 := \partial\text{Spr}/\partial S_{10}$ is obtained as a function of S_0 by replacing Φ in (4.4) by $\partial\Phi/\partial S_{10}$.

Double Fourier integrals like this can be approximated numerically by a two-dimensional FFT. Such approximations involve both a truncation and discretization of the integral, and the two properties that determine their accuracy are the decay of the integrand of (4.4) in u-space, and the decay of the function Spr in x-space. The remaining issue of computing the gamma function is not a real difficulty. Fast and accurate computation of the complex gamma function in for example, Matlab, is based on the Lanczos approximation popularized by [93][4].

---

[4]According to these authors, computing the gamma function becomes "not much more difficult than other built-in functions that we take for granted, such as $\sin x$ or e^x".

In this paper, we demonstrate how our method performs for computing spread options in three different two-asset stock models, namely geometric Brownian motion (GBM), a three factor stochastic volatility (SV) model and the variance gamma (VG) model. Section 2 provides the essential definitions of the three types of asset return models, including explicit formulas for their bivariate characteristic functions. Section 3 discusses how the two dimensional FFT can be implemented for our problem. Section 4 provides error analysis that shows how the accuracy and speed will depend on the implementation choices made. Section 5 describes briefly how the method extends to the computation of spread option Greeks. Section 6 gives the detailed results of the performance of the method in the three asset return models. In this section, the accuracy of each model is compared to benchmark values computed by an independent method for a reference set of option prices. We also demonstrate that the computation of the spread option Greeks in such models is equally feasible. Section 7 extends all the above results to several kinds of basket options on two or more assets. Although the formulation is simple, the resulting FFTs become in practice much slower to compute in higher dimensions, due to the so-called "curse of dimensionality": in such cases, one can implement the parallel partitioning approach of [71].

4.3   Three Kinds of Stock Models

4.3.1   The Case of Geometric Brownian Motion

In the two-asset Black-Scholes model, the vector $S_t = (S_{1t}, S_{2t})$ has components

$$S_{jt} = S_{j0} \exp[(r - \sigma_j^2/2)t + \sigma_j W_t^j], j = 1, 2$$

where $\sigma_1, \sigma_2 > 0$ and W^1, W^2 are risk-neutral Brownian motions with constant correlation $\rho, |\rho| < 1$. The joint characteristic function of $X_T = (\log S_{1T}, \log S_{2T})$ as a function of $u = (u_1, u_2)$ is of the form $e^{iuX_0'}\Phi(u; T)$ with

$$\Phi(u; T) = \exp[iu(rTe - \sigma^2 T/2)' - u\Sigma u' T/2] \tag{4.5}$$

where $e = (1, 1), \Sigma = [\sigma_1^2, \sigma_1\sigma_2\rho; \sigma_1\sigma_2\rho, \sigma_2^2]$ and $\sigma^2 = \text{diag } \Sigma$. We remind the reader that we use implied matrix multiplication, and that u' denotes the (unconjugated) matrix transpose. Substituting this expression into (4.4) yields the spread option formula

$$\text{Spr}(X_0; T) = (2\pi)^{-2} e^{-rT} \iint_{\mathbb{R}^2 + i\epsilon} e^{iuX_0'} \exp[iu(rTe - \sigma^2T/2)' - u\Sigma u'T/2]\hat{P}(u)d^2u .$$
(4.6)

As we discuss in Section 4, we recommend that this be computed numerically using the FFT.

4.3.2 Three Factor Stochastic Volatility Model

The spread option problem in a three factor stochastic volatility model was given as an example by Dempster and Hong [32]. Their asset model is defined by SDEs for $X_t = (\log S_{1t}, \log S_{2t})$ and the squared volatility v_t:

$$\begin{aligned}
dX_1 &= [(r - \delta_1 - \sigma_1^2/2)dt + \sigma_1\sqrt{v}dW^1] \\
dX_2 &= [(r - \delta_2 - \sigma_2^2/2)dt + \sigma_2\sqrt{v}dW^2] \\
dv &= \kappa(\mu - v)dt + \sigma_v\sqrt{v}dW^v
\end{aligned}$$

where the three Brownian motions have correlations:

$$\begin{aligned}
E[dW^1 dW^2] &= \rho dt \\
E[dW^1 dW^v] &= \rho_1 dt \\
E[dW^2 dW^v] &= \rho_2 dt.
\end{aligned}$$

As discussed in that paper, the asset return vector has the joint characteristic function $e^{iuX_0'}\Phi(u; T, v_0)$ where

$$\begin{aligned}
\Phi(u; T, v_0) &= \exp\left[\left(\frac{2\zeta(1 - e^{-\theta T})}{2\theta - (\theta - \gamma)(1 - e^{-\theta T})}\right)v_0 \right. \\
&\quad \left. +iu(re - \delta)'T - \frac{\kappa\mu}{\sigma_v^2}\left[2\log\left(\frac{2\theta - (\theta - \gamma)(1 - e^{-\theta T})}{2\theta}\right) + (\theta - \gamma)T\right]\right]
\end{aligned}$$

and

$$\begin{aligned}
\zeta &:= -\frac{1}{2}\left[\left(\sigma_1^2 u_1^2 + \sigma_2^2 u_2^2 + 2\rho\sigma_1\sigma_2 u_1 u_2\right) + i\left(\sigma_1^2 u_1 + \sigma_2^2 u_2\right)\right] \\
\gamma &:= \kappa - i(\rho_1\sigma_1 u_1 + \rho_2\sigma_2 u_2)\sigma_\nu \\
\theta &:= \sqrt{\gamma^2 - 2\sigma_v^2\zeta} \;.
\end{aligned}$$

4.3.3 Exponential Lévy Models

Many stock price models are of the form $S_t = e^{X_t}$ where X_t is a Lévy process for which the characteristic function is explicitly known. We illustrate with the example of the VG process introduced by [81], the three parameter process Y_t with Lévy characteristic triple $(0, 0, \nu)$ where the Lévy measure is $\nu(x) = \lambda[e^{-a_+ x}\mathbf{1}_{x>0} + e^{a_- x}\mathbf{1}_{x<0}]/|x|$ for positive constants $\lambda, a_\pm$. The characteristic function of Y_t is

$$\Phi_{Y_t}(u) = \left[1 + i\left(\frac{1}{a_-} - \frac{1}{a_+}\right)u + \frac{u^2}{a_- a_+}\right]^{-\lambda t}. \tag{4.7}$$

To demonstrate the effects of correlation, we take a bivariate VG model driven by three independent VG processes Y_1, Y_2, Y with common parameters $a_\pm$ and $\lambda_1 = \lambda_2 = (1-\alpha)\lambda$, $\lambda^Y = \alpha\lambda$. The bivariate log return process $X_t = \log S_t$ is a mixture:

$$X_{1t} = X_{10} + Y_{1t} + Y_t; \quad X_{2t} = X_{20} + Y_{2t} + Y_t \;. \tag{4.8}$$

Here $\alpha \in [0,1]$ leads to dependence between the two return processes, but leaves their marginal laws unchanged. An easy calculation leads to the bivariate characteristic function $e^{iuX_0'}\Phi(u;T)$ with

$$\begin{aligned}
\Phi(u;T) &= \left[1 + i\left(\frac{1}{a_-} - \frac{1}{a_+}\right)(u_1 + u_2) + \frac{(u_1 + u_2)^2}{a_- a_+}\right]^{-\alpha\lambda t} \\
&\times \left[1 + i\left(\frac{1}{a_-} - \frac{1}{a_+}\right)u_1 + \frac{u_1^2}{a_- a_+}\right]^{-(1-\alpha)\lambda t}\left[1 + i\left(\frac{1}{a_-} - \frac{1}{a_+}\right)u_2 + \frac{u_2^2}{a_- a_+}\right]^{-(1-\alpha)\lambda t}.
\end{aligned} \tag{4.9}$$

4.4 Numerical Integration by Fast Fourier Transform

To compute (4.4) in these models we approximate the double integral by a double sum over the lattice

$$\Gamma = \{u(k) = (u_1(k_1), u_2(k_2))|k = (k_1, k_2) \in \{0, \ldots, N-1\}^2\}, \quad u_i(k_i) = -\bar{u} + k_i\eta$$

for appropriate choices of $N, \eta, \bar{u} := N\eta/2$. For the FFT it is convenient to take N to be a power of 2 and lattice spacing η such that truncation of the u-integrals to $[-\bar{u}, \bar{u}]$ and discretization leads to an acceptable error. Finally, we choose initial values $X_0 = \log S_0$ to lie on the reciprocal lattice with spacing $\eta^* = 2\pi/N\eta = \pi/\bar{u}$ and width $2\bar{x}$, $\bar{x} = N\eta^*/2$:

$$\Gamma^* = \{x(\ell) = (x_1(\ell_1), x_2(\ell_2))|\ell = (\ell_1, \ell_2) \in \{0, \ldots, N-1\}^2\}, \ x_i(\ell_i) = -\bar{x} + \ell_i\eta^*, \ .$$

For any $S_0 = e^{X_0}$ with $X_0 = x(\ell) \in \Gamma^*$ we then have the approximation

$$\text{Spr}(X_0; T) \sim \frac{\eta^2 e^{-rT}}{(2\pi)^2} \sum_{k_1, k_2 = 0}^{N-1} e^{i(u(k) + i\epsilon)x(\ell)'} \Phi(u(k) + i\epsilon; T)\hat{P}(u(k) + i\epsilon) \ . \tag{4.10}$$

Now, as usual for the discrete FFT, as long as N is even,

$$iu(k)x(\ell)' = i\pi(k_1 + k_2 + \ell_1 + \ell_2) + 2\pi ik\ell'/N \pmod{2\pi i} \ .$$

This leads to the double inverse discrete Fourier transform (i.e. the Matlab function "ifft2")

$$\begin{aligned}
\text{Spr}(X_0; T) &\sim (-1)^{\ell_1 + \ell_2} e^{-rT} \left(\frac{\eta N}{2\pi}\right)^2 e^{-\epsilon x(\ell)'} \left[\frac{1}{N^2} \sum_{k_1, k_2 = 0}^{N-1} e^{2\pi ik\ell'/N} H(k)\right] \\
&= (-1)^{\ell_1 + \ell_2} e^{-rT} \left(\frac{\eta N}{2\pi}\right)^2 e^{-\epsilon x(\ell)'} [\text{ifft2}(H)](\ell) \tag{4.11}
\end{aligned}$$

where

$$H(k) = (-1)^{k_1 + k_2} \Phi(u(k) + i\epsilon; T)\hat{P}(u(k) + i\epsilon) \ .$$

4.5   Error Discussion

The selection of suitable values for ϵ, N and η when implementing the above FFT approximation of (4.4) is a somewhat subtle issue whose details depend on the asset model in question. We now give a general discussion of the pure truncation error and pure discretization error in (4.10): a more complete analysis of the combined errors using methods described in [70] will lead to the same broad conclusions.

The pure truncation error, defined by taking $\eta \to 0, N \to \infty$ while keeping $\bar{u} = N\eta/2$ fixed, can be made smaller than $\delta_1 \ll 1$ if the integrand of (4.4) is small and decaying outside the square $[-\bar{u} + i\epsilon_1, \bar{u} + i\epsilon_1] \times [-\bar{u} + i\epsilon_2, \bar{u} + i\epsilon_2]$. Corollary 12, proved in the Appendix, gives a uniform $O(|u|^{-2})$ upper bound on $\hat{P}$, while $\Phi(u)$ can generally be seen directly to have some u-decay. Thus the truncation error will be less than δ_1 if one picks $\bar{u}$ large enough so that $|\Phi| < O(\delta_1)$ and has decay outside the square.

The pure discretization error, defined by taking $\bar{u} \to \infty, N \to \infty$ while keeping $\bar{x} = \pi/\eta$ fixed, can be made smaller than $\delta_2 \ll 1$ if $e^{\epsilon X_0'}\mathrm{Spr}(X_0)$, taken as a function of $X_0 \in \mathbb{R}^2$, has rapid decay in X_0. This is related to the smoothness of $\Phi(u)$ and the choice of ϵ. The first two models are not very sensitive to ϵ, but in the VG model the following conditions are needed to ensure that singularities in u space are avoided:

$$-a_+ < \epsilon_1, \epsilon_2, \epsilon_1 + \epsilon_2 < a_- \ .$$

By applying the Poisson Summation Formula to $e^{\epsilon X_0'}\mathrm{Spr}(X_0)$, one can write the discretization error as

$$\mathrm{Spr}^{(\bar{x})}(X_0) - \mathrm{Spr}(X_0) = \sum_{\ell \in \mathbb{Z}^2 \backslash \{(0,0)\}} e^{2\bar{x}\epsilon\ell'}\mathrm{Spr}(X_0 + 2\bar{x}\ell) \ . \qquad (4.12)$$

One can verify using brute force bounds that the terms on the right hand side of (4.12) are all small and decay in all lattice directions, provided $\bar{x}$ is sufficiently large. Thus the discretization error will be less than δ_2 for all $X_0 \in [-c\bar{x}, c\bar{x}]^2$ with $0 < c \ll 1$ if one picks $\bar{x}$ large enough so that $|e^{\epsilon X_0'}\mathrm{Spr}(X_0)| < O(\delta_2)$ and has decay outside the square $[-\bar{x}, \bar{x}]^2$.

In summary, one expects that the combined truncation and discretization error will be close to $\delta_1 + \delta_2$ if $\bar{u} = N\eta/2$ and $\eta = \pi/\bar{x}$ are each chosen as above. We shall see in Section 6 that the observed errors are consistent with the above analysis that predicts an asymptotic exponential decay with the size N of the Fourier lattice for the models we address.

4.6 Greeks

The FFT method can also be applied to the Greeks, enabling us to tackle hedging and other interesting problems. It is particularly efficient for the GBM model, where differentiation under the integral sign is always permissible. For instance, the FFT formula for vega (the sensitivity to σ) takes the form:

$$
\begin{aligned}
\frac{\partial \mathrm{Spr}(S_0; T)}{\partial \sigma_1} &= (-1)^{\ell_1 + \ell_2} e^{-rT} \left(\frac{\eta N}{2\pi}\right)^2 e^{-\epsilon x(\ell)'}[\mathrm{ifft2}(\frac{\partial H}{\partial \sigma_1})](\ell) ; \\
\frac{\partial H(k)}{\partial \sigma_1} &= \left[-(u(k) + i\epsilon) \left(i\frac{\partial \sigma^{2'}}{\partial \sigma_1} + \frac{\partial \Sigma}{\partial \sigma_1}(u(k) + i\epsilon)'\right) T/2 \right] H(k) ,
\end{aligned}
$$

where $\frac{\partial \sigma^2}{\partial \sigma_1} = [2\sigma_1, 0]$ and $\frac{\partial \Sigma}{\partial \sigma_1} = [2\sigma_1, \rho\sigma_2; \rho\sigma_2, 0]$. Other Greeks including those of higher orders can be computed in similar fashion. This method needs to be used with care for the SV and VG models, since it is possible that differentiation leads to an integrand that decays slowly.

4.7 Numerical Results

Our numerical experiments were coded and implemented in Matlab version 7.6.0 on an Intel 2.80 GHz machine running under Linux with 1 GB physical memory. If they were coded in C++ with similar algorithms, we should expect to see faster performance.

The strength of the FFT method is demonstrated by comparison with accurate benchmark prices computed by an independent (usually extremely slow) method.

Based on a representative selection of initial log-asset value pairs $\log S_{10}^i = \frac{i\pi}{10}$, $\log S_{20}^j = -\frac{\pi}{5} + \frac{j\pi}{10}$, $i, j \in 1, 2, 3 \ldots 6$, the objective function we measure is defined as

$$\text{Err} = \frac{1}{36} \sum_{i,j=1}^{6} |\log(M^{ij}) - \log(B^{ij})| \tag{4.13}$$

where M^{ij} and B^{ij} are the corresponding FFT computed prices and benchmark prices. These choices cover a wide range of moneyness, from deep out-of-the-money to deep in-the-money. Since these combinations all lie on lattices Γ^* corresponding to $N = 2^n$ and $\bar{u}/10 = 2^m$ for integers n, m, all 36 prices M^{ij} can be computed simultaneously with a single FFT.

Figure 4.1 shows how the FFT method performs in the 2-dimensional Geometric Brownian motion model for different choices of N and $\bar{u}$. Since the two factors are bivariate normal, benchmark prices can be calculated to high accuracy by one dimensional integrations. In Figure 4.1 we can clearly see the effects of both truncation errors and discretization errors. For a fixed $\bar{u}$, the objective function decreases when N increases. The $\bar{u} = 20$ curve flattens out near 10^{-5} due to its truncation error of that magnitude. In turn, we can quantify its discretization errors with respect to N by subtracting the truncation error from the total error. The flattening of the curves with $\bar{u} = 40$, 80 and 160 near 10^{-14} should be attributed to Matlab round-off errors: because of the rapid decrease of the characteristic function Φ, their truncation error is negligible. For a fixed N, increasing $\bar{u}$ brings two effects: reducing truncation error and enlarging discretization error. These effects are well demonstrated in Figure 4.1.

For the stochastic volatility model, no analytical or numerical method we know is consistently accurate enough to serve as an independent benchmark. Instead, we computed benchmark prices using the FFT method itself with $N = 2^{12}$ and $\bar{u} = 80$. The resulting objective function shows similar behaviour to Figure 4.1, and is consistent with accuracies at the level of round-off. We also verified that the benchmark prices are consistent to a level of 4×10^{-4} with those resulting from an intensive Monte Carlo computation using $1,000,000$ simulations, each consisting of 2000 time steps. The computational cost to further reduce the Monte Carlo simulation error becomes prohibitive.

Figure 4.1: This graph shows the objective function Err for the numerical computation of the GBM spread option versus the benchmark. Errors are plotted against the grid size for different choices of $\bar{u}$. The parameter values are taken from [32]: $r = 0.1, T = 1.0, \rho = 0.5, \delta_1 = 0.05, \sigma_1 = 0.2, \delta_2 = 0.05, \sigma_2 = 0.1$.

Because the VG process has an explicit probability density function in terms of a Bessel function [80], rather accurate benchmark spread option values for the VG model can be computed by a three dimensional integration[5]. We used a Gaussian quadrature algorithm set with a high tolerance of 10^{-9} to compute the integrals for these benchmarks. The resulting objective function for various values of $\bar{u}, N$ is shown in Figure 4.3. The truncation error for $\bar{u} = 20$ is about 2×10^{-5}. The other three curves flatten out near 5×10^{-8}, a level we identify as the accuracy of the benchmark. A comparable graph (not shown), using benchmark prices computed with the FFT

---

[5]We thank a referee for this suggestion.
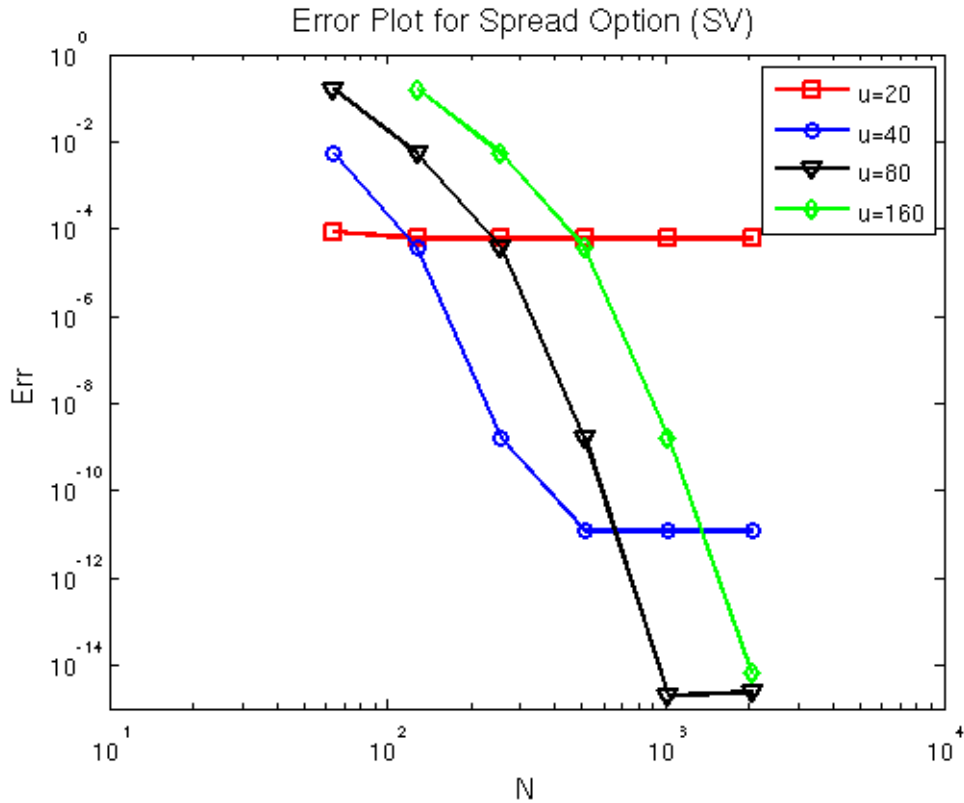
Figure 4.2: This graph shows the objective function Err for the numerical computation of the SV spread option versus the benchmark computed using the FFT method itself with parameters $N = 2^{12}$ and $\bar{u} = 80$. The parameter values are taken from [32]: $r = 0.1, T = 1.0, \rho = 0.5, \delta_1 = 0.05, \sigma_1 = 1.0, \rho_1 = -0.5, \delta_2 = 0.05, \sigma_2 = 0.5, \rho_2 = 0.25, v_0 = 0.04, \kappa = 1.0, \mu = 0.04, \sigma_v = 0.05$.

method with $N = 2^{12}$ and $\bar{u} = 80$, showed similar behaviour to Figures 4.1 and 4.2, and is consistent with the FFT method being capable of producing accuracies at the level of round-off.

The strength of the FFT method is further illustrated by the computation of individual prices and relative errors shown in Tables 4.1 to 4.3. One can observe that an FFT with $N = 256$ is capable of producing very high accuracy in all three models. It is interesting to note that FFT prices in almost all cases were biased low compared to the benchmark. Exceptions to this observation only seem to appear at a level of
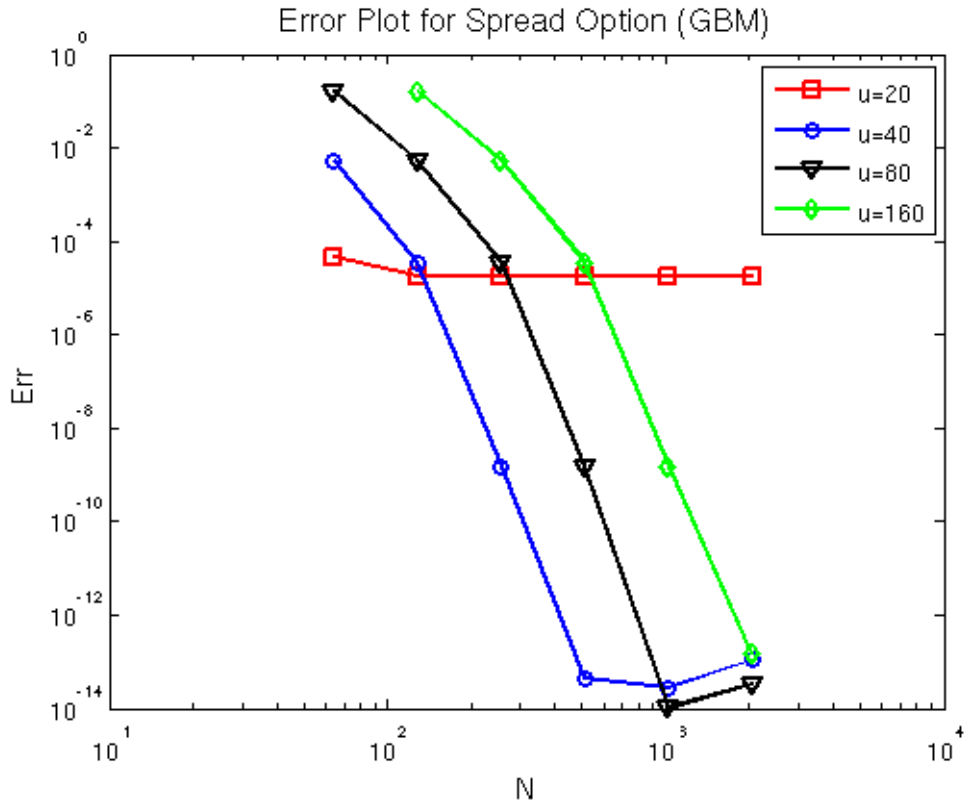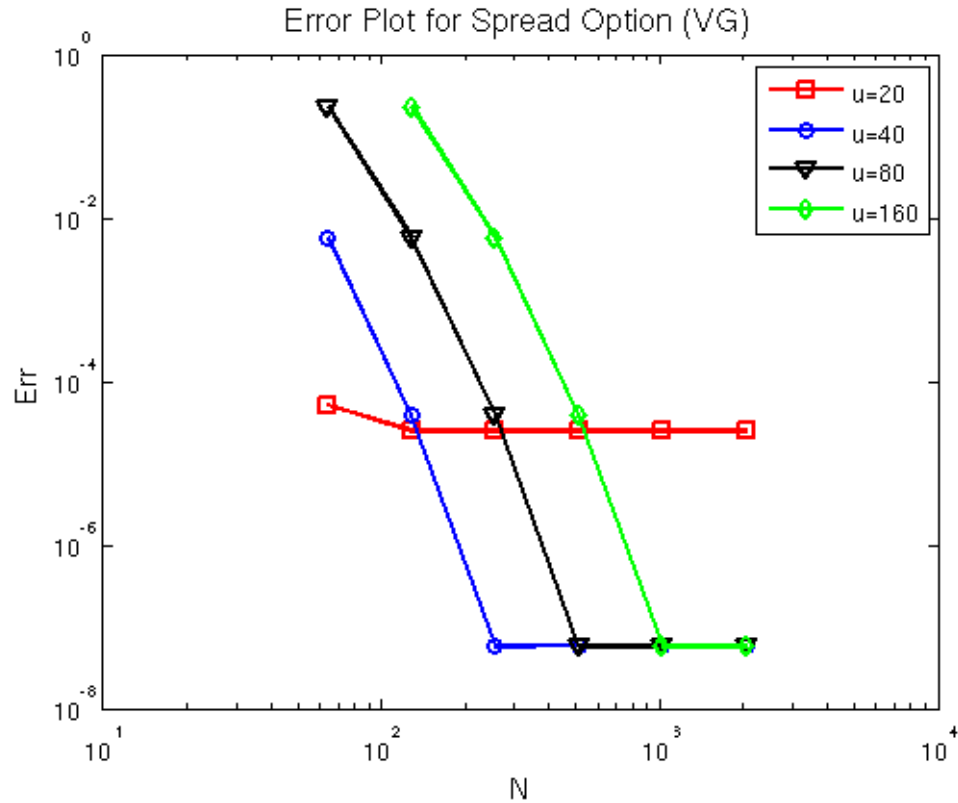
Figure 4.3: This graph shows the objective function Err for the numerical computation of the VG spread option versus the benchmark values computed with a three dimensional integration. Errors are plotted against the grid size for five different choices of $\bar{u}$. The parameters are: $r = 0.1, T = 1.0, \rho = 0.5, a_+ = 20.4499, a_- = 24.4499, \alpha = 0.4, \lambda = 10$.

the accuracy of the benchmark itself.

The FFT computes in a single iteration an $N \times N$ panel of prices *spread* corresponding to initial values $S_{10} = e^{x_{10}+\ell_1\eta^*}$, $S_{20} = e^{x_{20}+\ell_2\eta^*}$, $K = 1$, $(\ell_1, \ell_2) \in \{0, \ldots, N-1\}^2$. If the desired selection of $\{S_{10}, S_{20}, K\}$ fits into this panel of prices, or its scaling, a single FFT suffices. If not, then one has to match (x_{10}, x_{20}) with each combination, and run several FFTs, with a consequent increase in computation time. However, we have found that an interpolation technique is very accurate for practical purposes. For instance, prices for multiple strikes with the same

Table 4.1: Benchmark prices for the two-factor GBM model of [32] and relative errors for the FFT method with different choices of N. The parameter values are the same as Figure 4.1 except we fix $S_{10} = 100, S_{20} = 96, \bar{u} = 40$. The interpolation is based on a matrix of prices with discretization of $N = 256$ and a polynomial with degree of 8.

Strike K	Benchmark	64	128	256	512	Interpolation
0.4	8.312461	-3.8	-4.5E-4	-1.9E-8	-1.7E-14	1.9E-8
0.8	8.114994	-3.8E-1	-4.6E-4	-2.0E-8	-7E-15	2.0E-8
1.2	7.920820	-7.3E-2	-4.6E-4	-2.0E-8	-2.8E-14	2.0E-8
1.6	7.729932	-7.2E-2	-4.7E-4	-2.0E-8	-4.8E-14	2.0E-8
2.0	7.542324	-7.3E-2	-4.8E-4	-2.1E-8	-4.9E-14	2.1E-8
2.4	7.357984	-7.5E-2	-4.9E-4	-2.1E-8	-7.3E-14	2.1E-8
2.8	7.176902	-7.6E-2	-5.0E-4	-2.2E-8	-6.8E-14	2.2E-8
3.2	6.999065	-7.8E-2	-5.1E-4	-2.2E-8	-9.7E-14	2.2E-8
3.6	6.824458	-8.0E-2	-5.3E-4	-2.3E-8	-8.2E-14	2.3E-8
4.0	6.653065	-8.1E-2	-5.4E-4	-2.3E-8	-9.0E-14	2.3E-8

S_{10} and S_{20} are approximated by a polynomial fit along the diagonal of the price panel: $\mathrm{Spr}(S_0; K_1) = K_1 \cdot spread(1,1)$, $\mathrm{Spr}(S_0; K_1 e^{-\eta^*}) = K_1 e^{-\eta^*} \cdot spread(2,2)$, $\mathrm{Spr}(S_0; K_1 e^{-2\eta^*}) = K_1 e^{-2\eta^*} \cdot spread(3,3) \dots$. The results of this technique are recorded in Tables 4.2 to 4.3 in the column "Interpolation". We can see this technique generates very accurate results and moreover, saves computational resources.

Finally, we computed first order Greeks using the method described at the beginning of Section 4.4 and compared them with finite differences. As seen in Table 4.4, the two methods come up with very consistent results. The Greeks of our at-the-money spread option exhibit some resemblance to those of the at-the-money European put/call option. The delta of S_1 is close to the delta of the call option, which is about 0.5. And the delta of S_2 is close to the delta of the put option, which is also about 0.5. The time premium of the spread option is positive. The option price is much more sensitive to S_1 volatility than to S_2 volatility. It is an important feature that the option price is negatively correlated with the underlying correlation: Intuitively speaking, if the two underlyings are strongly correlated, their co-movements diminish the probability that S_{1T} develops a wide spread over S_{2T}. This result is consistent

Table 4.2: Benchmark prices for the 3 factor SV model of [32] and relative errors for the FFT method with different choices of N. The parameter values are the same as Figure 4.2 except we fix $S_{10} = 100, S_{20} = 96, \bar{u} = 40$. The interpolation is based on a matrix of prices with discretization of $N = 256$ and a polynomial with degree of 8.

Strike K	Benchmark	64	128	256	512	Interpolation
2.0	7.548502	-7.3E-2	-4.8E-4	-2.1E-8	1.6E-11	-2.1E-8
2.2	7.453536	-7.4E-2	-4.9E-4	-2.1E-8	1.2E-11	-2.1E-8
2.4	7.359381	-7.5E-2	-4.8E-4	-2.1E-8	8.6E-12	-2.1E-8
2.6	7.266037	-7.5E-2	-5.0E-4	-2.1E-8	4.6E-12	-2.1E-8
2.8	7.173501	-7.6E-2	-5.0E-4	-2.2E-8	6.1E-13	-2.2E-8
3.0	7.081775	-7.7E-2	-5.1E-4	-2.2E-8	-3.5E-12	-2.2E-8
3.2	6.990857	-7.8E-2	-5.2E-4	-2.2E-8	-7.7E-12	-2.2E-8
3.4	6.900745	-7.9E-2	-5.2E-4	-2.2E-8	-1.2E-11	-2.2E-8
3.6	6.811440	-8.0E-2	-5.3E-4	-2.3E-8	-1.7E-11	-2.3E-8
3.8	6.722939	-8.1E-2	-5.3E-4	-2.3E-8	-2.0E-11	-2.3E-8
4.0	6.635242	-8.1E-2	-5.4E-4	-2.3E-8	-2.4E-11	-2.3E-8

with observations made by [35].

Since the FFT method naturally generates a panel of prices, and interpolation can be implemented accurately with negligible additional computational cost, it is appropriate to measure the efficiency of the method by timing the computation of a panel of prices. Such computing times are shown in Table 4.5. For the FFT method, the main computational cost comes from the calculation of the matrix H in (4.11) and the subsequent FFT of H. We see that the GBM model is noticeably faster than the SV and VG models: This is due to a recursive method used to calculate the H matrix entries of the GBM model, which is not applicable for the SV and VG models. The number of calculations for H is of order N^2 which for large N exceeds the $N\log N$ of the FFT of H, and thus the advantage of this efficient algorithm for GBM is magnified as N increases. However, our FFT method is still very fast for the SV and VG models and is able to generate a large panel of prices within a couple of seconds.

Table 4.3: Benchmark prices for the VG model and relative errors for the FFT method with different choices of N. The parameter values are the same as Figure 4.3 except we fix $S_{10} = 100, S_{20} = 96, \bar{u} = 40$. The interpolation is based on a matrix of prices with discretization of $N = 256$ and a polynomial with degree of 8.

Strike K	Benchmark	64	128	256	512	Interpolation
2.0	9.727458	-5.9E-2	-3.9E-4	1.5E-8	3.2E-8	1.5E-8
2.2	9.630005	-5.9E-2	-3.9E-4	1.7E-8	3.4E-8	1.7E-8
2.4	9.533199	-6.0E-2	-3.9E-4	1.8E-8	3.5E-8	1.8E-8
2.6	9.437040	-6.0E-2	-4.0E-4	2.0E-8	3.7E-8	2.0E-8
2.8	9.341527	-6.0E-2	-4.0E-4	2.5E-8	4.3E-8	2.5E-8
3.0	9.246662	-6.1E-2	-4.0E-4	2.5E-8	4.3E-8	2.5E-8
3.2	9.152445	-6.1E-2	-4.1E-4	2.3E-8	4.1E-8	2.3E-8
3.4	9.058875	-6.2E-2	-4.1E-4	3.0E-8	4.8E-8	3.0E-8
3.6	8.965954	-6.2E-2	-4.1E-4	3.0E-8	4.8E-8	3.0E-8
3.8	8.873681	-6.3E-2	-4.2E-4	2.8E-8	4.6E-8	2.8E-8
4.0	8.782057	-6.4E-2	-4.2E-4	2.9E-8	4.7E-8	2.9E-8

4.8 High Dimensional Basket Options

The ideas of Section 2 turn out to extend naturally to two particular classes of basket options on $M \geq 2$ assets.

Proposition 10. *Let $M \geq 2$.*

1. *For any real numbers $\epsilon = (\epsilon_1, \ldots, \epsilon_M)$ with $\epsilon_m > 0$ for $2 \leq m \leq M$ and $\epsilon_1 < -1 - \sum_{m=2}^M \epsilon_m$*

$$\left(e^{x_1} - \sum_{m=2}^M e^{x_m} - 1 \right)^+ = (2\pi)^{-M} \int_{\mathbb{R}^M + i\epsilon} e^{iux'} \hat{P}^M(u) d^M u \qquad (4.14)$$

where for $u = (u_1, \ldots, u_M) \in \mathbb{C}^M$

$$\hat{P}^M(u) = \frac{\Gamma(i(u_1 + \sum_{m=2}^M u_m) - 1) \prod_{m=2}^M \Gamma(-iu_m)}{\Gamma(iu_1 + 1)}. \qquad (4.15)$$

2. *For any real numbers $\epsilon = (\epsilon_1, \ldots, \epsilon_M)$ with $\epsilon_m > 0$ for all $m \leq M$*

$$\left(1 - \sum_{m=1}^M e^{x_m} \right)^+ = (2\pi)^{-M} \int_{\mathbb{R}^M + i\epsilon} e^{iux'} \hat{Q}^M(u) d^M u \qquad (4.16)$$

Table 4.4: The Greeks for the GBM model compared between the FFT method and the finite difference method. The FFT method uses $N = 2^{10}$ and $\bar{u} = 40$. The finite difference uses a two-point central formula, in which the displacement is $\pm 1\%$. Other parameters are the same as Table 4.1 except that we fix the strike $K = 4.0$ to make the option at-the-money.

	Delta(S1)	Delta(S2)	Theta	Vega(σ_1)	Vega(σ_2)	$\partial Spr/\partial \rho$
FD	0.512648	-0.447127	3.023823	33.114315	-0.798959	-4.193749
FFT	0.512705	-0.447079	3.023777	33.114834	-0.798972	-4.193728

Table 4.5: Computing time of FFT for a panel of prices.

Discretization	GBM	SV	VG
64	0.091647	0.083326	0.109537
128	0.099994	0.120412	0.139276
256	0.126687	0.234024	0.220364
512	0.240938	0.711395	0.621074
1024	0.609860	2.628901	2.208770
2048	2.261325	10.243228	8.695122

where for $u = (u_1, \ldots, u_M) \in \mathbb{C}^M$

$$\hat{Q}^M(u) = \frac{\prod_{m=1}^{M} \Gamma(-iu_m)}{\Gamma(-i \sum_{m=1}^{M} u_m + 2)}. \tag{4.17}$$

Remark: Clearly, these two results can be applied directly to obtain an M-dimensional FFT method to price M-asset basket options that payoff either $(S_{1T} - S_{2T} - \cdots - S_{MT} - 1)^+$ or $(1 - S_{1T} - S_{2T} - \cdots - S_{MT})^+$. However, it is important to also note that by a generalized "put-call parity", one can also price options that payoff either $(1 + S_{2T} + \cdots + S_{MT} - S_{1T})^+$ or $(S_{1T} + S_{2T} + \cdots + S_{MT} - 1)^+$.

Proof: The proof of both parts of the above Proposition is based on a simple lemma proved in the Appendix:

Lemma 11. *Let $z \in \mathbb{R}$ and $u = (u_1, \ldots, u_M)' \in \mathbb{C}^M$ with $\Im m(u_m) > 0$ for all $m \leq M$. Then*

$$\int_{\mathbb{R}^M} e^z \delta(e^z - \sum_{m=1}^{M} e^{x_m}) e^{-iux'} d^M x = \frac{\prod_{m=1}^{M} \Gamma(-iu_m)}{\Gamma(-i \sum_{m=1}^{M} u_m)} e^{-i(\sum_{m=1}^{M} u_m)z} . \qquad (4.18)$$

To prove (4.15), we need to compute for $u \in \mathbb{C}^M$,

$$\hat{P}^M(u) = \int_{\mathbb{R}^M} (e^{x_1} - \sum_{m=2}^{M} e^{x_m} - 1)^+ e^{-i\tilde{u}\tilde{x}} d^M x.$$

We introduce the factor $1 = \int_{\mathbb{R}} \delta(e^z - \sum_{m=2}^{M} e^{x_m}) e^z dz$ and interchange the z integral with the x integrals. Then using Lemma 11 one finds

$$\begin{aligned}
\hat{P}^M(u) &= \int_{\mathbb{R}^2} (e^{x_1} - e^z - 1)^+ \left[\int_{\mathbb{R}^{M-1}} e^z \delta(e^z - \sum_{m=2}^{M} e^{x_m}) e^{-iux'} dx_2 \ldots dx_M \right] dx_1 dz \\
&= \frac{\prod_{m=2}^{M} \Gamma(-iu_m)}{\Gamma(-i \sum_{m=2}^{M} u_m)} \int_{\mathbb{R}^2} e^{-iu_1 x_1} e^{-i(\sum_{m=2}^{M} u_m)z} (e^{x_1} - e^z - 1)^+ dx_1 dz
\end{aligned}$$

We can then apply Theorem 9 and obtain the result.

The proof of (4.17) is similar to the proof of (4.15), where the two dimensional problem can be deduced first and extended to higher dimension with the application of Lemma 11.

$\square$

4.9   Conclusion

This paper presents a new approach to the valuation of spread options, an important class of financial contracts. The method is based on a newly discovered explicit formula for the Fourier transform of the spread option payoff in terms of the gamma function. In the final section we extended this formula to spread options in all dimensions, and a certain class of basket options.

This mathematical result leads to simple and transparent algorithms for pricing spread options and other basket options in all dimensions. We have shown that

the powerful tool of the Fast Fourier Transform provides an accurate and efficient implementation of the pricing formula in low dimensions. For implementation of higher dimensional problems, the curse of dimensionality sets in, and such cases should proceed using parallel partitioning methods as introduced in [71]. The difficulties and pitfalls of the FFT, of which there are admittedly several, are by now well understood, and thus the reliability and stability properties of our method are clear. We present a detailed discussion of errors, and show which criteria determine the optimal choice of implementation parameters.

Many important processes in finance, particularly affine models and Lévy jump models, have well known explicit characteristic functions, and can be included in the method with little difficulty. Thus the method can be easily applied to important problems arising in energy and commodity markets.

Finally, the Greeks can be systematically evaluated for such models, with similar performance and little extra work.

While our method provides a basic analytic framework for spread options, much as has been done for one-dimensional options, it is certainly possible to add refinements that will improve convergence rates. Such techniques might include, for example, analytic computation of residues combined with contour deformation.

4.10   Appendix: Proof of Theorem 9 and Lemma 11

Proof of Theorem 9:   Suppose $\epsilon_2 > 0, \epsilon_1 + \epsilon_2 < -1$. One can then verify either directly or from the argument that follows that $e^{\epsilon \cdot x} P(x), \epsilon = (\epsilon_1, \epsilon_2)$ is in $\mathbb{L}^2(\mathbb{R}^2)$. Therefore, application of the Fourier inversion theorem to $e^{\epsilon \cdot x} P(x), \epsilon = (\epsilon_1, \epsilon_2)$ implies that

$$P(x) = (2\pi)^{-2} \iint_{\mathbb{R}^2 + i\epsilon} e^{iu \cdot x} g(u) d^2 u \qquad (4.19)$$

where

$$g(u) = \iint_{\mathbb{R}^2} e^{-iu \cdot x} P(x) d^2 x \ .$$

By restricting to the domain $\{x : x_1 > 0, e^{x_2} < e^{x_1} - 1\}$ we have

$$
\begin{aligned}
g(u) &= \int_0^\infty e^{-iu_1x_1} \left[\int_{-\infty}^{\log(e^{x_1}-1)} e^{-iu_2x_2}[(e^{x_1}-1) - e^{x_2}]dx_2 \right] dx_1 \\
&= \int_0^\infty e^{-iu_1x_1}(e^{x_1}-1)^{1-iu_2} \left[\frac{1}{-iu_2} - \frac{1}{1-iu_2} \right] dx_1 .
\end{aligned}
$$

The change of variables $z = e^{-x_1}$ then leads to

$$
g(u) = \frac{1}{(1-iu_2)(-iu_2)} \int_0^1 z^{iu_1} \left(\frac{1-z}{z} \right)^{1-iu_2} \frac{dz}{z} .
$$

The beta function

$$
B(a,b) = \frac{\Gamma(a)\Gamma(b)}{\Gamma(a+b)}
$$

is defined for any complex a, b with $\Re e(a), \Re e(b) > 0$ by

$$
B(a,b) = \int_0^1 z^{a-1}(1-z)^{b-1}dz .
$$

From this, and the property $\Gamma(z) = (z-1)\Gamma(z-1)$ follow the formulas

$$
g(u) = \frac{\Gamma(i(u_1+u_2)-1)\Gamma(-iu_2+2)}{(1-iu_2)(-iu_2)\Gamma(iu_1+1)} = \frac{\Gamma(i(u_1+u_2)-1)\Gamma(-iu_2)}{\Gamma(iu_1+1)} . \tag{4.20}
$$

$\square$

The above derivation also leads to the following bound on $\hat{P}$.

Corollary 12. *Fix $\epsilon_2 = \epsilon, \epsilon_1 = -1 - 2\epsilon$ for some $\epsilon > 0$. Then*

$$
|\hat{P}(u_1, u_2)| \leq \frac{\Gamma(\epsilon)\Gamma(2+\epsilon)}{\Gamma(2+2\epsilon)} \cdot \frac{1}{Q(|u|^2/5)^{1/2}} \tag{4.21}
$$

where $Q(z) = (z + \epsilon^2)(z + (1+\epsilon)^2)$.

Proof: First note that for $z_1, z_2 \in \mathbb{C}$, $|B(z_1, z_2)| \leq B(\Re e(z_1), \Re e(z_2))$. Then (4.20) and a symmetric formula with $u_2 \leftrightarrow -1 - u_1 - u_2$ leads to the upper bound

$$
|\hat{P}(u_1 - i(\epsilon+1), u_2 + i\epsilon)| \leq B(\epsilon, 2+\epsilon) \min\left(\frac{1}{Q(|u_2|)}, \frac{1}{Q(|u_1+u_2|)} \right) .
$$

But since Q is monotonic and $|u| \leq \sqrt{5} \max(|u_2|, |u_1 + u_2|)$ for all $u \in \mathbb{R}^2$, the required result follows. $\qquad\square$

Proof of Lemma 11: We make the change of variables $p = e^z$ and $q_m = e^{x_m}$ and prove by induction that

$$\int_{\mathbb{R}^M} p\delta(p - \sum_{m=1}^M q_m) \prod_{m=1}^M q_m^{-iu_m-1} d^M q = \frac{\prod_{m=1}^M \Gamma(-iu_m)}{\Gamma(-i\sum_{m=1}^M u_m)} p^{-i(\sum_{m=1}^M u_m)} . \qquad (4.22)$$

The above equation trivially holds when $M = 1$. Supposing it holds for $M = N$, then for $M = N+1$ one finds

$$
\begin{aligned}
LHS &= \int_{\mathbb{R}^{N+1}} p\delta(p - q_{N+1} - \sum_{m=1}^N q_m) q_{N+1}^{-iu_{N+1}-1} \prod_{m=1}^N q_m^{-iu_m-1} d^{N+1}q \\
&= \frac{\prod_{m=1}^N \Gamma(-iu_m)}{\Gamma(-i\sum_{m=1}^N u_m)} \int_0^p \frac{p}{p - q_{N+1}} (p - q_{N+1})^{-i(\sum_{m=1}^N u_m)} q_{N+1}^{-iu_{N+1}-1} dq_{N+1} \quad (4.23)
\end{aligned}
$$

The proof is complete when one notices that the q_{N+1} integral is simply $p^{-i(\sum_{m=1}^{N+1} u_m)}$ multiplied by a beta function with parameters $-i(\sum_{m=1}^N u_m)$ and $-iu_{N+1}$.

$\qquad\square$

4.11   Additional Material

In section 4.7, we plot the objective function for the SV spread option using the benchmark computed using the FFT method itself with parameters $N = 2^{12}$ and $\bar{u} = 80$. Here we present the objective function using the benchmark computed using Monte Carlo simulation in Figure 4.4. The Monte Carlo computation errors are consistent to a level of 4×10^{-4}, where the objective function levels off.

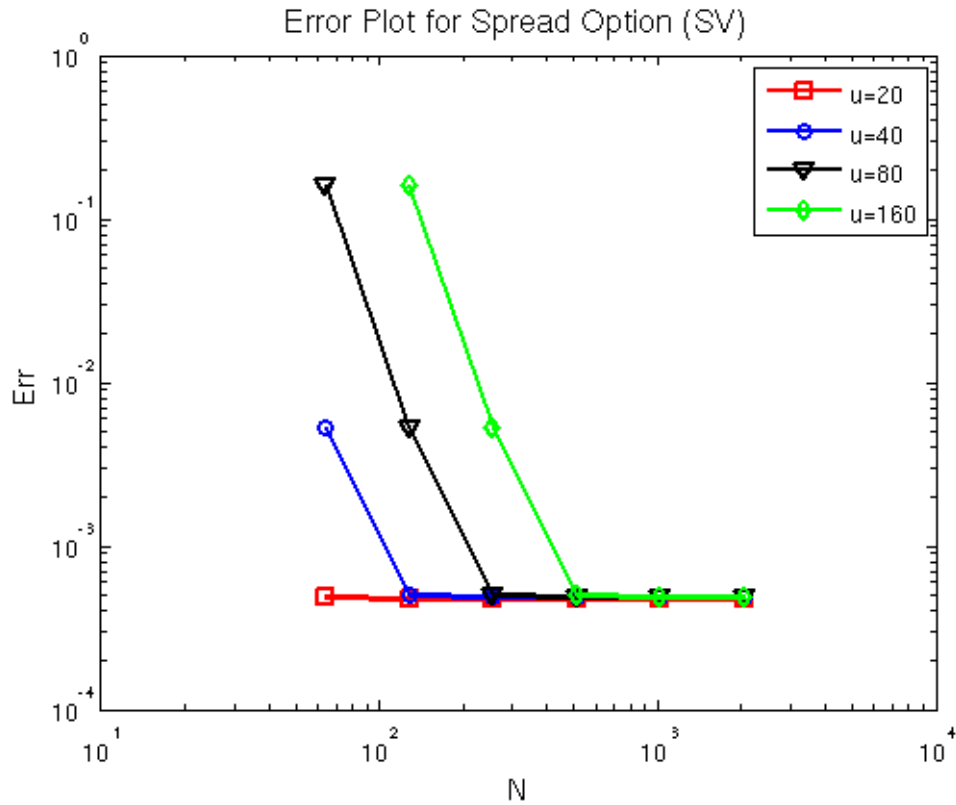Figure 4.4: This graph shows the objective function Err for the numerical computation of the SV spread option versus the benchmark computed using $1,000,000$ simulations, each consisting of 2000 time steps. The parameter values are taken from [32]: $r = 0.1, T = 1.0, \rho = 0.5, \delta_1 = 0.05, \sigma_1 = 1.0, \rho_1 = -0.5, \delta_2 = 0.05, \sigma_2 = 0.5, \rho_2 = 0.25, v_0 = 0.04, \kappa = 1.0, \mu = 0.04, \sigma_v = 0.05$.

Chapter 5

Summary

Hindered by the shortcomings of a firm's infrequent quarterly financial reports, investors have difficulties obtaining more dynamic information on the firms capital structure. We have shown that one way this difficulty can be addressed is by interpreting market traded instruments in terms of capital structure through mathematical modeling and statistical inference methods.

Of course, this undertaking is far from being trivial. Traditional capital structure modeling is equivalent to modeling a firm's log-leverage ratio. As a first step, in chapter 2 we consider structural credit risk modeling in the important special case where the log-leverage ratio of the firm is a time-changed Brownian motion (TCBM) with the time-change taken to be an independent increasing process. Following the approach of Black and Cox, one defines the time of default to be the first passage time for the log-leverage ratio to cross the level zero. Rather than adopting the classical notion of first passage, with its associated numerical challenges, we accept an alternative notion applicable for TCBMs introduced by Hurd [57] called "first passage of the second kind". We demonstrate how statistical inference can be efficiently implemented in this new class of models. This allows us to compare the performance of two versions of TCBMs, the variance gamma (VG) model and the exponential jump model (EXP), to the Black-Cox model. When applied to a 4.5 year long data set of weekly credit default swap (CDS) quotes for Ford Motor Co, the conclusion is that the two TCBM models, with essentially one extra parameter, can significantly

outperform the classic Black-Cox model. Therefore, we demonstrate that observations of a firm's CDS term structures contain rich and accessible information about its capital structure.

While the structural credit risk modeling and statistical inference are well illustrated by the case study of Ford Motor Co., we can easily extend the scope to cover more firms. It would be interesting to see for a pool of thousands of firms how the model implied log leverage ratios are correlated to their balance sheet parameters. In particular, we can plot model implied leverage ratios against accounting leverage ratios and observe their dependence by a regression analysis. If a significant linear fit exists for certain firms or certain industry sectors, we can confidently monitor the dynamics of their accounting leverage ratios through market CDS prices, without having to wait for the release of quarterly financial reports. This will help us understand a firm's true financial status, especially its creditworthiness, on a timely basis. Practically, it can serve as an important supplementary tool for rating agencies dedicated to fundamental analysis. On the other hand, if regression fitting deviates dramatically from the expected linear specification, we can also draw crucial information. We might want to ask questions such as: Is this deviation typical for certain firms or industry sectors, or just an outlier? Does the deviation vanish in time or persist? If it does disappear in time, one can trade CDS contracts of two firms whose deviations are opposite in sign, and expect that their prices will evolve to be consistent with the balance sheet in time. Then there could exist statistical arbitrage opportunities. Or even, does the financial report reflect the true situation of the firm? Investors can always take a firm released information with a grain of salt and the regression analysis can provide them with the necessary quantitative evidence.

This chapter also points to the potential for further mathematical and statistical results. For example, the linearized inference method seems deserving of further study, to understand better its advantages and limitations, as well as its relation to other methods of filtering.

Another interesting topic is recovery modeling. Similar to the Black-Cox model and its common variants, in this thesis we model the default event and the recovery rate independently. In particular, we model a constant recovery of par for CDS pric-

ing. In contrast, a Merton type model is able to integrate the default and recovery treatment so that given a default at the maturity, the difference between debt face value and asset "overshoot" value, the residual of asset, is considered as the recovery for debt holders. This assumption seems natural in structural models, which assume that cashflows for stakeholders are essentially the allocation of the asset value. However, to our knowledge, this type of recovery modeling is rarely used in the literature, mainly due to its lack of tractability in jump-diffusion models. However, we can still implement this alternative approach by Monte Carlo simulation in our TCBM models.

In chapter 3 we extend the pure structural credit risk models to a unification of equity and credit modeling. We assume both a firm's asset and debt to follow exponential TCBM, leading to a two-factor capital structure model. Consistent with the arbitrage pricing theory, we consider the firm's equity and credit derivatives as contingent claims on the underlying asset and debt. The equity formula is derived as the difference of the values of asset and debt. The credit risk modeling is identical to the TCBM modeling in chapter 2, both in its analytical setup and numerical implementation. On the equity side, we are able to price the European call option as a two dimensional Fourier transform. Numerical experiments show that this capital structure model is able to produce flexible implied volatility surfaces and CDS term structures that could not be easily accommodated by other existing models. We demonstrate its practical effectiveness by calibrating Ford Motor Co. to equity option quotes and CDS quotes simultaneously. Not surprisingly, since the credit modeling uses the same approach as the previous chapter, the modeled CDS term structure fits market data quite well. Moreover, the modeled implied volatility surface fits the market data quite well across both maturity and moneyness, a quality not usually seen in one-factor equity Lévy models [67]. The calibration demonstrates that the model is able to capture risks simultaneously in both equity markets and credit markets.

The joint modeling of equity and credit risk reveals much more of a firm's capital structure than the pure credit risk modeling. So the potential explorations for the TCBM credit modeling of many firms we described above applies to the joint credit/equity modeling as well. One has better insight into a firm's financial status

by looking jointly at its model implied asset and debt. We can plot model implied assets against accounting assets, and model implied debts against accounting debts[1], and hope to see a significant dependence coming out of a regression analysis.

Besides looking at the deviations between model implied assets/debts and accounting assets/debts, we have several other dimensions to explore. For example, is our model consistently biased? If yes, it might be caused by limitations of mathematical modeling. We notice that Ford Motor Co. shows negative equity in its balance sheets for several years. Impossible in our modeling framework, this inconsistency requires a corporate finance interpretation. Is there anything surprising about calibration in our model? We recall that we obtained zero implied recovery rates for our VG and EXP model, and attributed these implausibly low rates to a pricing inconsistency between equity and credit markets. In other words, in a world of positive recovery, either the market CDS is too high or the market implied volatility is too low for our model. Observing this inconsistency and uncovering its evolution can be of practical significance. If the inconsistency has a tendency to diminish over time, one can attempt a capital structure arbitrage in single name stocks, options and CDS trading, with long positions in relatively underpriced instruments and short positions in relatively overpriced instruments. Alternatively, we can use accounting asset and debt values of balance sheets as inputs to compute model implied stocks, options and CDS prices. The differences between model prices and market prices may also lead to strategies for capital structure arbitrage. For example, Yu [110] studied similar strategies for stocks and CDS trading using CreditGrades [45].

One challenge for the realization of the above programs is the statistical inference of the assets and debts alike what we did in chapter 2. One notices that in chapter 3 we make only single day calibrations rather than a full multi-period MLE. This is because the bivariate transition density function is much more difficult to manage. Brute force computation will be slow and numerical errors will be much higher than those in chapter 2. One might investigate simplifications that lead to efficient approximations of the transition density function: Given the potential power of this model such efforts

---

[1]It is at researchers' discretion to select total assets, current assets, total debt, short-term debts *etc.*

may be well justified.

Last but not least, in chapter 4 we present a new approach to the valuation of spread options, an important class of financial contracts. The fact we find that pricing the equity option in the capital structure context breaks down into pricing two spread options makes this chapter part of the backbone of the entire thesis. The method is based on a newly discovered explicit formula for the Fourier transform of the spread option payoff in terms of the complex gamma function. We were also able to extend this formula to spread options in higher dimensions, and a certain class of basket options.

This mathematical result leads to simple and transparent algorithms for pricing spread options and other basket options in all dimensions. We have shown that the powerful tool of the FFT provides an accurate and efficient implementation of the pricing formula in low dimensions. For implementation of higher dimensional problems, the curse of dimensionality sets in, and such cases should proceed using parallel partitioning methods as introduced in [71]. The difficulties and pitfalls of the FFT, of which there are admittedly several, are by now well understood, and thus the reliability and stability properties of our method are clear. We presented a detailed discussion of errors, and showed which criteria determine the optimal choice of implementation parameters.

Many important processes in finance, particularly affine models and Lévy jump models, have well known explicit characteristic functions, and can be included in the method with little difficulty. Thus the method can be easily applied to other important models arising in energy and commodity markets. Finally, the Greeks can be systematically evaluated for such models, with similar performance and little extra work.

While our method provides a basic analytic framework for spread options, much as has been done for one-dimensional options, it is certainly possible to add refinements that will improve convergence rates. Such techniques might include, for example, analytic computation of residues combined with contour deformation.

In the end, while we have demonstrated that our mathematical models provide alternatives to accounting balance sheets published quarterly in financial statements

to understand the dynamics of a firm's capital structure, we would like to reiterate that the model implied asset and debt values are indeed market values rather than accounting values of the firm. The detailed correspondence between these two points of view may prove to be a fruitful avenue for future exploration.

Bibliography

[1] E. Altman. Financial ratios: discriminant analysis, and the prediction of corporate bankruptcy. *Journal of Finance*, 23:589–609, 1968.

[2] A. Antonov and M. Arneguy. Analytical formulas for pricing CMS products in the LIBOR market model with the stochastic volatility. *SSRN eLibrary*, 2009.

[3] D. Applebaum. *Lévy processes and stochastic calculus*. Cambridge University Press, 2004.

[4] O.E. Barndorff-Nielsen and N. Shephard. Non-Gaussian Ornstein-Uhlenbeck-based models and some of their uses in financial economics (with discussion). *J. Royal Stat. Soc. B*, 63:167–241, 2001.

[5] M. Baxter. Dynamic modelling of single-name credits and CDO tranches. *www.defaultrisk.com*.

[6] A. Benos and G. Papanastasopoulos. Extending the Merton model: A hybrid approach to assessing credit quality. *Mathematical and computer modeling*, 46:47–68, 2007.

[7] A. Bensoussan, M. Crouhy and D. Galai. Stochastic equity volatility, and the capital structure of the firm. *Mathematical Models in Finance.* In D. D. Howison, F. P. Kelly and P. Wilmott, eds., The Royal Society/Chapman and Hall, 1995.

[8] A. Biere and M. Scherer. Robust calibration of a structural-default model with jumps. *http://www.defaultrisk.com*, 2008.

[9] BIS quarterly review. *http://www.bis.org*, March 2011.

[10] F. Black and J. C. Cox. Valuing corporate securities. *J. Finance*, 31:351–367, 1976.

[11] F. Black and M. Scholes. The pricing of options and corporate liabilities. *Journal of Political Economy*, 81:659–683, 1973.

[12] C. Blanchet-Scalliet and F. Patras. Counterparty risk valuation for cds. *http://www.defaultrisk.com*, 2008.

[13] D. Brigo, F. Mercurio, F. Rapisarda and R. Scotti. Approximated moment-matching dynamics for basket-options simulation. *http://www.papers.ssrn.com*, 2002.

[14] D. Brigo and M. Tarenghi. Credit default swap calibration and equity swap valuation under counterparty risk with a tractable structural model. *http://www.defaultrisk.com*, 2005.

[15] E. Briys and F. de Varenne. Valuing risky fixed rate debt: an extension. *Journal of Financial and Quantitative Analysis*, 32(2):239–248, 1997.

[16] J. Cariboni and W. Schoutens Pricing credit default swaps under Lévy models. *Journal of Computational Finance*, 10(4):1–21, 2007.

[17] R. Carmona and V. Durrleman Pricing and hedging spread options. *SIAM Review*, 45:627–685, 2003.

[18] R. Carmona and V. Durrleman Pricing and hedging spread options in a log-normal model. *Technical report*, Princeton University, 2003.

[19] P. Carr, H. Geman, D. Madan and M. Yor. Stochastic volatility for lévy processes. *Mathematical Finance*, 13:345–382, 2003.

[20] P. Carr, H. Geman, D. Madan and M. Yor. Self decomposability and option pricing. *Mathematical Finance*, 17:31–57, 2007.

[21] P. Carr and R. Lee. Volatility derivatives. *Annu. Rev. Financ. Econ.*, 1:1–21, 2009.

[22] P. Carr and V. Linetsky A jump to default extended CEV model: an application of Bessel processes *Finance and Stochastics*, 2006.

[23] P. Carr and D. Madan Option valuation using the fast Fourier transform. *Journal of Computational Finance*, 2, 2000.

[24] P. Carr and D. Madan. A note on sufficient conditions for no arbitrage. *Finance Research Letters*, 2:125–130, 2005.

[25] P. Carr and L. Wu. Time-changed Lévy processes and option pricing. *Journal of Financial Economics*, 71:113–141, 2004.

[26] P. Carr and L. Wu. Stock options and credit default swaps: a joint framework for valuation and estimation. *Journal of Financial Econometrics*, 1–41, 2009.

[27] U. Cetin, R. Jarrow, P. Protter and Y. Yildirim. Modeling credit risk with partial information. *Annals of Applied Probability*, 14(3):1167–1178, 2004.

[28] R. Cont, A. Moussa and E. B. Santos. Network structure and systemic risk in banking systems. *http://papers.ssrn.com*, 2010.

[29] R. Cont and P. Tankov. *Financial Modeling with Jump Processes*. CRC Press Company, 2004.

[30] P. Crosbie. Modeling default risk. *KMV technical document*, 2002.

[31] F. Delbaen and W. Schachermayer. A general version of the fundamental theorem on asset pricing. *Mathematishe Annalen*, 300:463–520, 1994.

[32] M. A. H. Dempster and S. S. G. Hong Spread option valuation and the fast Fourier transform. *Technical report*, Cambridge University, 2000.

[33] M. Dempster, E. Medova and K. Tang. Long term spread option valuation and hedging. *Journal of Banking & Finance*, 32:2530–2540, 2008.

[34] S. Deng, M. Li and J. Zhou. Multi-asset spread option pricing and hedging. *http://papers.ssrn.com*, 2007.

[35] S. Deng, M. Li and J. Zhou Closed-form approximations for spread option prices and greeks. SSRN: http://ssrn.com/abstract=952747, 2006.

[36] E. Derman and P. Wilmott. The financial modeler's manifesto. *Emanuel Derman's Blog in http://www.wilmott.com*, 2009.

[37] J. Duan. Maximum likelihood estimation using price data of the derivatives contract. *Mathematical Finance*, 4:155–167, 1994.

[38] D. Duffie and D. Lando. Term structures of credit spreads with incomplete accounting information. *Econometrica*, 69:633–664, 2001.

[39] D. Duffie and K. Singleton. *Credit Risk*. Princeton University Press, 2003.

[40] D. Duffie, K. Singleton and J. Pan. Transform analysis and asset pricing for affine jump-diffusions. *Econometrica*, 68:1343–1376, 2000.

[41] E. Eberlein and D. Madan. Unlimited liabilities, reserve capital requirements and the taxpayer put option. *http://papers.ssrn.com*, 2010.

[42] Y. Eom, J. Helwege and J. Huang. Structural models of corporate bond pricing: An empirical analysis. *Review of Financial Studies*, 17(2):499–544, 2004.

[43] J. Ericsson and J. Reneby. The valuation of corporate liabilities: theory and tests. *Working paper, McGill University*, 2001.

[44] Fang Fang, Henrik Jönsson, Cornelis W. Oosterlee, and Wim Schoutens. Fast Valuation and Calibration of Credit Default Swaps Under Levy Dynamics. *Journal of Computational Finance*, 2010.

[45] C. Finger. Creditgrades technical document. *RiskMetrics Group, Inc.*, 2002.

[46] K. Giesecke. Correlated default with incomplete information. *Journal of Banking and Finance*, 28:1521–1545, 2004.

[47] M. Gordy. Model foundations for the supervisory formula approach. *Structured Credit Products: Pricing, Rating, Risk Management and Basel II, Risk Books.* In William Perraudin eds., 2004.

[48] J. Harrison and J. Kreps. Martingales and arbitrage in multiperiod securities markets. *Journal of Economic Theory*, 11:418–443, 1981.

[49] J. Harrison and S. Pliska. Martingales and stochastic integrals in the theory of continous trading. *Stochastic Processes & Applications*, 11:215–260, 1981.

[50] J. Helwege and C. M. Turner. The slope of the credit yield curve for speculative grade issuers. *Journal of Finance*, 54:1869–1885, 1999.

[51] J. Hull. The credit crunch of 2007: What went wrong? why? what lessons can be learned? *http://www.defaultrisk.com*, 2009.

[52] J. Hull. OTC derivatives and central clearing: can all transaction be cleared? *http://www.defaultrisk.com*, 2010.

[53] J. Hull. *Options, futures and other derivatives, 8th Edition.* Prentice Hall, 2011.

[54] J. Hull, M. Predescu and A. White. The valuation of correlation-dependent credit derivatives using a structural model. *http://www.defaultrisk.com*, 2009.

[55] J. Hull and A. White. Valuing credit default swaps II: Modeling default correlations. *Journal of Derivatives*, 8(3):12–22, 2001.

[56] J. Hull and A. White. Valuation of a cdo and nth to default cds without monte carlo simulation. *Journal of Derivatives*, 12(2):8–23, 2001.

[57] T. R. Hurd. Credit risk modeling using time-changed Brownian motion. *Int. J. Theor. App. Fin.*, 12:1213–1230, 2009.

[58] T. R. Hurd and A. Kuznetsov. On the first passage time for Brownian motion subordinated by a Lévy process. *J. Appl. Probab.*, 46:181–198, 2009.

[59] T. Hurd and Z. Zhou. A Fourier transform method for spread option pricing. *SIAM J. Financial Math.*, 1:142–157, 2010.

[60] T. Hurd and Z. Zhou. Statistical Inference for Time-changed Brownian Motion Credit Risk Models. *http://www.defaultrisk.com*, 2011.

[61] T. Hurd and Z. Zhou. Two-factor capital structure models for equity and credit. *In preparation*, 2011.

[62] K. R. Jackson, S. Jaimungal, and V. Surkov Fourier space time-stepping for option pricing with Lévy models. *J. Comp. Finance*, 12, 2008.

[63] R. Jarrow and A. Rudd. Approximate option valuation for arbitrary stochastic processes. *Journal of Financial Economics*, 10:347–369, 1982.

[64] R. Jarrow and S. Turnbull. Pricing Derivatives on Financial Securities Subject to Credit Risk. *Journal of Finance*, 50, 1995.

[65] I. Karatzas and S. Shreve. *Brownian motion and stochastic calculus-2nd Ed.* Springer Press, 1991.

[66] E. Kirk. Correlations in the energy markets, in managing energy price risk. *Risk Publications and Enron*, 1995.

[67] M. Konikov and D. Madan. Stochastic volatility via Markov chains. *Review of Derivatives Research*, 5: 81–115, 2002.

[68] S. G. Kou and H. Wang. First passage times of a jump diffusion process. *Adv. in Appl. Probab.*, 35(2):504–531, 2003.

[69] D. Lando. *Credit Risk Modeling: Theory and Applications.* Princeton University Press, 2004.

[70] R. Lee. Option pricing by transform methods: Extensions, unification, and error control. *Journal of Computational Finance*, 7:51–86, 2004.

[71] C. C. W. Leentvaar and C. W. Oosterlee Multi-asset option pricing using a parallel Fourier-based technique. *J. Comp. Finance*, 12, 2008.

[72] H. Leland. Risky debt, bond covenants and optimal capital structure. *Journal of Finance*, 49:1213–1252, 1994.

[73] H. Leland and K. Toft. Optimal capital structure, endogenous bankruptcy and the term structure of credit spreads. *Journal of Finance*, 50:789–819, 1996.

[74] A. Lewis. A simple option formula for general jump-diffusion and other exponential lévy processes. *Envision Financial Systems and OptionCity.net*, 2001.

[75] A. Lipton and A. Sepp. Credit value adjustment for credit default swaps via the structural default model. *Journal of Credit Risk*, 5(2):123–146, 2001.

[76] R. Litterman and T. Iben. Corporate bond valuation and the term structure of credit spreads. *Journal of Portfolio Management*, pages 52–64, 1991.

[77] A. Lo and M. Mueller. Warning: physics envy may be hazardous to your wealth! *http://papers.ssrn.com*, 2010.

[78] R. Lord, F. Fang, F. Bervoets, and K. Oosterlee A fast and accurate FFT-based method for pricing early-exercise options under Lévy processes. *SIAM J. Sci. Comput.*, 30:1678–1705, 2008.

[79] A. Mbafeno. Co movement term structure and the valuation of energy spread options. *Mathematics of Derivative Securities*. In M. Dempster and S. Pliska, eds., Cambridge University Press, UK, 1997.

[80] D. Madan, P. Carr, and E. Chang The variance gamma model and option pricing. *European Finance Review*, 3, 1998.

[81] D. Madan and E. Seneta. The VG model for share market returns. *Journal of Business*, 63:511–524, 1990.

[82] W. Margrabe The value of an option to exchange one asset for another. *Journal of Finance*, 33:177–186, 1978.

[83] P. Mella-Barral and W. Perraudin. Strategic debt service. *Journal of Finance*, 51, 1997.

[84] Rafael Mendoza-Arriaga, Peter Carr, and Vadim Linetsky. Time-changed markov processes in unified credit-equity modeling. *Mathematical Finance*, 20(4):527–569, 2010.

[85] R. Merton. The theory of rational option pricing. *Bell Journal of Economics and Management Science*, 4:141–183, 1973.

[86] R. C. Merton. On the pricing of corporate debt: the risk structure of interest rates. *J. Finance*, 29:449–470, 1974.

[87] T. Moosbrucker. Pricing CDOs with correlated Variance Gamma distributions. Working paper `http://www.defaultrisk.com/pp_crdrv103.htm`, 2006.

[88] *http://en.wikipedia.org/wiki/Mortgage-backed_security.*

[89] M. Musiela and M. Rutkowski. *Martingale methods in financial modeling.* Springer Verlag, Berlin Heidelberg New York, 1997.

[90] Whitney K. Newey and Kenneth D. West. A simple, positive semidefinite, heteroskedasticity and autocorrelation consistent covariance matrix. *Econometrica*, 55(3):703–08, 1987.

[91] L. T. Nielsen, J. Saá-Requejo and P. Santa-Clara. Default risk and interest rate risk: The term structure of default spreads. *Working paper, INSEAD*, 1993.

[92] G. Poitras. Spread options, exchange options, and arithmetic brownian motion. *Journal of Futures Markets*, 18:487–517, 1998.

[93] W. H. Press, S. A. Teukolsky, W. T. Vetterling, and B. P. Flannery Numerical Recipes 3rd Edition: The Art of Scientific Computing. *Cambridge University Press*, 2007.

[94] F. Salmon. Recipe for disaster: The formula that killed wall street. *http://www.wired.com*, 2009.

[95] O. Sarig and A. Warga. Some empirical estimates of the risk structure of interest rates. *Journal of Finance*, 44:1351–1360, 1989.

[96] R. Schöbel. A note on the valuation of risky corporate bonds. *OR Spektrum*, 21:35–47, 1999.

[97] P. Schönbucher. *Credit Derivatives Pricing Models: Models, Pricing and Implementation.* Wiley Finance, 2003.

[98] D. Shimko. Options on future spreads: Hedging, speculating, and valuation. *Journal of Futures Markets*, 14:183–213, 1997.

[99] S. Shreve. *Stochastic calculus for finance-volume II.* Springer Finance, 2003.

[100] S. Shreve. Steve Shreve on Pablo Triana's the flawed maths of financial models. *http://www.quantnet.com*, 2010.

[101] Securities Industry and Financial Markets Association. http://sifma.org. *Global CDO issuance*, 2010.

[102] P. Triana. The flawed maths of financial models. *http://www.ft.com*, 2010.

[103] Q. H. Vuong. Likelihood ratio tests for model selection and non-nested hypotheses. *Econometrica*, 57:307–333, 1989.

[104] D. Wilcox. Energy futures and options: Spread options in energy markets. *Goldman Sachs, New York*, 1990.

[105] J. Williams, S. Haka, M. Bettner and J. Carcello. *Financial & Managerial Accounting*. McGraw-Hill Irwin, 2008.

[106] P. Wilmott. The use, misuse and abuse of mathematics in finance. *Phil. Trans. R. Soc. Lond. A*, 358:63–73, 2000.

[107] P. Wilmott. The problem with derivatives, quants, and risk management today. *http://www.qfinance.com*, 2010.

[108] Y. Yildirim. Modeling default risk: A new structural approach. *Finance Research Letters*, 3(3):165–172, 2006.

[109] F. Yu. Introduction to special issue on capital structure arbitrage. *Banque & Marchés*, 80:5–6, 2006.

[110] F. Yu. How profitable is capital structure arbitrage? *Financial Analysts Journal*, 62(5):47–62, 2006.

[111] C. Zhou. The term structure of credit spreads with jump risk. *Journal of Banking & Finance*, 25:2015-2040, 2001.